2012

Identification of a Post-Transcriptional Mechanism Regulating Epithelial-Mesenchymal Transition

George S. Hussey
Cleveland State University

IDENTIFICATION OF A POST-TRANSCRIPTIONAL MECHANISM

REGULATING EPITHELIAL-MESENCHYMAL TRANSITION

GEORGE S. HUSSEY

Bachelor of Science in Biology

University of Akron

May, 2007

Submitted in partial fulfillment of requirements for the degree

DOCTOR OF PHILOSOPHY IN REGULATORY BIOLOGY

at the

CLEVELAND STATE UNIVERSITY

December, 2012

This dissertation has been approved

For the Department of BIOLOGICAL, GEOLOGICAL, AND ENVIRONMENTAL

SCIENCES and the College of Graduate Studies of Cleveland State University

by

_____Date:_____
Dr. Philip H Howe, CSU-BGES
Major Advisor

_____Date:_____
Dr. Crystal Weyman, CSU-BGES
Advisory Committee Member

_____Date:_____
Dr. Valentin Boerner, CSU-BGES
Advisory Committee Member

_____Date:_____
Dr. Aaron Severson, CSU-BGES
Advisory Committee Member

_____Date:_____
Dr. Paul L Fox, CCF-Cell Biology/CSU-BGES
Advisory Committee Member

_____Date:_____
Dr. Barsanjit Mazumder, CSU-BGES
Internal Examiner

_____Date:_____
Dr. Véronique Lefebvre, CCF-Cell Biology
External Examiner

This thesis is dedicated to my parents.

For their endless love, support and encouragement.

ACKNOWLEDGMENTS

IDENTIFICATION OF A POST-TRANSCRIPTIONAL MECHANISM

REGULATING EPITHELIAL-MESENCHYMAL TRANSITION

George S. Hussey

ABSTRACT

A major challenge in the clinical management of human cancers is to accurately stratify patients according to risk and likelihood of a favorable response. Stratification is confounded by significant phenotypic heterogeneity in some tumor types, often without obvious criteria for subdivision. Despite intensive transcriptional array analyses, the identity and validation of cancer specific 'signature genes' remains elusive, partially because the transcriptome does not mirror the proteome. The simplification associated with transcriptomic profiling does not take into consideration changes in the relative expression among transcripts that arise due to post-transcriptional regulatory events. Transcript-selective translational regulation of epithelial-mesenchymal transition (EMT) by transforming growth factor-β (TGFβ) is directed by the hnRNP E1-containing TGFβ-activated-translational (BAT) mRNP complex. Herein, eukaryotic elongation factor-1 A1 (eEF1A1) is identified as an integral component of the BAT complex. Translational silencing of Dab2 and ILEI, two EMT-transcripts, is mediated by binding of hnRNP E1 and eEF1A1 to their 3'-UTR BAT element, whereby hnRNP E1 stalls translational elongation by inhibiting the release of eEF1A1 from the ribosomal A site. TGFβ-mediated hnRNP E1

phosphorylation, through Akt2, disrupts the BAT complex, thereby restoring translation of target EMT-transcripts. Attenuation of hnRNP E1 expression in non-invasive breast epithelial cells induced not only EMT, but also enabled cells to form metastatic lesions *in vivo*. Thus, translational regulation by TGFβ, at the elongation stage, represents a critical checkpoint coordinating the expression of EMT-transcripts involved during tumorigenesis and metastatic progression. Using a genome-wide combinatorial approach involving expression profiling and RIP-Chip analysis, we have identified an EMT gene signature comprised of a cohort of translationally regulated mRNAs that are induced during TGFβ-mediated EMT and follow the same pattern of regulation as Dab2 and ILEI. Translational regulation by hnRNP E1 constitutes a post-transcriptional regulon thus enabling the cell to rapidly and coordinately regulate multiple EMT-facilitating genes.

TABLE OF CONTENTS

LIST OF TABLES

LIST OF FIGURES

CHAPTER I

INTRODUCTION

1.1. TGFβ signaling and EMT

TGFβ, and its related factors, modulate essential cellular functions ranging from cellular proliferation and differentiation to apoptosis (Shi & Massague, 2003; Howe, 2003). TGFβ exerts its biological effects by inducing the formation of an oligomeric complex of type I and type II serine/threonine kinase receptors. The activated receptor complex phosphorylates and activates the receptor-regulated Smads, Smad2 and Smad3. Once activated, these Smads complex with the common mediator Smad4, translocate to the nucleus, wherein the Smads regulate transcription of target genes through their interaction with a wide variety of transcriptional regulators (Howe, 2003; Siegel & Massague, 2003). In addition to the canonical Smad pathway, TGFβ has also been reported to signal through components of the MAPK and PI3K/Akt pathways (Howe, 2003; Siegel &

Massague, 2003). TGFβ has been shown to activate extracellular signal regulated kinase (ERK) (Hartsough & Mulder, 1995; Mucsi *et al.*, 1996), Jun N-terminal kinase (JNK) (Afti *et al.*, 1997; Hocevar *et al.*, 1999), and p38 mitogen activated protein kinase (p38) (Hanafusa *et al.*, 1999). The TGFβ responses regulated by these kinases are varied ranging from reporter construct transactivation, to regulation of cellular proliferation and apoptosis. It has been demonstrated that expression of the cytosolic adaptor molecule Disabled-2 (Dab2) was able to restore both Smad-dependent and Smad-independent TGFβ responses to a TGFβ-signaling-deficient mutant cell line (Hocevar *et al.*, 1999).

Human carcinomas exhibit a wide range of signaling events to promote cell migration and invasion. Recent studies demonstrate the conversion of epithelial cancer cells to a more mesenchymal-like phenotype, a process termed epithelial-mesenchymal transition (EMT), to facilitate cell invasion and metastasis (Brabletz et al., 2005). Numerous studies have suggested that members of the TGFβ superfamily represent these inductive signals which mediate the transition to a mesenchymal state (Sanford et al., 1997; Thiery and Sleeman, 2006). TGFβ-induced EMT is largely characterized by disruption of the polarized morphology of epithelial cells and acquisition of a spindle shaped phenotype (Savagner, 2001). It is accompanied by a downregulation and relocalization of the epithelial marker E-cadherin from cell junctions, whereas fibroblastic markers vimentin, and N-cadherin are upregulated (Buck et al., 2007).

1.2. Significance of Dab2 and ILEI in TGFβ-mediated EMT.

A predominant *in vitro* model for studying TGFβ-induced EMT is normal murine mammary gland epithelial (NMuMG) cells. Using this model, two candidate EMT genes were defined, Disabled-2 (Dab2) and FAM3C or *Interleukin like EMT inducer (ILEI)*. Dab2 is a cytosolic adaptor protein that is involved in the organization and formation of signalsome complexes in clathrin coated pits and in early endosomes following growth factor stimulation of cells. It has also been shown to be an important regulator of cellular differentiation in several models including megakaryocytic, visceral endoderm, and in EMT (Tseng *et al.*, 2001; Smith *et al.,* 2001; Prunier & Howe, 2005). Dab2 is a positive mediator of TGFβ signaling and functions as an adaptor protein bridging the TGFβ receptor complex to the Smad proteins (Hocevar *et al.*, 2001; Hocevar *et al.,* 2005). Treatment of NMuMG cells with TGFβ induces an alteration in cell morphology from the cuboidal appearance characteristic of epithelial cells to an elongated, spindle-shaped form characteristic of fibroblasts, and induces an upregulation of Dab2 concomitant with EMT in these cells. Confirming the morphologic analysis of a TGFβ-mediated EMT, treatment of cells with TGFβ induces an accompanying increase in N-cadherin expression, characteristic of fibroblastic cells (Prunier & Howe, 2005). ILEI was initially identified as a candidate gene for autosomal recessive nonsyndromic hearing loss locus 17 (DFNB17) and was subsequently identified as a member of a recently discovered gene family (FAM3A-D). In an expression profiling analysis of polysome bound-mRNA during TGFβ-mediated EMT in EpRas cells, ILEI was shown to be

translationally upregulated during EMT (Waerner *et al.*, 2006). This data suggests that post-transcriptional control of Dab2 and ILEI gene expression is an important regulatory mechanism and that translational control may be the underlying mechanism.

1.3. Translational Control of Gene Expression.

Translation is usually initiated by binding of a cap-binding complex, recruitment of the 40S small ribosomal subunit, scanning of the 40S subunit to the first AUG initiation codon, and joining of the 60S large ribosomal subunit to form a translational-competent 80S ribosome (Holcik & Sonenberg, 2005; Gebauer & Hentze, 2004; Mazumder *et al.*, 2003). Translational control can be categorized into two general modes: global control, which regulates the synthesis of many proteins; and transcript-specific control in which the translation of one (or several) protein(s) is regulated. Global regulation occurs mainly through modification of translation-initiation factors, whereas transcript-specific regulation occurs by association with an RNA-binding protein to a *cis*-acting structural element in the 5'- or 3'-untranslated region (UTR) of the target mRNA. In early studies of *cis*-acting sequences that regulate translation, attention has been mostly directed to the 5'-UTR. More recently, however, the 3'-UTR has become increasingly recognized as an important regulator of mRNA translation (Mazumder *et al.*, 2003). *Trans*-acting factors that bind the 3'-UTR repress the translation of multiple transcripts, including ceruloplasmin (Mazumder & Fox, 1999), 15-lipoxygenase (Ostareck et al., 1999), myocyte enhancer factor 2 (MEF-2) (Black et al., 1997), β-F1 ATPase (Izquierdo & Cuerva, 1997), amyloid

4

precursor protein (Mbongolo Mbella *et al.*, 2000), p53 (Fu & Benchimol, 1997) and cyclin B (De Moor & Richter, 1999) to name a few. Recently, it has also been reported that 3'-UTR-mediated translation control is a mechanism that is used to modulate gene expression in a wide range of biological situations. From early embryonic development to cell differentiation and apoptosis, translation has been demonstrated to fine-tune protein levels in both a temporal and spatially-dependent manner (Preiss & Hentze, 1999; Mazumder *et al.*, 2003; De Moor *et al.*, 2005).

CHAPTER II

IDENTIFICATION OF AN mRNP COMPLEX REGULATING

TUMORIGENESIS AT THE TRANSLATIONAL ELONGATION STEP[1]

2.1 Abstract

Transcript-selective translational regulation of epithelial-mesenchymal transition (EMT) by transforming growth factor-β (TGFβ) is directed by the hnRNP E1-containing TGF$\underline{\beta}$-$\underline{a}$ctivated-$\underline{t}$ranslational (BAT) mRNP complex. Herein, eukaryotic elongation factor-1 A1 (eEF1A1) is identified as an integral component of the BAT complex. Translational silencing of Dab2 and ILEI, two EMT-transcripts, is mediated by binding of hnRNP E1 and eEF1A1 to their 3'-UTR BAT element, whereby hnRNP E1 stalls translational elongation by inhibiting the release of eEF1A1 from the ribosomal A site. TGFβ-mediated hnRNP E1 phosphorylation, through Akt2, disrupts the BAT complex, thereby

---

restoring translation of target EMT-transcripts. Attenuation of hnRNP E1 expression in two non-invasive breast epithelial cells (NMuMG and MCF-7) induced not only EMT, but also enabled cells to form metastatic lesions *in vivo*. Thus, translational regulation by TGFβ, at the elongation stage, represents a critical checkpoint coordinating the expression of EMT-transcripts required during development and in tumorigenesis and metastatic progression.

2.2 Introduction

Metastasis is a process resulting in the spread of cancer cells from primary tumors to distant sites and is responsible for more than 90% of cancer-related deaths (Ma et al., 2010). Cells in the primary tumor are triggered by stromal signals to undergo structural and phenotypic changes allowing them to become more motile and invasive, ultimately leading to dissociation from the primary tumor, invasion of surrounding tissue, intravasation into lymphatic or vascular vessels, and extravasation and proliferation at secondary sites (Mouneimne and Brugge, 2009). It is postulated that epithelial cancer cells revert to an embryonic state during the invasive phase of metastasis, undergoing a developmental switch from a polarized, epithelial phenotype to a highly motile mesenchymal phenotype (Thiery and Sleeman, 2006). This epithelial to mesenchymal transition (EMT) is induced by numerous cytokines, including transforming growth factor-β (TGFβ) (Massague, 2008). TGFβ-induced EMT is indispensable during embryonic development for neural crest, heart, and craniofacial structure formation (Massague, 2008), but can also be aberrantly reactivated during tumorigenesis (Zavadil and Bottinger, 2005). TGFβ-mediated EMT integrates Smad, as well as non-Smad signaling pathways (Bakin et al., 2000) and is usually accompanied by a loss of epithelial cell markers; mainly E-cadherin and zonula occludens (ZO-1) (Massague, 2008) and expression of different mesenchymal cell markers like N-cadherin and Twist (Yang et al., 2004; Prunier and Howe, 2005).

Recent studies suggest that regulation of gene expression at the post-transcriptional level plays an important role in TGFβ-mediated EMT (Chaudhury et al., 2010). We have described a transcript-selective translational regulatory pathway in which a ribonucleoprotein (mRNP) complex, containing heterogeneous nuclear ribonucleoprotein E1 (hnRNP E1), binds to a 33-nucleotide (33-nt) structural element in the 3'-UTR of *Disabled-2 (Dab2)* and *Interleukin like EMT inducer (ILEI)*, two mRNAs involved in mediating EMT, and inhibits their translation. The 33-nt RNA element, which we have designated 'BAT' for TGFbeta activated translational element, is sufficient to mediate translational inhibition. TGFβ stimulation activates a kinase cascade terminating in the phosphorylation of hnRNP E1, by isoform-specific stimulation of Akt2, inducing its release from the 3'-UTR BAT element, resulting in reversal of translational silencing and increased expression of these EMT-transcripts (Chaudhury et al., 2010).

Herein, we identify eukaryotic elongation factor-1 A1 (eEF1A1) as an integral component of the BAT mRNP complex. We demonstrate that the BAT element, hnRNP E1 and eEF1A1 form a complex which mediates translational silencing at the translational elongation step. Mechanistically, hnRNP E1 binding to eEF1A1 effectively blocks progression of the 80S ribosome by preventing the release of eEF1A1 from the ribosomal A site post GTP hydrolysis. Akt2-mediated hnRNP E1 phosphorylation, following TGFβ stimulation, induces its release from the BAT element and eEF1A1, allowing eEF1A1-mediated translational elongation to proceed. Remarkably, modulation of hnRNP E1 expression, or its

9

Akt2 targeted Ser43 phosphorylation site, transforms otherwise normal, non-tumorigenic breast epithelial cells to highly invasive cells and enables these to form tumor allografts with accompanying lung metastases.

2.3 Results

eEF1A1 and hnRNP E1 are integral components of the BAT mRNP complex.

The isolation of hnRNP E1, its selective binding to the BAT element, and its phosphorylation and release from the BAT element following TGFβ stimulation has been described (Chaudhury et al., 2010). To identify other proteins in the mRNP complex, we employed size exclusion chromatography, followed by *in vitro* translation (IVT) analysis of a chimeric luciferase BAT (Luc-BAT) reporter construct to isolate fractions that demonstrated translational silencing activity (Figure 2.1 A, B). Cytosolic S100 extracts isolated from non-stimulated (-) murine mammary epithelial (NMuMG) cells displayed translational silencing activity, whereas lysates isolated from 24 h TGFβ-treated cells (+) did not (Figure 2.1 B). Maximal translational silencing activity was observed in chromatography fractions 37-41 (Figure 2.1 B). These fractions were pooled and affinity purified by precipitation with wild-type (WT) BAT cRNA or BAT mutant (BAT-M) coupled to sepharose beads. The BAT-M contains a U to A substitution at position 10 that by Mfold analysis is predicted to unfold the stem loop structure (Figure 2.1 B) (Zuker, 2003). The precipitates were analyzed by SDS-PAGE and visualized by silver stain (Figure 2.1 C, left panel). The resulting bands were compared to corresponding bands in a silver stained gel of a BAT pull down from rabbit reticulocyte lysate (RRL) (Figure 2.1 C, right panel). The lower band (~40 kDa) corresponded with the previously identified BAT element binding protein hnRNP E1. The band at ~50 kDa, present in pooled chromatographic fractions and RRL, bound to the WT BAT, but not the BAT-M. The band was excised, subjected to

11

mass spectrometric analysis and identified as eukaryotic elongation factor-1 A1 (eEF1A1). Additionally, we used two repetitive differentiation control elements (DICE) (Ostareck et al., 1997) in an RNA pull-down experiment from RRL to test the specificity of eEF1A1 binding to the BAT element. hnRNP E1 and heterogenous nuclear ribonucleoprotein K (hnRNP K) have been shown to bind to DICE in the 3-'UTR of *15-lipoxygenase* (Ostareck et al., 1997) and *L2* mRNAs (Collier et al., 1998) and mediate their translational regulation. DICE cRNA precipitated hnRNP E1 and K (Figure 2.1 C, right panel), but not eEF1A1. Immunoblot (IB) analysis of the chromatographic fractions confirmed that eEF1A1 and hnRNP E1 eluted selectively in those fractions that exhibited translational silencing activity (Figure 2.1 D).

In vitro reconstitution of translational silencing was performed with eEF1A1 and hnRNP E1 in stoichiometric ratios to evaluate their indispensability in rendering translational silencing activity. Purified eEF1A1 or recombinant full-length (FL) hnRNP E1 expressed as a GST-fusion product, when excluded from the reaction, or when added individually, had no effect on translational silencing (Figure 2.1 E, lanes 1-3). eEF1A1 (1 – 4 pM) added with low doses (0.8 pM) of hnRNP E1 also had no effect on translation of Luc-BAT (Figure 2.1 E, lanes 4-6); however, eEF1A1 (1 pM) when added with increasing concentrations (1.2 – 3.2 pM) of hnRNP E1 resulted in translational silencing (Figure 2.1 E, lanes 7-9). The last 3 lanes demonstrated that phosphorylated hnRNP E1 (p-hnRNP E1), phosphorylated at Ser43 by recombinant Akt2 *in vitro*, when added with eEF1A1, did not result in translational silencing.

eEF1A1 interacts with hnRNP E1 and the BAT element *in vitro* and *in vivo.*

We examined the temporal association of eEF1A1 with hnRNP E1 and the BAT element. WT BAT and BAT-M were used to precipitate eEF1A1 (Figure 2.2 A, top panel) or hnRNP E1 (Figure 2.2 A, middle panel) from NMuMG cell lysates treated ± TGFβ. eEF1A1 and hnRNP E1 were both precipitated by WT BAT from non-stimulated lysates, but TGFβ treatment induced the loss of eEF1A1 and hnRNP E1 binding in a time-dependent manner. Additionally, purified eEF1A1 alone interacted with the WT BAT in a dose-dependent manner, but not with the BAT-M (Figure 2.2 A, lower panel).

The kinetics of interaction between hnRNP E1 or eEF1A1 with the BAT element were investigated using surface plasmon resonance (SPR) by BIAcore. WT-BAT, BAT-M, and BAT-C (C26 point deletion which removed the asymmetric bulge on the stem of the BAT element) were used in these analyses. The Mfold generated structures of the WT-BAT, BAT-M, and BAT-C are depicted in Figure 2.2 B (Zuker, 2003). These cRNAs were synthesized carrying a 5'-biotin tag and immobilized onto a streptavidin-coated sensor chip. FL-hnRNP E1, purified eEF1A1, or p-hnRNP E1 were serially diluted to concentrations ranging from 1 - 500 nM, and injected across the ligand-immobilized surface. eEF1A1 and hnRNP E1 displayed high affinity binding to the WT BAT, with diminished affinity for either the BAT-M or BAT-C structural mutants (Figure 2.2 C, eEF1A1; $K(a)(M)=$ 1.58 x 10^7; $K(d)(M)=$ 6.32 x 10^{-8} ; hnRNP E1; $K(a)(M)=$ 3.10 x 10^7; $K(d)(M)=$ 3.22 x 10^{-7}), whereas p-hnRNP E1 exhibited complete lack of binding to the WT BAT or its derivative mutants (Figure 2.2 C, lower panel).

13

In vivo interaction of hnRNP E1 and eEF1A1 in NMuMG cells treated ± TGFβ was investigated by co-immunoprecipitation. Anti-hnRNP E1 co-immunoprecipitated eEF1A1 from cell lysates in a TGFβ- and PI3K-sensitive manner (Figure 2.2 D). Interaction was observed in non-stimulated lysates but lost, in a time-dependent fashion, in extracts from TGFβ-treated cells (Figure 2.2 D, top panel). Pre-treatment of cells with the PI3K inhibitor LY294002, blocked the ability of TGFβ to modulate hnRNP E1/eEF1A1 interactions (Figure 2.2 D, top panel), consistent with our previous observation that inhibition of the PI3K/Akt pathway blocked hnRNP E1 Ser43 phosphorylation (Chaudhury et al., 2010). TGFβ or LY294002 had no effect on the expression levels of hnRNP E1 and eEF1A1 (Figure 2.2 D, lower panels).

In vitro binding studies were performed to confirm hnRNP E1/eEF1A1 binding and to determine respective interaction domains. FL-hnRNP E1 precipitated eEF1A1 in a dose-dependent manner (Figure 2.2 E, top panel) while addition of BAT cRNA with low concentrations of eEF1A1 enhanced interactions, suggesting that eEF1A1/hnRNP E1 interactions are stabilized in the presence of the BAT element. p-hnRNP E1 failed to precipitate and interact with eEF1A1 (Figure 2.2 E, middle panel), indicating that phosphorylation of hnRNP E1 contributes to the attenuation of protein-protein and protein-RNA interactions.

We determined the domains of interaction between hnRNP E1, eEF1A1 and the BAT element. eEF1A1 and hnRNP E1 are RNA binding proteins with well characterized domains (Dejgaard and Leffers, 1996; Yan et al., 2008). eEF1A1 or its domains were expressed *in vitro* as [^{35}S]-labeled products (Figure

2.3 A) and precipitated with FL-hnRNP E1 (Figure 2.3 B) or WT BAT (Figure 2.3 C); resolved by SDS-PAGE and analyzed by autoradiography. The results can be summarized as follows; Domains 1 and 3 of eEF1A1, but not domain 2, bind to hnRNP E1, whereas only domain 3 binds the BAT element.

Reciprocally, FL-hnRNP E1 and its KH1-3 domains were expressed as GST-fusion products (Figure 2.3 D, left panel) and precipitated with WT BAT (Figure 2.3 D, right upper panel) or eEF1A1 (Figure 2.3 D, right bottom panel); resolved by SDS-PAGE and probed with α-GST or α-eEF1A1 antibodies, respectively. The results can be summarized as follows: the KH1 and KH3 domains bind the BAT element (Figure 2.3 D, right upper panel), whereas KH1 and KH2 domains bind eEF1A1 (Figure 2.3 D, right bottom panel). A schematic summarizing these results is depicted in Figure 2.3 F. Consistent with these binding data, only FL-hnRNP E1 and its KH1 domain, which bound both eEF1A1 and the BAT element, were functional in repression of Luc-BAT in an IVT assay (Figure 2.3 E). FL-hnRNP E1 repressed translation by >80%, whereas the KH1 domain repressed translation by ~70%. KH2 and KH3 domains were unable to reconstitute translational silencing *in vitro*.

The BAT complex inhibits translation at the elongation stage

The effect of hnRNP E1/eEF1A1 interactions on translation elongation were investigated. We created a synthetic construct harboring the WT BAT or BAT-M element downstream of a poly(uridylic) acid template (poly(U)-BAT) corresponding to $(UUU)_{37}$ codons. poly(U)-BAT cRNA was used in an IVT assay ± hnRNP E1. These conditions allowed the ribosome to enter a correct reading

frame by attachment to any three nucleotides of a UUU codon in the absence of specific initiation and direct incorporation of [^{3}H]-phenylalanine. Accumulation of [^{3}H]-Phe readily occurred in control reactions (Figure 2.4 A), whereas incorporation of [^{3}H]-Phe was inhibited when equimolar concentration of hnRNP E1 relative to eEF1A1 was added to the reaction, and ~60% inhibition was observed when 4X-fold excess of hnRNP E1 was added. As control, p-hnRNP E1 did not inhibit [^{3}H]-Phe incorporation (Figure 2.4 A). Furthermore, the poly(U)-BAT-M failed to inhibit [^{3}H]-Phe incorporation in the presence or absence of hnRNP E1 (Figure 2.4 B).

Ribosome sedimentation analyses were performed to determine the position of a stalled ribosome at either the initiation (40S) or elongation (80S) stage of translation (Anthony and Merrick, 1992). A schematic of the procedure is outlined in Figure 2.4 C. A 20-mer oligodeoxynucleotide was 5'-end labeled with [γ-^{32}P]-ATP and hybridized downstream of the AUG codon of Luc-BAT. The hybrid was incubated with RRL to allow formation of ribosome-mRNA complexes. As controls, the initiation inhibitor GMP-PNP and the elongation inhibitor anisomycin were used to compare radioactivity profiles with reactions ± hnRNP E1. Following incubation, the reaction was layered over a sucrose gradient, centrifuged, and fractions collected from the top and used for scintillation counting. In reactions containing GMP-PNP or anisomycin inhibitors, the [^{32}P]-labeled primer was detected in the 40S (initiation) or 80S (elongation) mRNA complexes, respectively (Figure 2.4 D). In the absence of inhibitors and of hnRNP E1, the [^{32}P]-labeled primer segregated with the free RNA fraction with a

16

minor 80S-mRNA peak observed, indicating that the primer had been displaced from the hybrid, due to the helicase activity of the 80S ribosome, resulting in its accumulation in the free RNA fraction (Figure 2.4 E). In the presence of hnRNP E1, the ribosome-mRNA complexes co-sediment with the 80S fraction, indicating that translation was stalled after formation of the 80S ribosomal complex (Figure 2.4 E). When p-hnRNP E1 was added to the reaction, the radioactivity profile resembled that of the control reaction, indicating that p-hnRNP E1 had no effect on progression of the 80S ribosome (Figure 2.4 F). These results provided evidence that the BAT mRNP complex was targeting the elongation step of protein biosynthesis.

To further localize the action of hnRNP E1, we examined eEF1A1-dependent (enzymatic) and -independent (non-enzymatic) binding of aminoacyl-tRNA. Purified 80S ribosomes and poly(U)-BAT were incubated with [^{3}H]-Phe-tRNA^{Phe} in the presence or absence of eEF1A1 ± hnRNP E1. eEF1A1-dependent and -independent binding of [^{3}H]-Phe-tRNA^{Phe} was not affected by the addition of hnRNP E1 or p-hnRNP E1 (Figure 2.4 G), indicating that hnRNP E1 allows both enzymatic and non-enzymatic binding of aminoacyl-tRNA. Additionally, we tested the effect of hnRNP E1 on the intrinsic GTPase activity of eEF1A1, but found that hnRNP E1 had no effect on GTP hydrolysis (Figure 2.4 H).

hnRNP E1 prevents the release of eEF1A1 from the ribosomal A site.

Since hnRNP E1 had no effect on aminoacyl-tRNA binding or GTPase activity of eEF1A1, we hypothesized that it may be preventing release of eEF1A1 from the ribosome. To investigate this scenario, a ternary complex of Phe-

tRNA^{Phe}, eEF1A1, and [8-^{3}H]-GTP was incubated with 80S ribosomes, poly(U)-BAT ± hnRNP E1 to allow for at least one round of eEF1A1 binding, followed by GTP hydrolysis and eEF1A1 release (Figure 2.5 A). The reaction mix was then analyzed by gel filtration chromatography. This assay allowed us to monitor the presence of eEF1A1 as either free, or ribosome-bound since [8-^{3}H]-GTP retains its radiolabel after hydrolysis, with the resultant [8-^{3}H]-GDP remaining attached to the elongation factor. Aliquots of each fraction were used to measure absorbance at 280 nm, radioactivity via liquid scintillation, or for IB analysis. In control reactions (Figure 2.5 B), eEF1A1 eluted in the lighter fractions (11-14), while the ribosomes eluted in the heavy fractions (7-8) as indicated by the radioactivity profile (graph) and IB analysis with α-eEF1A1 or α-ribosomal protein L30 (RPL30) (Figure 2.5 B). Thus, eEF1A1 is released from the ribosome. When hnRNP E1 was added to the reaction, the radioactivity profile shifted towards the heavy fractions indicating that the eEF1A1 eluted with the ribosomes (Figure 2.5 C; graph), and IB analysis confirmed the presence of eEF1A1 and hnRNP E1 in the ribosomal fractions (Figure 2.5 C). When p-hnRNP E1 was added to the reaction, no [^{3}H] radiolabel was found associated with ribosomes (Figure 2.5 D; graph), and IB analysis confirmed the presence of eEF1A1 in the light fractions (Figure 2.5 D).

In a separate set of reactions, by replacing [^{3}H]-GTP with [γ-^{32}P]-GTP in the ternary complex, we identified the form of the nucleotide bound to eEF1A1 as GDP since [γ-^{32}P]-GTP will lose its radiolabel upon hydrolysis. As shown, (Figure 2.5 B, C, D) the [^{32}P] radiolabel eluted with the lighter fractions in the absence

(panel B) or presence of hnRNP E1 (panel C) or p-hnRNP E1 (panel D), confirming that hnRNP E1 had no effect on GTPase activity. These results demonstrated that hnRNP E1 prevents the release of eEF1A1-GDP from the ribosome thus blocking translation at the eEF1A1-dependent elongation step.

Modulation of the BAT complex alters *in vivo* inhibition of translation elongation.

We examined whether modulation of hnRNP E1 levels in cells regulated translation elongation *in vivo*. We utilized NMuMG cells and derivatives of these that we have previously described (Chaudhury et al., 2010), in which hnRNP E1 expression levels were either stably overexpressed (E23 cells), silenced by shRNA (SH14 cells), or in which the silenced expression was rescued (knock-in) with a wild-type (WT) (KIWT6 cells) or a phosphomutant form, (S43A substitution) of hnRNP E1 (KIM2 cells). We investigated the effect of hnRNP E1 expression levels, or its phosphorylation status, on translational inhibition by monitoring the translocation of *ILEI* mRNA from the non-translating, non-polysomal pool to the actively translating, polysomal pool in non-stimulated and TGFβ-treated cells (Figure 2.6 A). In NMuMG and KIWT6 cells, *ILEI* mRNA was primarily associated with the non-polysomal fractions in non-stimulated cells but translocated to the polysomal fractions after 24 h of TGFβ treatment. In SH14 cells, *ILEI* mRNA was abundant in the polysomal fractions irrespective of TGFβ treatment, whereas in E23 and KIM2 cells, *ILEI* mRNA failed to translocate to the polysomal fractions even in the presence of TGFβ.

In cell-free IVT assays (Figure 2.6 B), cytosolic extract from non-stimulated NMuMG and KIWT6 cells inhibited translation of Luc-BAT, an inhibition that was reversed after a 24 h TGFβ treatment. Extracts from SH14 cells failed to inhibit translation of Luc-BAT even in the absence of TGFβ, whereas translational silencing was observed even in the presence of TGFβ-treated E23 and KIM2 cell extracts. Furthermore, supplementation of the SH14 extracts, or the TGFβ-treated NMuMG and KIWT6 extracts with non-phosphorylated FL-hnRNP E1 was able to reconstitute translational silencing.

Ribosome sedimentation analyses were performed to determine if extracts from hnRNP E1-modulated cells could affect the ribosome association status of a target mRNA (Figure 2.6 C). In reactions containing extracts from non-stimulated NMuMG cells, the [^{32}P]-labeled primer segregated in the 80S (elongation) fraction, whereas only a minor 80S peak was observed in reactions containing extracts from TGFβ−treated NMuMG cells (Figure 2.6 C; left top panel). Supplementation of TGFβ-treated NMuMG extracts with FL-hnRNP E1 caused the [^{32}P]-labeled primer to again co-sediment with the 80S fractions, thereby blocking translation at the elongation step (Figure 2.6 C; right top panel). Alternatively, in reactions performed in the presence of SH14 cell extract, the [^{32}P]-labeled primer segregated with the free RNA fraction (Figure 2.6 C; left bottom panel), while supplementation of SH14 extracts with FL-hnRNP E1 caused the ribosome-mRNA complexes to co-sediment with the 80S fraction. In reactions containing extracts from E23 cells, the [^{32}P]-labeled primer was

detected in 80S (elongation) mRNA complexes irrespective of TGFβ-treatment (Figure 2.6 C; right bottom panel).

As depicted in our model (Figure 2.6 D), eEF1A1 forms a complex with hnRNP E1 and the BAT element. Given the necessity for cognate-codon interaction with the ribosomal A site, it is likely that the formation of the BAT mRNP complex occurs post-delivery of the aminoacyl-tRNA to the ribosome. The ability of the BAT mRNP complex to inhibit eEF1A1-dependent elongation suggests that the 3'-UTR is interacting with the 5'-UTR in a circularized model to facilitate its proximity to the 80S ribosome. It has been suggested that translatable mRNAs are likely to be found in circular forms due to interaction between PABP, eIF4G, and the cap binding protein eIF4E (Wells et al., 1998). In addition, numerous studies have demonstrated the importance of mRNA circularization in translational regulation, most notably during expression of ceruloplasmin in the GAIT-mediated translational regulatory system (Mazumder et al., 2003). While such a circularized model remains to be firmly established, our preliminary data is suggestive of such a scenario in that the poly(A) tail is required for efficient translational silencing (Figure 2.7).

Modulation of the BAT complex alters *in vitro* migratory and invasive capacity and *in vivo* tumorigenesis and metastasis.

Since acquisition of the mesenchymal state is associated with changes in the proliferative, invasive, and migratory properties of cells, we investigated these phenotypes using a combination of *in vitro* assays. In proliferation assays, SH14 cells resulted in a 2X-fold increase in the proliferative index compared to the

parental or derivative clones of NMuMG cells (Figure 2.8 A). In TGFβ-mediated wound healing migration assays, SH14 cells resulted in complete wound closure in 24 h, even in the absence of TGFβ, suggestive of an inherent migratory capacity (Figure 2.8 B). In NMuMG and KIWT6 cells, wound closure was observed only following a 24 h TGFβ treatment, whereas in E23 and KIM2 cells, wound closure was not observed even in the presence of TGFβ, suggesting that they were deficient in migratory capacity (Figure 2.8 B). In trans-well *in vitro* invasion assays, SH14 cells were invasive even in the absence of TGFβ, whereas the NMuMG and KIWT6 cells showed invasiveness only when TGFβ was added to the lower chamber (Figure 2.8 C). In this assay, E23 and KIM2 cells failed to invade the basement membrane under all conditions. To assess anchorage-independent growth, we performed soft-agar colony-formation assays (Figure 2.8 D). Only the SH14 cells formed colonies in the absence of TGFβ, whereas NMuMG and KIWT6 cells formed colonies only in the presence of TGFβ.

Anchorage-independent growth in soft agar is often predictive of tumorigenicity *in vivo*; we therefore inoculated NMuMG cells and hnRNP E1-modulated derivatives subcutaneously into 6-week old athymic nude mice and compared rates of tumor growth. The SH14 allograft induced large, slowly growing tumors (n=5) with a mean volume of 198 ± 16 mm^3, while NMuMG, E23, KIWT6 and KIM2 cells only formed small, rapidly regressing nodules (Figure 2.8 E & Figure 2.9 A) at 96 days post-inoculation. SH14 cells formed tumors in >75%

of inoculations and these tumors reached a mean volume nearly 10X-fold that of the KIWT6 allograft at 96 days post-inoculation ($p<0.05$) (Figure 2.9B).

Hematoxylin and eosin (H&E) staining revealed that tumors produced by the SH14 cells were characterized by accelerated growth, decreased differentiation, and acquisition of a spindle phenotype in comparison to the slow growing, well differentiated and regressing nodules formed by NMuMG cells (Figure 2.9 C, top panel). Immunohistochemical (IHC) staining of tumor sections revealed an overall pattern suggestive of an *in vivo* EMT in SH14 injected mice, including increased vimentin and ILEI staining, and loss of E-cadherin (Figure 2.9 C, bottom three panels). IB analysis of SH14 cells and cultured tumor cells from SH14 injected mice displayed increased vimentin and ILEI expression and decreased E-cadherin and hnRNP E1 expression as compared to parental NMuMG cells (Figure 2.9 D).

We investigated whether modulating hnRNP E1 levels can directly dictate *in vivo* metastasis, distinct from effects on tumor initiation. We used the tumorigenic but non-invasive human breast cancer cell line MCF7 (Micalizzi et al., 2009), and generated a stable shRNA-mediated hnRNP E1 knockdown (MCF7 E1-/-) derivative. The MCF7 E1-/- cells displayed increased expression of ILEI and the EMT marker vimentin compared to the parental MCF7 cells (Figure 2.10 A). The parental MCF7 and NMuMG cells, as well as their hnRNP E1 knockout derivatives, SH14 and MCF7 E1-/-, were stably transfected with a constitutively expressed luciferase construct (Figure 2.10 B); injected intravenously (tail vein) into nude mice (1 x 10^5 cells/injection) and analyzed for

metastasis following 30 days. As detected by *in vivo* bioluminescence imaging (Figure 2.10 C), no metastases were observed in nude mice injected with parental MCF7 or NMuMG cells, whereas metastases were observed in mice injected with MCF7 E1$^{-/-}$ or SH14 cells (Figure 2.10 C). *Ex vivo* bioluminescence imaging (Figure 2.10 D) detected metastatic lesions in lungs of mice injected with MCF7 E1-/- or SH14 cells, whereas no lesions where detected in mice injected with the parental lines (Figure 2.10 D). Together, these results suggest that shRNA-mediated silencing of hnRNP E1 alters *in vivo* EMT and enables distant organ colonization.
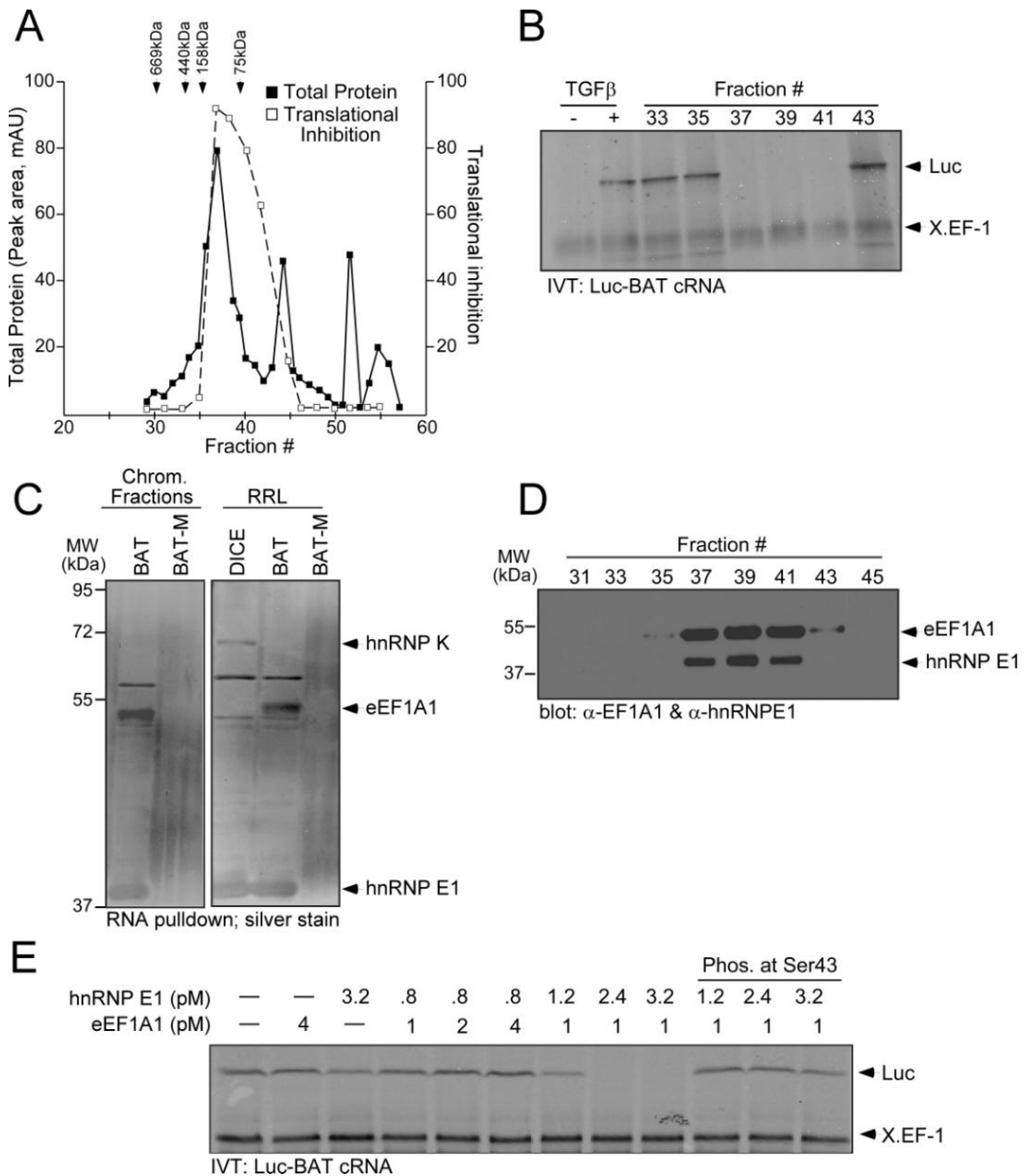
Figure 2.1: eEF1A1 and hnRNP E1 are integral and functional components of the mRNP complex. (A & B) Purification of the mRNP complex binding to the BAT element by size exclusion chromatography of S100 cytosolic extract prepared from non-stimulated NMuMG cells followed by IVT assay for translation inhibitory activity of Luc-BAT cRNA. Protein content of chromatographic fractions was quantitated at 280 nm (■) and compared to protein standards; translation inhibition was quantitated by NIH ImageJ software and compared to inhibitory capacity of unfractionated, control S100 extract (□). (C) Silver stain of RNA pull down from chromatographic fractions (left panel) or rabbit reticulocyte lysates RRL (right panel) with WT BAT or BAT-M (D) IB analysis of chromatographic fractions with α-eEF1A1 and α-hnRNP E1 antibody. (E) IVT analysis was performed using Luc-BAT cRNA and *X. EF-1* mRNA as a control.

25
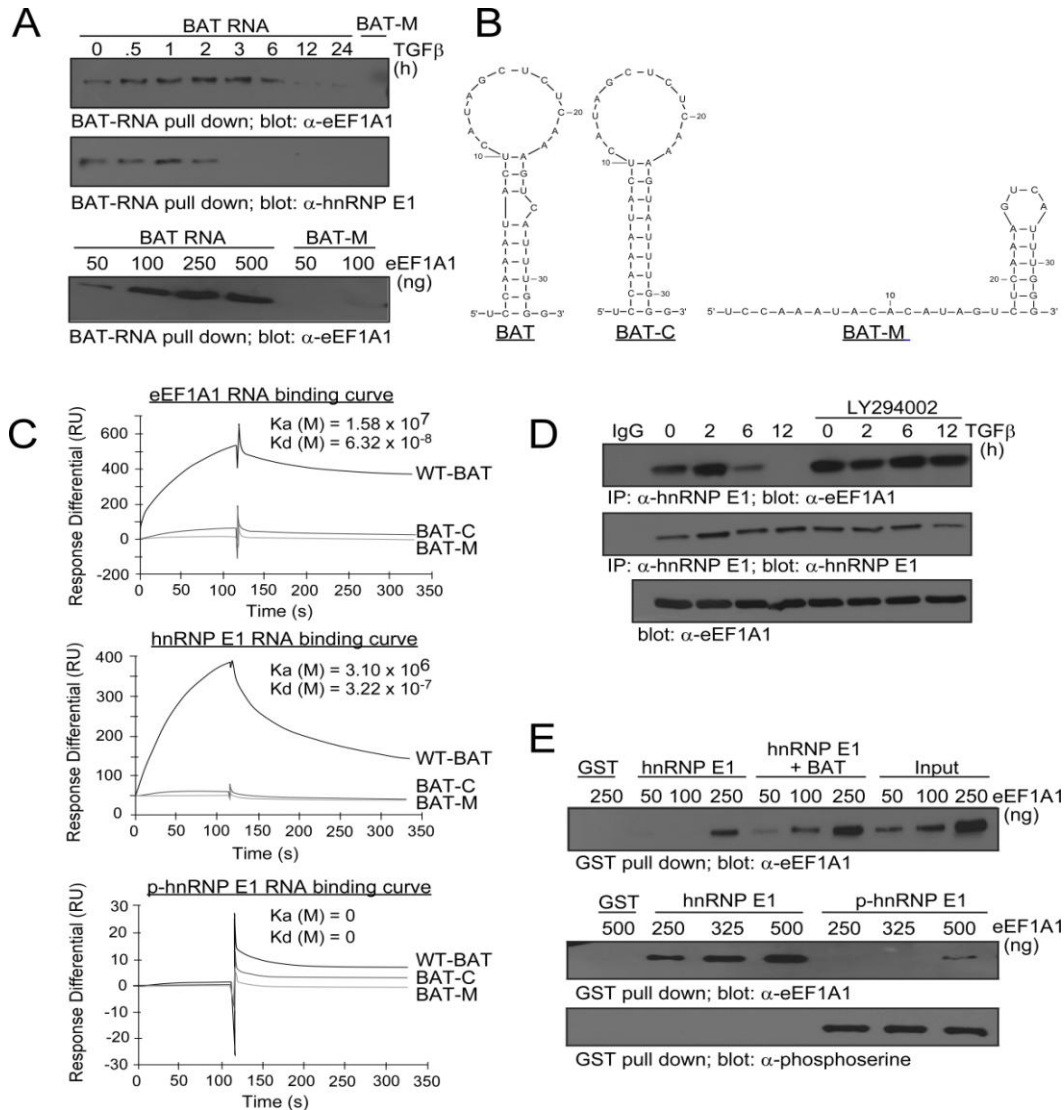
Figure 2.2: eEF1A1 interacts with hnRNP E1 and the BAT element *in vitro* and *in vivo.* (A) BAT RNA pull down from NMuMG cell lysates treated ± TGFβ (top panels), or from purified eEF1A1 added at indicated concentrations (bottom panel) was separated by SDS-PAGE and analyzed by IB with α-eEF1A1 or α-hnRNP E1 antibodies (B) Secondary structures of WT BAT, BAT-C and the BAT-M element as predicted by the Mfold algorithm. (C) Binding of eEF1A1, hnRNP E1, or p-hnRNP E1 to the BAT element was determined by SPR and expressed as resonance units (RU). Sensograms of 500 nM protein binding to WT BAT, BAT-M and BAT-C elements are overlayed. (D) Lysates prepared from NMuMG cells treated ± TGFβ for the times indicated in the presence or absence of LY294002 were immunoprecipitated with α-hnRNP E1 antibodies followed by IB analysis with α-eEF1A1 (top panel) or α-hnRNP E1 (middle panel). IB analysis with α-eEF1A1 antibody of whole cell lysate used in the co-immunoprecipitation analysis (bottom panel). (E) GST pull down followed by IB analyses with α-eEF1A1 antibody of GST-hnRNP E1 (0.5 µg) or GST-hnRNP E1 + BAT cRNA (100 ng) incubated with increasing concentrations of purified eEF1A1 (top panel). GST pull down followed by IB analyses with α-eEF1A1 or α-phosphoserine antibody of GST-hnRNP E1 (0.5 µg) or *in vitro* Akt2-phosphorylated GST-hnRNP E1 (0.5 µg) with increasing concentration of purified eEF1A1 (lower panels).
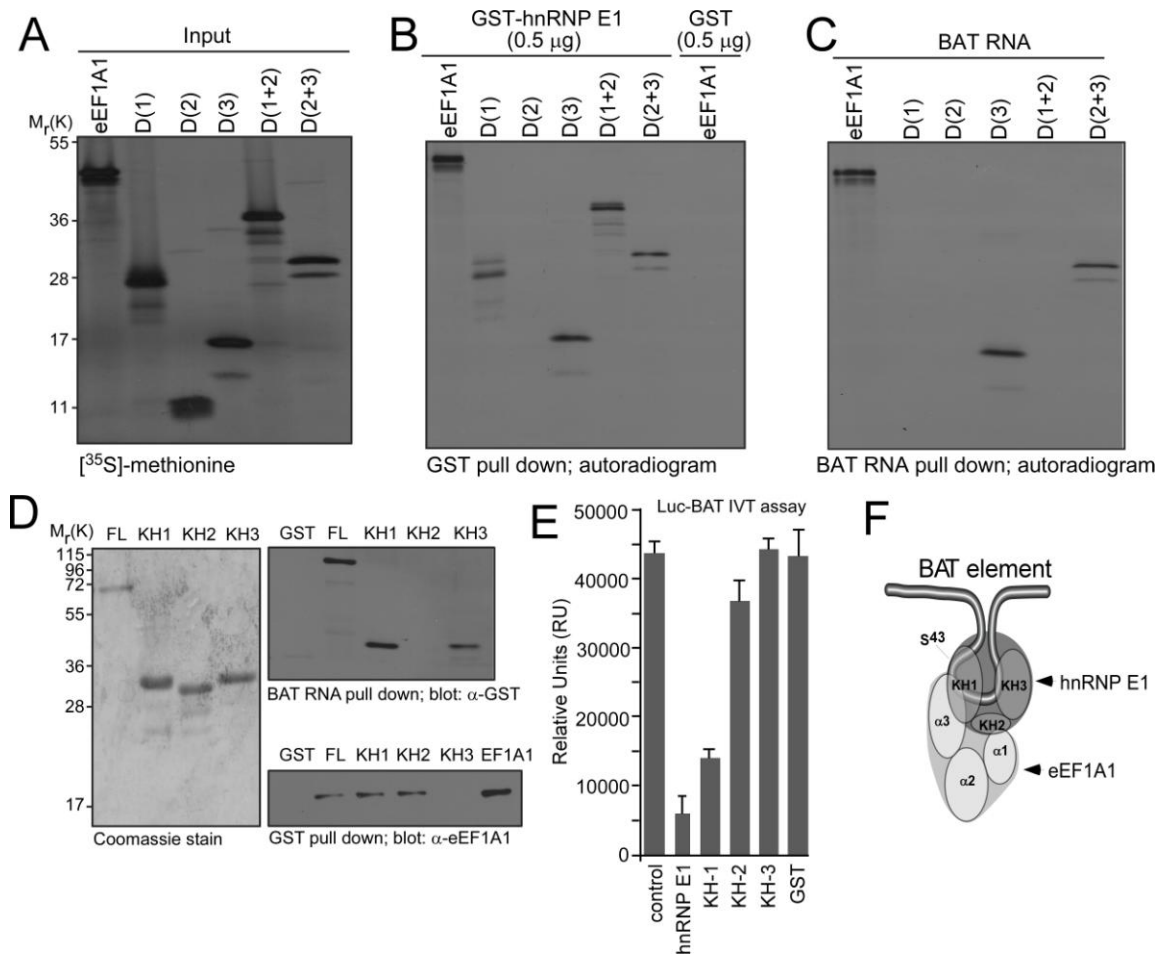
Figure 2.3: eEF1A1 and hnRNP E1 interact with each other and with the BAT element (A) Mammalian expression versions of FL-eEF1A1, and eEF1A1 domain constructs eEF1A1-D1 (amino acids 1-239), eEF1A1-D2 (amino acids 240-328), eEF1A1-D3 (amino acids 329-462), eEF1A1-D(1+2)(amino acids 1-328), and eEF1A1-D(2+3)(amino acids 240-462) were labeled in vitro with [^{35}S]-methionine, resolved by SDS-PAGE and analyzed by autoradiogram. (B, C) GST and RNA affinity pull down of [^{35}S]-methionine labeled eEF1A1 and key domain constructs. Interactions were resolved by SDS-PAGE and analyzed by autoradiogram. RNA affinity pull down (left panels) and GST pull down (right panels) using (D) Recombinant FL and key KH domains of hnRNP E1 expressed as a GST fusion protein, resolved by SDS-PAGE and analyzed by coomassie stain. RNA affinity and GST pull down assay (d, right panels) of full length hnRNP E1 and key KH domains. Interactions were analyzed by immunoblotting using a-EF1A1 and a-GST. (E) In vitro luciferase assay. Capped and poly(A)-tailed template RNAs were translated in RRL (Promega). Purified eEF1A1 (1pM), or recombinant GST-hnRNP E1 (3 pM), or GST-KH domains 1-3 (3 pM) were added and pre-incubated with the RNAs before addition of the translation system. Recombinant GST (3 pM) was used as a control. Luciferase expression was detected by luminescence. Data are presented as means ± s.e.m. for n=3 sample per group. (F) Model of the protein-protein, protein-RNA interactions of eEF1A1, hnRNP E1 and the BAT element.
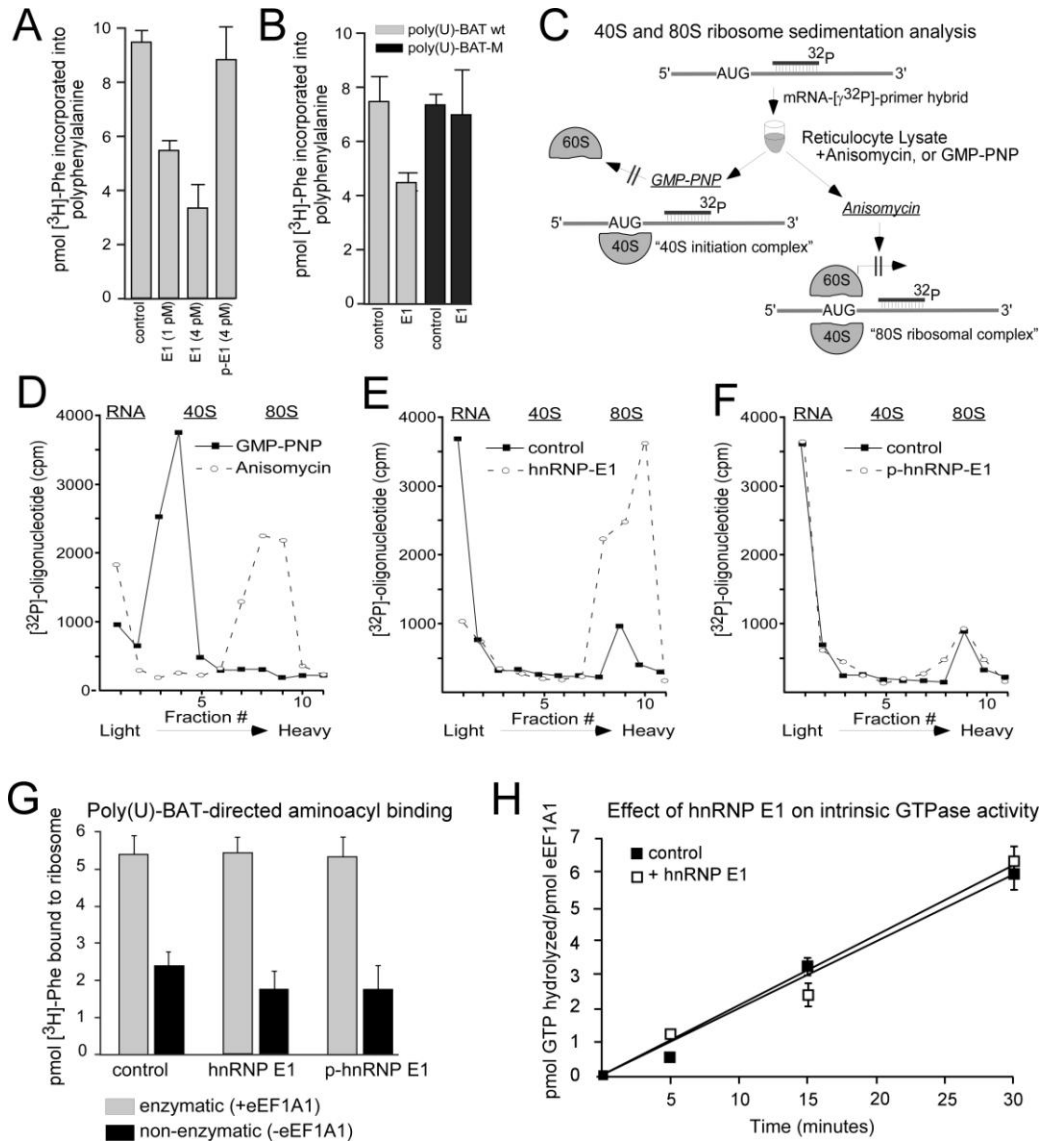
Figure 2.4: hnRNP E1 and eEF1A1 inhibit translation at the elongation stage of protein biosynthesis. (A) Translation of poly(U)-BAT mRNA was performed using RRL devoid of added cold amino acids and supplemented with 5 mM MgCl2 and [^{3}H]-phenylalanine, 1 pM eEF1A1, and hnRNP E1 where indicated. The activity was measured as [^{3}H]-phenylalanine incorporation as a function of counts per minute (cpm). Data are presented as means ± s.d., *n*=3. (B) Translation of wild type (wt) versus mutant (M) poly(U)-BAT mRNA. Data are presented as means ± s.d., *n*=3. (C) A schematic depicting the experimental procedure of 40S and 80S ribosome sedimentation analysis. (D, E, F) Ribosome sedimentation analyses. The efficiency of formation of the 40S and 80S ribosomal complexes was monitored via liquid scintillation spectroscopy. The position of sedimentation of free RNA, 40S ribosomal subunits, and 80S ribosomes are marked at the top of each figure. Graph of scintillation counts versus sucrose gradient fraction number is represented for reactions in the presence of GMP-PNP, or anisomycin-treated lysates (E); or for reaction reactions in the absence (control) or presence of hnRNP E1 (E); and for reactions in the presence of p-hnRNP E1 (F). (G) Aminoacyl binding assays. Activities ± eEF1A1 are denoted as enzymatic and non-enzymatic, respectively. Data are presented as means ± s.d., *n*=3. (H) GTPase assay measuring effect of hnRNP E1 on intrinsic eEF1A1 GTPase activity. Data are presented as means ± s.d., *n*=3.

28
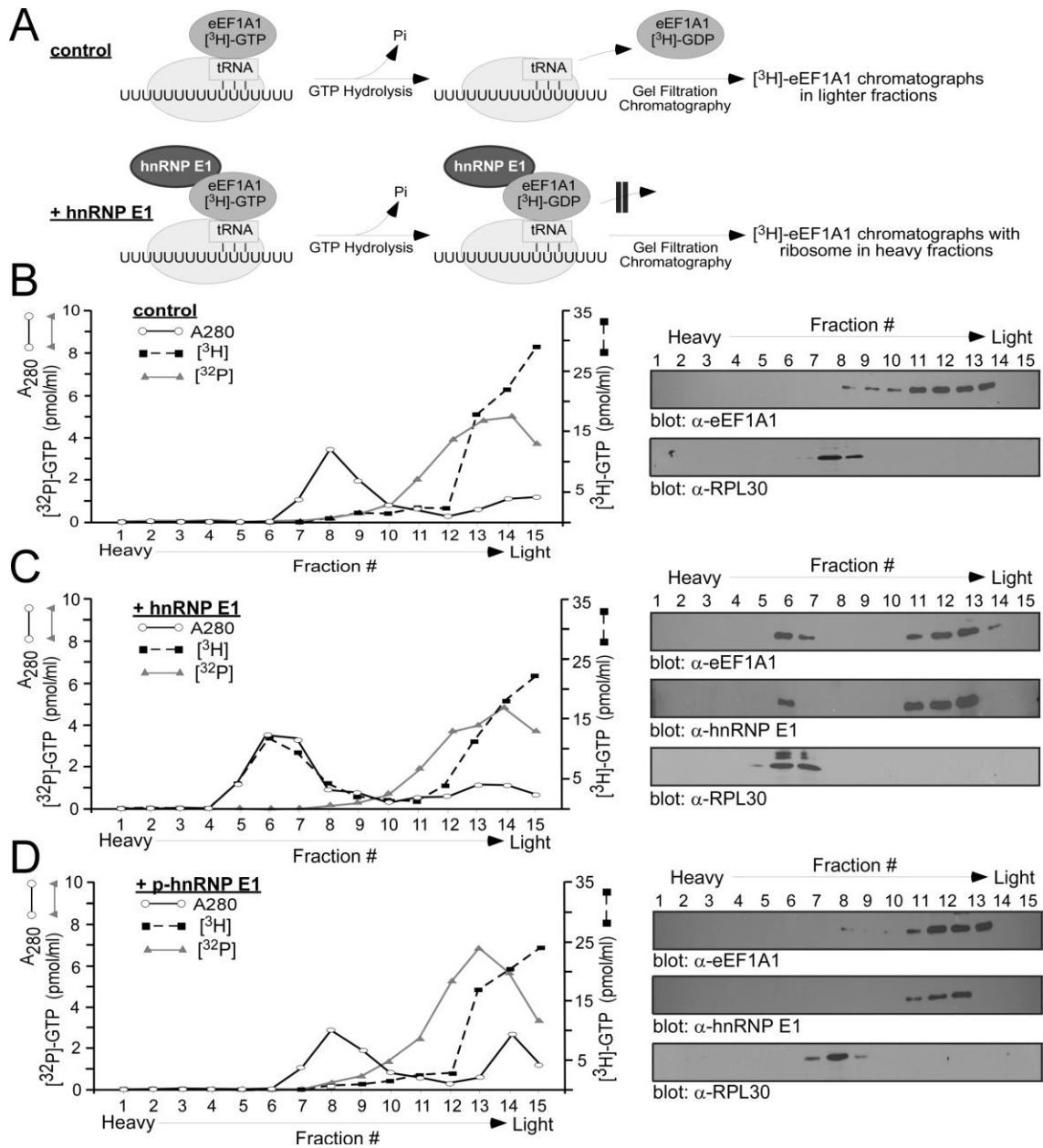
Figure 2.5: hnRNP E1 prevents the release of eEF1A1 from the ribosome. (A) Schematic depicting the binding of eEF1A1 to the 80S ribosome, GTP hydrolysis and subsequent release or arrest of eEF1A1 on the ribosome in the absence (control) or presence of hnRNP E1. A ternary complex of Phe-tRNA[Phe]-eEF1A1-[3H]-GTP was incubated with 80S ribosomes and poly(U)-BAT in the absence (B) or presence (C) of hnRNP E1, and the resultant reaction mix analyzed by gel filtration chromatography assay. p-hnRNP E1 was used as a control (D). Aliquots of each fraction were used to determine absorbance at 280 nm (○) and for detection of [3H] (■), or [32P] radioactivity (Δ). IB analyses of fractions were performed with antibodies against eEF1A1, ribosomal protein L30 (RPL30), or hnRNP E1.
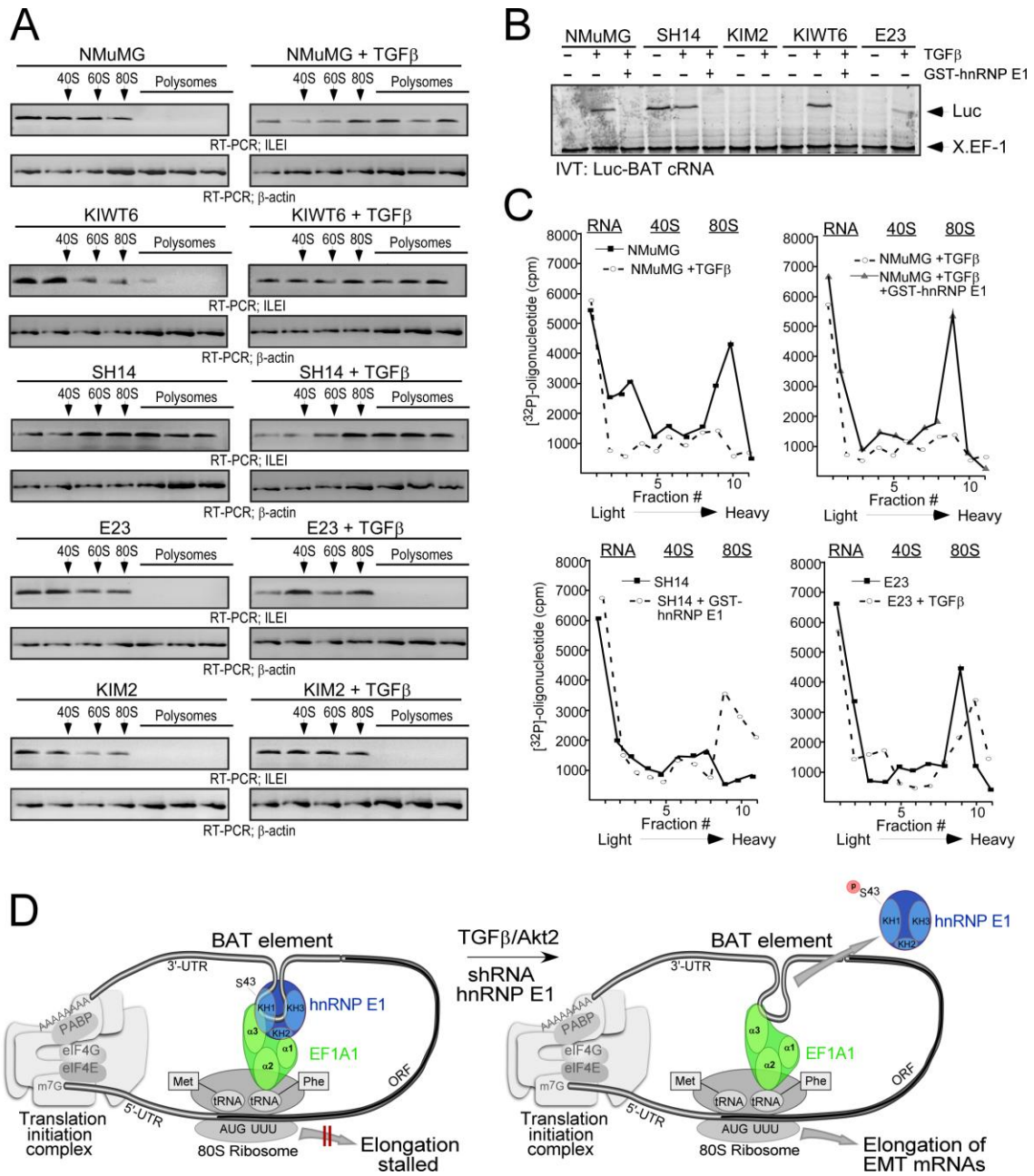
Figure 2.6: hnRNP E1 expression levels control inhibition of translation elongation *in vivo*. (A) Polysome profiling of parental and derivative NMuMG cells treated ± TGFβ. Translocation of *ILEI* mRNA from the non-polysomal pool to the polysomal pool was analyzed by semiquantitative RT–PCR. (B) In *vitro* translation (IVT) assay for inhibitory activity of Luc-BAT cRNA. Cell lysates (5 μg) were supplemented with FL-hnRNP E1 (0.5 μg) where indicated, and pre-incubated with the RNAs before addition of the translation system. *X.EF-1* cRNA was used as an internal control. (C) Ribosome sedimentation analyses. Graph of scintillation counts versus sucrose gradient fraction number for reactions containing lysates from NMuMG, SH14, and E23 cells treated ± TGFβ, and supplemented with FL-hnRNP E1 (0.5 μg) as indicated. (D) Model depicting the BAT regulatory mechanism (described in text).
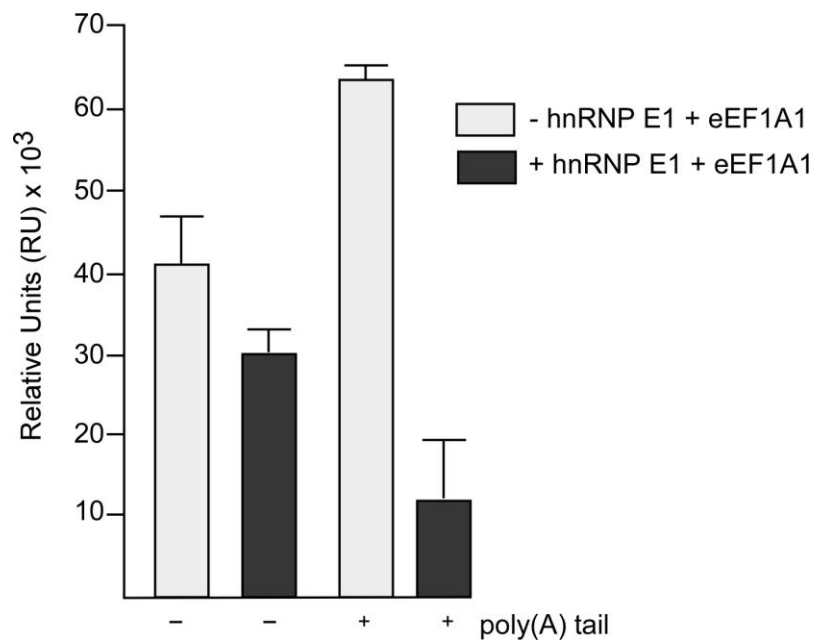
Figure 2.7: Poly(A) tail is required for efficient BAT-mediated translational silencing. *In vitro* luciferase assay. 5'-capped and -/+ poly(A)-tailed Luc-BAT cRNAs were generated using the mMessage mMachine transcription kit. The synthetic RNAs were translated in RRL. eEF1A1 (1 pM) and GST-hnRNP E1 (2 pM) were added as indicated and pre-incubated with the RNAs before addition of the translation system. 10 μl aliquots were used to detect luciferase expression by luminescence. Data are presented as means ± s.e.m., n=3.
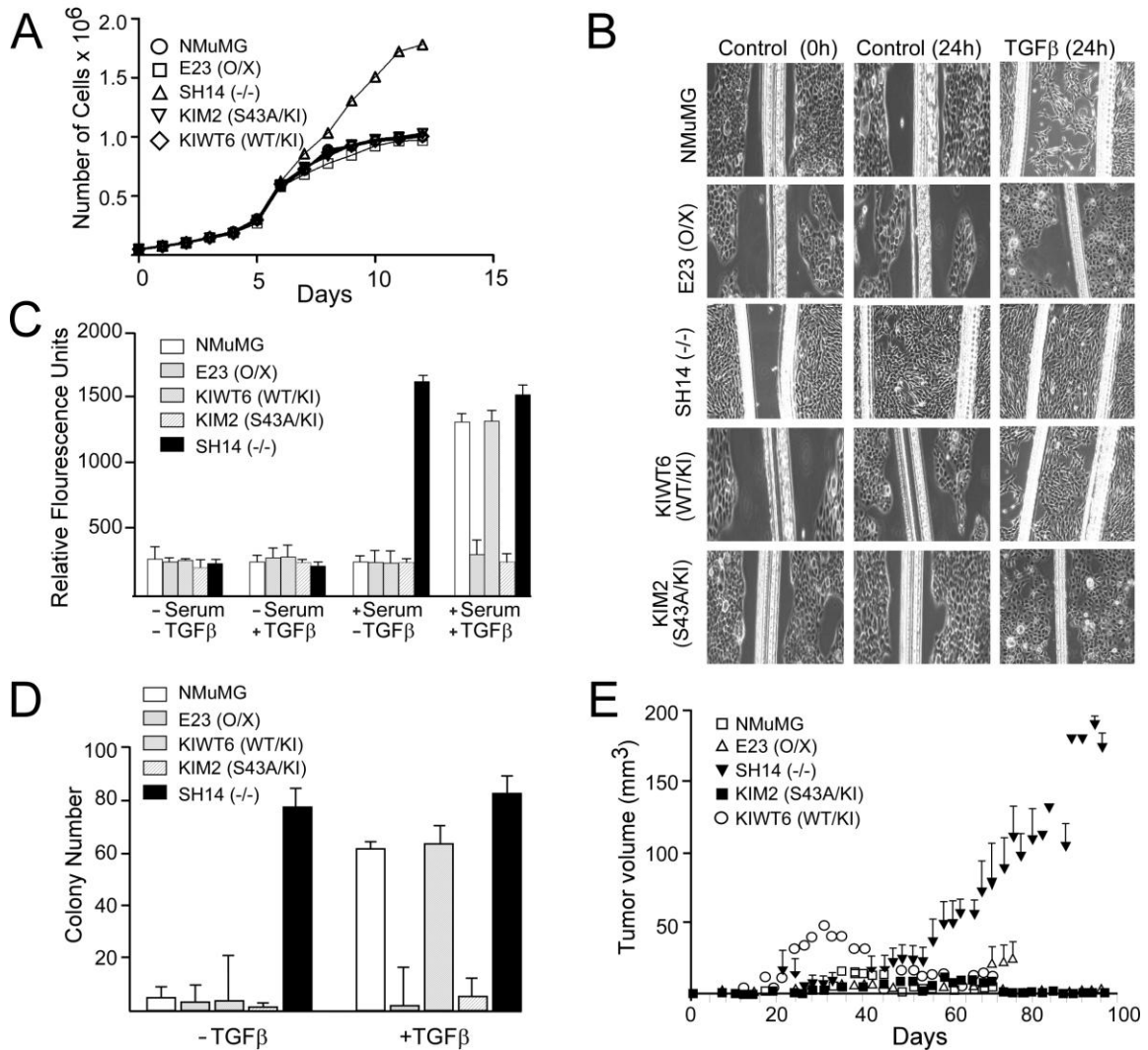
Figure 2.8: hnRNP E1 expression levels control *in vitro* migratory and invasive capacity, and *in vivo* tumorigenecity. (A) Cell proliferation assay. Cells (1 x 10^5 /well) of a particular cell type were plated in a 6-well tissue culture plates, trypsinized and counted through a hemocytometer chamber up to 12 days following initial seeding. Data is represented as means ± s.e.m. of 3 independent experiments. (B) Wound healing assay. Cell monolayers were wounded with a plastic tip after 24 h of seeding and images obtained using a phase-contrast microscope at 5X magnification. Cells were incubated ± TGFβ for 24 h at 37°C before being photographed again at 5X magnification. (C) Cell invasion assay. Cells (2 x 10^5) were added to the membrane chamber -/+ serum and TGFβ in the feeder tray. Cell invasion was assayed fluorimetrically at 480 nm/520 nm per manufacturer's instructions. Data is represented as means ± s.e.m. of 3 independent experiments. (D) Anchorage-independent growth assay. Cells (1 x 10^4) were suspended in 2 ml of 0.4% soft-agar in DMEM containing 10% FBS and were overlaid on 2 ml of 0.8% soft agar in 35 mm diameter dishes. Colonies were visualized under an inverted light microscope after 3 weeks. (E) Subcutaneous inoculation of 1 x 10^5 cells in the hind flank (each side) of six week old BalbC athymic nude mice (nu/nu). Tumor volume was determined 3 times a week with a vernier caliper. Five animals were used for each cell type. Data is represented as mean ± s.e.m. (n=5).
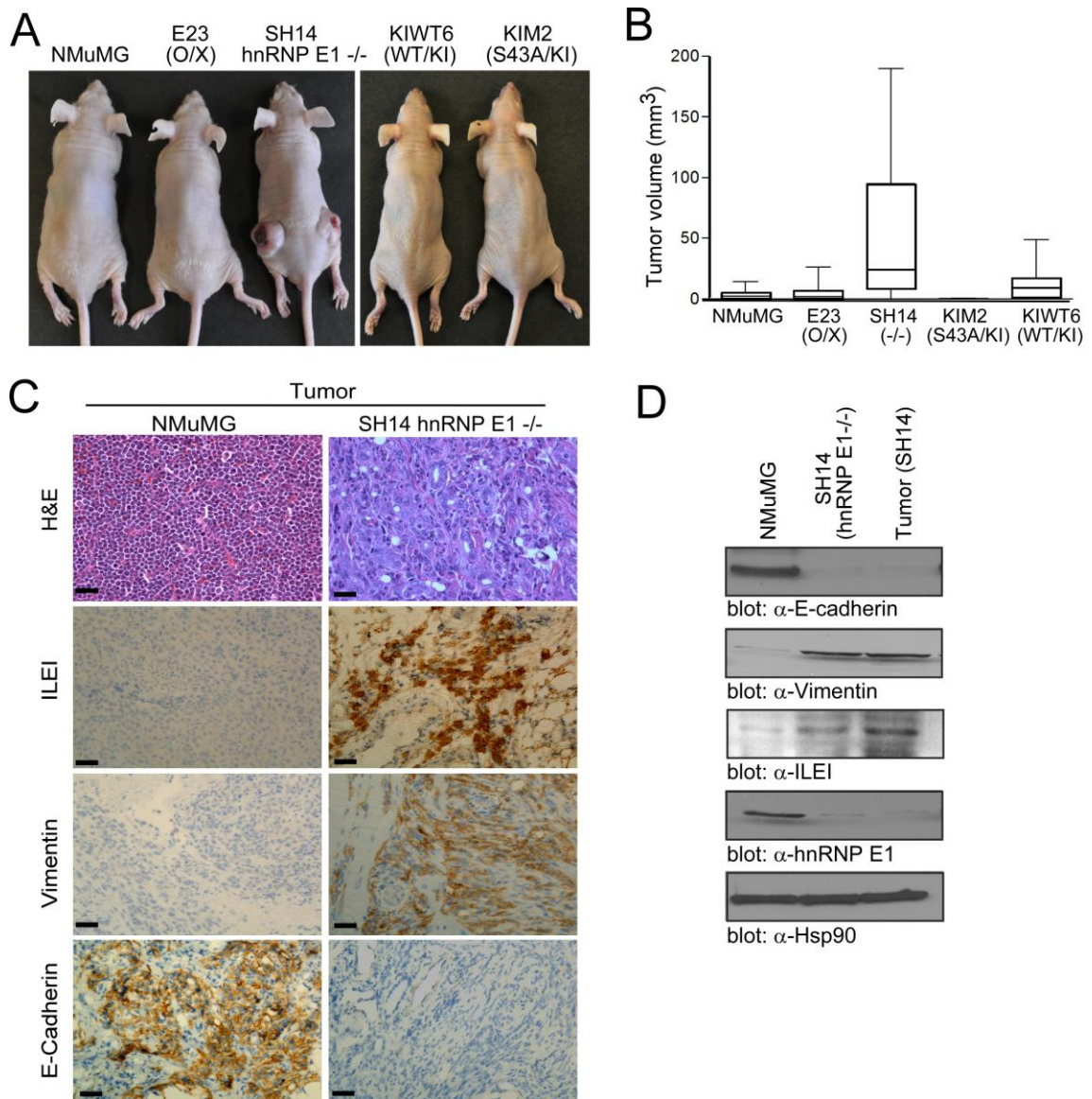
Figure 2.9: hnRNP E1 expression levels alter *in vivo* tumorigenicity (A) Subcutaneous inoculation of 1 x 10^5 cells in hind flanks of 6-week old BalbC athymic nude mice (*nu/nu*) was performed. Images were taken 96 d post-injection. (B) Tumor volume (mm^3) was evaluated as Box-and-Whisker plot to analyze differences between median tumor volumes among the various cells used for inoculation. Data are presented as means ± s.e.m (*P*< 0.05) for n=5 samples per group. (C) H&E staining of excised tumors was performed according to standard protocols. IHC of paraffin sections from excised tumors was performed with α-E-Cadherin; α-Vimentin; and α-ILEI. The stain was observed with a 40X objective lens. (D) IB analysis of NMuMG, SH14 and cultured tumor cells from SH14 injected mice using α-E-Cadherin, α-Vimentin, α-ILEI, α-hnRNP E1, and α-Hsp90 antibodies.

33
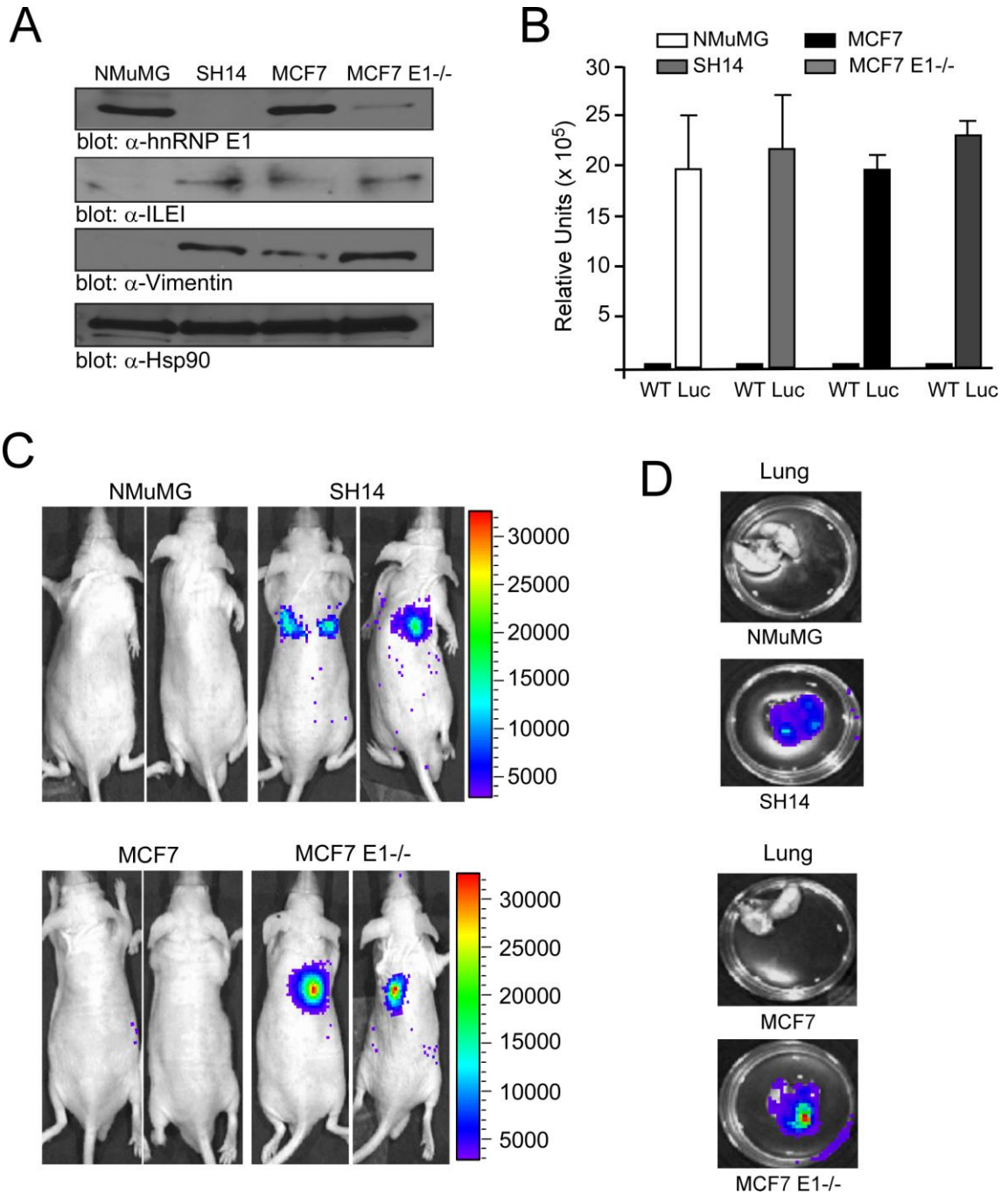
Figure 2.10: shRNA-mediated silencing of hnRNP E1 enables distant organ colonization.
(A) IB analysis of NMuMG, SH14, MCF7, and MCF7 E1-/- cells using α-hnRNP E1, α-Vimentin, α-ILEI and α-Hsp90 antibodies. (B) *In vitro* luciferase expression in NMuMG, MCF7, SH14 and MCF7 E1-/- cells stably transfected with the CMV firefly luciferase (Luc) construct compared to the wild-type (WT) non-transfected cells. Data are presented as means ± s.d. (*n*=3). (C) *In vivo* bioluminescent imaging of nude mice 30 d post intravenous injection. The luminescence signal is represented by the overlaid false-color image. (D) *Ex vivo* bioluminescence imaging. Excised lungs were imaged in a 35mm culture dish.

2.4 Discussion

In the present study, we provide evidence for a regulatory mechanism in which hnRNP E1 and eEF1A1 coordinate transcript-specific repression of genes required for EMT. The canonical function of eEF1A1 is to facilitate binding of aminoacyl-tRNA to the ribosomal A site in the form of a ternary complex, eEF1A1-GTP-aminoacyl-tRNA (Negrutskii and El'skaya, 1998). Codon-anticodon recognition is followed by GTP hydrolysis on eEF1A1, with subsequent release of eEF1A1-GDP from the ribosome. Our data suggests that interaction between eEF1A1 and hnRNP E1 inhibits eEF1A1 release following hydrolysis of GTP, so that eEF1A1-GDP remains on the ribosome, thereby preventing the subsequent translocation of the aminoacyl-tRNA to the peptidyl moiety of the growing peptide chain. The ribosome is thus stalled at the eEF1A1-dependent elongation stage, resulting in translational silencing. The interaction between eEF1A1 and hnRNP E1 is largely mediated by their independent BAT element binding capacity, thus allowing for a transcript-specific translational silencing activity in mRNAs which harbor a 33-nt BAT element in their 3'-UTR. The transcript-specific restriction of the BAT element is conferred by its structural fidelity rather than a conserved sequence homology, as is evident by the fact that *Dab2* and *ILEI* mRNA differ in the nucleotide sequence of their respective BAT elements (Chaudhury et al., 2010). Furthermore, the binding affinity of both hnRNP E1 and eEF1A1 is impaired by mutations which alter the structure of the BAT element.

Insight into the structure-function relationships of eEF1A1 and hnRNP E1 may aid in providing an understanding of how hnRNP E1 prevents release of eEF1A1 from the ribosome. Similar to other GTP-binding proteins, eEF1A1

35

undergoes structural changes following hydrolysis. It has been shown that upon GTP hydrolysis, domains 2 and 3 of eEF1A1 rotate as a rigid body with respect to domain 1, thus resulting in a GTP-mediated conformational change (Berchtold et al., 1993). *In vitro* binding studies demonstrated that hnRNP E1 is capable of binding to eEF1A1 via its domains 1 and 3. Possibly, hnRNP E1 binding may be affecting the interface of domain 1-3 in eEF1A1, thereby preventing the post-GTP hydrolysis conformation change necessary for eEF1A1 release. It has also been proposed that isoform-specific functions of elongation factor 1-alpha play an important role in cancer (Edmonds et al., 1996), and while the eEF1A1 isoform was used in the present study, we cannot rule out a potential role for eEF1A2 in BAT-mediated translational silencing.

While translational regulation, through 5' and 3'-UTR regulatory elements, has most often been demonstrated to modulate the initiation stage, several reports suggest that control may occur at the post-initiation level. For example, the translational repression of *nanos* mRNA in *Drosophila* embryos has been shown to be mediated by *nanos* 3'-UTR sequences, resulting in an altered polyribosome profile, indicating a block after initiation of translation (Clark et al., 2000). Additionally, during *C. elegans* larval development, repression of *lin-14* mRNA has been shown to be directed by a small *lin-4* RNA which binds the 3'-UTR of *lin-14 mRNA* and mediates translational repression at a post-initiation stage of translation (Olsen and Ambrose, 1999). Alternatively, in cell-free translation assays, it has been demonstrated that phosphorylation of eukaryotic elongation factor-1B, a guanine nucleotide exchange factor for eEF1A1, by

CDK1/cyclin B, results in decreased elongation rates (Monnier et al., 2001). While these examples are suggestive of regulation at an event post- initiation, our identification of regulation being mediated at the elongation stage, precisely through modulation of eEF1A1 function, provide a mechanistic demonstration of such a translation control mechanism.

The biological implications of the BAT-mediated translational silencing mechanism are profound. Both *in vitro* and in mice, knockdown of hnRNP E1 in NMuMG caused these otherwise normal, non-invasive epithelial cells to display an inherent tumorigenic and metastatic capacity. In allograftic tumor studies, SH14 cells readily formed large, slowly growing tumors. In contrast, the parental cells formed tiny, regressing nodules consisting of normal epithelial cells as evidenced by strong E-cadherin expression in tumor tissue sections. Downregulation of E-cadherin expression in SH14-derived tumors, as well as upregulation of the EMT marker vimentin and strong expression of ILEI, corroborate our morphological analysis and substantiate the findings that ILEI is necessary for tumor formation (Waerner et al., 2006). In addition, knockdown of hnRNP E1 in the human breast cancer line MCF7 caused these cells to acquire EMT markers and to form lung metastases when injected intravenously. While these results support a direct role for hnRNP E1 in EMT and metastasis, further studies are needed to address earlier steps of metastasis such as invasion and intravasation.

While the process of EMT in development and cancer progression has been shown to encompass a wide continuum of alterations in epithelial plasticity

in response to numerous signaling pathways, an important finding of this study is that a single factor, hnRNP E1, is responsible for silencing a TGFβ-mediated EMT program normally functional during embryonic development. Whereas Dab2 and ILEI protein expression is directly regulated by the BAT-mediated translational silencing mechanism, our data suggests that the combined expression of Dab2 and ILEI alone is not sufficient for mediating EMT (Chaudhury et al., 2010). Rather, we postulate that the BAT regulatory mechanism operates upstream of key cellular pathways contributing to metastatic progression and tumor development.

An understanding of the molecular mediators that control epithelial plasticity may aid in elucidating the downstream cellular pathways that are affected by activation of silenced EMT-transcripts. A key step in EMT is disintegration of adherens junctions associated with redistribution and repression of the E-cadherin. (Thiery and Sleeman, 2006). Snail-related zinc-finger transcriptional repressors (Snail and Slug), as well as bHLH transcription factors Twist and E12/E47, are the most prominent suppressors of E-cadherin transcription (Zavadil and Bottinger, 2005). Interestingly, a recent report has demonstrated that translational regulation mediated by Y-box binding protein-1 (YB-1) is upstream of, and regulates the expression of transcription factors implicated in repression of E-cadherin (Evdokimova et al., 2009). Enhanced expression of YB-1 was shown to promote EMT and the metastatic potential of normal breast epithelial cells by activating cap-independent translation of Snail1. Similarly, our findings that shRNA-mediated knockdown of hnRNP E1 results in

38

downregulation of E-cadherin and EMT, irrespective of TGFβ-treatment, may be indicative of activated downstream EMT transcriptional programs leading to downregulation of epithelial-related genes and activation of mesenchymal genes. Numerous studies have shown that secretion of TGFβ by tumor cell-stimulated autocrine loops and loss of sensitivity to the antiproliferative effects of TGFβ are classical hallmarks during metastatic progression of tumors (Bierie and Moses, 2006). Additionally, activation of the PI3K/Akt pathway, as well as increased expression of Akt2 have both been shown to lead to EMT and increased cell invasiveness in tumor cells (Irie et al., 2005; Gershtein et al., 1999). Attenuation of the BAT mRNP complex *via* TGFβ/Akt2-mediated phosphorylation of hnRNP E1 may therefore represent a downstream target of cytokine-mediated activation of EMT during tumorigenesis and metastatic progression. Although our findings suggest that the proposed translational regulatory mechanism is functionally significant in the metastatic progression of tumors, further studies are needed to determine whether this pathway is deregulated in cancer cells and tissues. Given the necessity of hnRNP E1 in the BAT mRNP complex we speculate that expression levels and/or phosphorylation status of p-Akt2 and hnRNP E1, as well as the expression of *Dab2* and *ILEI* may be directly correlative with metastatic progression of tumors.

2.5 Materials and Methods

Reagents: Mouse α-hnRNP E1 (1:3000) and α-RPL30 (1:5000) antibodies were obtained from Novus Biologicals. Rabbit α-hnRNP E1 (1:3000) was from Lifespan Biosciences. α-ILEI was obtained from Abcam. α-phosphoserine (clone PSR-45; 1:1000) antibody was obtained from Sigma-Aldrich and α-eEF1A1 (1:3000) from US Biologicals. α-GST (#2622, 1:2000), α-Vimentin and recombinant Akt2 kinase were purchased from Cell Signaling Technology. α-E-Cadherin was purchased from BD Biosciences. α-Hsp90 (H-114, 1:5000), and normal mouse and rabbit IgG were purchased from Santa Cruz Biotechnology. Secondary antibodies, α-mouse and α-rabbit-IgG-HRP were obtained from GE Healthcare Bio-Sciences. Rabbit reticulocyte lysate and RiboMAX Large Scale RNA Production kit were purchased from Promega. MAXIscript and mMESSAGE mMACHINE T7 Ultra kits were purchased from Ambion. Primers and oligonucleoties were purchased from Integrated DNA Technologies. Translation grade [^{35}S]-methionine, [γ-^{32}P]-ATP and [γ-^{32}P]-GTP were purchased from Perkin Elmer Life Sciences. [^{3}H]-phenylalanine and [8-^{3}H]-GTP was purchased from American Radiolabeled Chemicals, Inc. LY294002 was obtained from Alexis-Biochemicals.

Cell culture and treatments: TGFβ2 was a generous gift from Genzyme Inc. and was used at a final concentration of 5 ng/ml. NMuMG and MCF7 cells, and all derivatives, were maintained in Dulbecco's modified Eagle's medium supplemented with 10% fetal bovine serum, 10 μg/ml insulin, and antibiotics/antimycotics (100 units/ml penicillin G, 100 mg/ml streptomycin,

40

and 0.25 μg/ml amphotericin B). Where indicated, cells were treated with 10 μM of LY294002 30 min before TGFβ treatment. SH14, E23, KIM2, and KIWT6 cells lines were generated in the laboratory and have been previously described (Chaudhury et al., 2010).

Plasmids construction and protein expression: The 33-nt BAT, BAT-M, and BAT-C oligonucleotides were synthesized by Integrated DNA Technologies with T7 promoter sequence, and annealed to a complementary oligonucleotide containing the T7 promoter sequence in STE buffer (0.1 M NaCl, 10 mM Tris-HCl [pH, 8.0], 1 mM EDTA). The oligonucleotides were PAGE purified before annealing. The Luc-*Dab2*/BAT was generated in the laboratory and has been previously described (Chaudhury et al., 2010). For construction of the poly(U)-*Dab2*/BAT, the oligonucleotide 5'-TAATACGACTCACTATAGGG-$(TTT)_{37}$-TCCAAATACTCATAGCTCTCAAA GTCATTTGGG-3' was synthesized by Integrated DNA Technologies, and PAGE purified. The oligonucleotide was amplified by PCR using 5'-TAATACGACTCACTATAGGGTTTT-3' and 5'-CCCAAATGACTTTGAGAGCT ATG-3' forward and reverse primers respectively, separated on a 2% agarose gel, and purified using QiaQuick gel extraction kit (Qiagen). RiboMax kit (Promega) was used to generate milligram quantity of cRNA. eEF1A1 purified from human reticulocytes was maintained in #3344 buffer (100 mM KCl, 0.1 mM EDTA, 1 mM DTT, 20 mM Tris-HCl, pH 7.5, and 25% glycerol. pSilencer neo-shRNA-human hnRNP E1-3' UTR (shRNA against 3' UTR of hnRNP E1) was constructed by annealing shRNA template oligonucleotides and cloned

into pSilencer neo vector. pCMV-LL luciferase construct was generated as previously described (Chaudhury et al., 2010).

Preparation of cell lysates, immunoblot analysis, and immunoprecipitation: For immunoprecipitation and immunoblot analysis, cells were lysed in buffer D and immunoprecipitation was performed as described previously (Hocevar et al., 1999).

Preparation of cytosolic extract (S100 Fraction): S100 fractions were prepared from control and TGFβ-treated NMuMG cells as previously described (Mazumder and Fox, 1999) with minor modifications. Briefly, the buffer used for cytosolic extraction contained 20 mM Hepes (pH 7.5), 10 mM KCl, 1.5 mM MgCl2, 1 mM EGTA, 1 mM EDTA, 1 mM dithiothreitol and protease inhibitor cocktail (Hampton et al., 1998).

Size-Exclusion chromatography: Size exclusion chromatography was performed as described previously (Sampath et al., 2004). Briefly, 5 mg of control cytosolic extract from NMuMG cells were applied to a Superose-6 FPLC column and eluted at a flow rate of 0.5 ml/min. Ferritin (440 kDa), aldolase (158 kDa) and conalbumin (75 kDa) were used as molecular weight standards. Fractions were subjected to *in vitro* translation reaction using pCMVLuc-*Dab2*/BAT to assay for translation inhibitory activity.

RNA pull down: RiboMax kit (Promega) was used to generate milligram quantity of synthetic 33-nt RNA from template DNA. WT BAT and BAT-M cRNA were bound to CNBr-activated Sepharose beads and incubated with 100 μg of cytosolic extracts from NMuMG cells treated ± TGFβ for 2 h at 4 ^{0}C. Following

incubation, beads were washed with 0.2 M NaCl and resolved by SDS-PAGE. Size-exclusion fractions that displayed translational silencing activity were subjected to RNA pull down as described above. The indicated bands were excised, and peptide sequences determined by capillary liquid chromatography-electrospray mass spectrometry. The data obtained were analyzed using TurboSequest software to query the NCBI nonredundant protein database. Matching spectra was confirmed by manual interpretation using Mascot and FASTA software.

In Vitro binding studies: GST-hnRNP-E1 (0.5 μg) was immobilized onto glutathione-agarose beads (Sigma), and incubated with indicated concentrations of purified eEF1A1. The bead were then washed to remove non-specific binding, and subjected to SDS-PAGE and IB analysis. The mouse pGADT7-heEF1A1 and pGADT7 domain constructs eEF1A1-D1 (amino acids 1-239), eEF1A1-D2 (amino acids 240-328), eEF1A1-D3 (amino acids 329-462), eEF1A1-D(1+2)(amino acids 1-328), and eEF1A1-D(2+3)(amino acids 240-462) have been described previously (Mansilla et al., 2008). The constructs were used to generate [^{35}S]-methionine metabolically labeled proteins using the TNT Quick Coupled Transcription/Translation system (Promega). The GST-tagged hnRNP E1 was a gift from Dr. Kumar and has been described previously (Meng et al., 2007). The KH1-3 domain constructs of hnRNP E1 have been previously described (Sidiqi et al., 2005). The GST constructs were expressed in *E. coli,* purified by affinity chromatography using Glutathione Sepharose 4B beads (Amersham Biosciences) and eluted by 50 mM Tris (pH

7.4) containing 10 mM reduced glutathione. Recombinant GST protein was made in parallel for use in control experiments.

In Vitro luciferase assay: *In vitro* luciferase assay was performed as described previously. (Mazumder and Fox, 1999) In brief, capped and poly(A)-tailed template RNAs were generated using the mMessage mMachine transcription kit. The synthetic RNAs were translated in RRL in the presence of a methionine-free amino acid mixture and translation grade [^{35}S]-methionine. Indicated amounts of purified eEF1A1, or recombinant GST-hnRNP E1 were added and pre-incubated with the RNAs before addition of the translation system. Reactions were resolved by 10% SDS-PAGE and visualized by autoradiography.

Polysome analysis: Polysome analysis was performed as described previously (Merrick & Hensold, 2001). Briefly, cell lysates were layered onto a 10%-50% sucrose gradient and centrifuged at 100,000 x g at 4^{0}C for 4 h. Gradient fractions were collected using a fraction collector with continuous monitoring of absorbance at 254 nm. RNA was extracted with Trizol, and analyzed by semiquantitative RT-PCR.

Surface Plasmon Resonance (SPR): SPR was performed using a BIAcore 3000 optical sensor. Fifty response units (RU) of biotinylated cRNA probe were immobilized onto a streptavidin-coated sensor chip (GE Healthcare). Purifed eEF1A1 and GST-hnRNP E1 protein were diluted in HBS-P buffer [0.01 M HEPES, pH 7.4, 0.15 M NaCl, 0.0005% Surfactant P20) to a final concentration ranging from 1 to 500 nM, and injected for 120 seconds

through four flow cells (flow cell 1, blank; flow cell 2; BAT-C; flow cell 3, BAT-M; flow cell 4, WT BAT) at a flow rate of 25 μl/min. The response value of the reference cell (flow cell 1, blank) was subtracted from flow cells 2-4 to correct for nonspecific binding. Association and dissociation rates were calculated using BIAevaluation 3.0 software (BIAcore). Sensograms were transformed to align injection points.

Poly(U)-directed synthesis assay: Translation of poly(U)-BAT was performed as previously described (Monnier et al., 2001), with minor modifications. In brief, RRL devoid of cold amino acids was supplemented with 5 mM $MgCl_2$. Assays were performed with 1 μCi [^{3}H]-phenylalanine (120 Ci/mmol), 2.0 μg poly(U)-BAT cRNA, 14 μl lysate extract, 1 pmol eEF1A1, and 1-4 pmol hnRNP E1 where indicated, in a total volume of 20 μl and incubated for 1 h at 30°C. 2 μl aliquots were withdrawn from each reaction, and diluted in 1 ml decolorizing solution (0.5 N NaOH, 0.75% hydrogen peroxide). Samples were precipitated with 1 ml cold 25% TCA (w/v) and filtered through Whatman filters. Precipitated proteins were counted in scintillation fluid.

Sedimentation Analysis: Analysis using sucrose density gradients were performed as previously described (Anthony and Merrick, 1992). Briefly, Luc-BAT cRNA was hybridized to [$\gamma-^{32}$P]-ATP-end labeled 18-mer primer (5'-GCTCTCCAGCGGTTCCAT-3') complementary to a region 53-nt downstream of the initiation codon. Labeled hybrid was incubated with RRL for 10 min at 30°C in the presence or absence of 0.1 mM Anisomycin (Sigma), 1 mM GMP-PNP (Sigma), 80 pmol hnRNP E1, or 5.0 μg cytosolic extract supplemented ±

80 pmol GST-hnRNP E1 where indicated. Following incubation, the reaction was layered on 10-35% linear sucrose gradients and centrifuged for 4 h at 4°C. Gradients were fractionated (1 ml fractions) and 0.3 ml of each fraction was counted via liquid scintillation spectrometry. A graph of scintillation counts versus sucrose gradient fraction number was plotted to determine the quantity of labeled primer present at each sedimentation coefficient (S) value.

Aminoacyl Binding assay: Aminoacyl binding assays were performed as described previously (Agafonov et al., 2001) with some modifications. Briefly, 15 pmol eEF1A1 were added to 100 μl reaction mix containing 100 mM KCl, 20 mM Tris-HCl, pH 7.5, 1.0 mM GTP, 2.1 mM phosphoenolpyruvate (PEP), 0.3 U pyruvate kinase, 1 mM DTT, 10 mM Mg(CH$_3$CO$_2$), 0.5 A$_{260}$ salt washed ribosomes, 10.0 μg poly(U)-BAT cRNA, 15 pmol [^{3}H]-Phe-tRNA (*Escherichia coli*; Sigma), and 30 pmol hnRNP E1. After 10 min incubation at 37°C, the reaction mixture was filtered through a 0.45 mm nitrocellulose membrane and the filter-retained radioactivity measured. The non-enzymatic [^{3}H]-Phe-tRNA^{Phe} binding was similarly performed, but eEF1A1 was omitted from the reaction mixture.

GTPase Assay: Analysis of intrinsic GTPase activity was performed using the QuantiChromTM ATPase/GTPase Kit from BioAssay Systems according to the manufacturers protocol.

Gel Filtration on Sepharose 4B columns: Gel filtration on Sepharose 4B columns was performed as previously described (Wolf et al., 1977) with minor modifications. Briefly, 100 pmol eEF1A1 were added to 150 μl reaction

mix containing standard buffer (100 mM KCl, 20 mM Tris-HCl, pH 7.5, 1 mM DTT, 10 mM $Mg(CH_3CO_2)$, 2.1 mM phosphoenolpyruvate (PEP), 0.3 U pyruvate kinase, 150 pmol Phe-tRNA, 100 pmol [8-^{3}H]-GTP (15 Ci/mmol), and 0.5 A_{260} salt washed ribosomes (RRL) were pre-incubated with 10.0 μg poly(U)-BAT cRNA, and 200 pmol hnRNP E1. Reaction was incubated 5 min. at 37°C; chilled to 0°C and analyzed on Sepharose 4B columns equilibrated with standard buffer. Fractions of 150 μl were collected. Aliquots (15 μl) were dissolved in scintillation liquid and measured for radioactivity. Absorbance at 280 nm was determined on a NanoDrop 1000 Spectrophotometer (Thermo Scientific).

Wound healing (migration) assay: Wound healing assays were performed as described previously (Lamouille and Derynck, 2007) with brief modifications. Cell monolayers were wounded with a plastic tip after 24 h of seeding and images obtained using a phase-contrast microscope at 10X magnification. The cells were incubated in a humidified chamber with 5% carbon dioxide ± TGFβ for 24 h at 37°C before being photographed again at 10X magnification.

Cell proliferation assay: 1 x 10^5 cells/well were plated in triplicates in a 6-well tissue culture plate. Cells were trypsinized and resuspended in 1 ml of media, before being counted through a hemocytometer chamber up to 12 days following initial seeding. Data is represented as means ± s.e.m. of 3 independent experiments.

Anchorage-independent growth assay (soft-agar colony formation assay): Anchorage-independent growth assay was performed as described earlier (Pietenpol et al., 1989). Approximately 1×10^4 cells were suspended in 2 ml of 0.4% soft-agar in DMEM containing 10% fetal bovine serum and were overlaid on 2 ml of 0.8% soft agar in the same medium in 35 mm diameter dishes. Each cell line was tested in triplicate wells. Colonies were visualized under an inverted light microscope after 3 weeks.

Invasion assay: Cell invasion assay was performed using a CytoSelect™ 96-well Cell Invasion Assay Kit (Cell Biolabs, San Diego, CA) as per the manufacturer's protocol. The experiment was performed with the addition of the 2×10^5 cells to the membrane chamber and ± TGFβ in the feeder tray. Cell invasion was assayed by using the provided cell lysis buffer and CyQuant® dye fluorimetrically at 480 nm/520 nm. Data are presented as means ± s.e.m. of 3 independent experiments.

Tumorigenesis assay: Tumorigenesis was determined by subcutaneous injection of 1×10^5 cells in the hind flank (each side) of 6-week old BalbC athymic nude mice (*nu/nu*), according to approved protocols of Institutional Animal Care and Use Committee (IACUC), Cleveland Clinic. Tumor volume (mm^3) was determined by using the standard formula $a^2 \times b/2$, where '*a*' is the width and '*b*' is the length of the horizontal tumor perimeter, determined 3 times a week with a vernier caliper. Five animals were used for each cell type. The data was analyzed by one-way ANOVA and is represented as mean ± s.e.m ($P < 0.05$).

Hematoxylin/eosin staining: After determination of tumor weight and/or photography, excised tumors were fixed with paraformaldehyde (4%, 18 h, 4°C) and post-fixed (70% ethanol, 16 h) before dehydration and paraffin embedding. Paraffin sections were stained with hematoxylin/eosin according to standard protocols.

Immunohistochemistry: Excised tissues were fixed in formalin and embedded with paraffin. For IHC, tissue sections were deparaffinized and rehydrated sequentially through to distilled water (dH$_2$O) before being immersed in 0.5% hydrogen peroxide/methanol for 10 min. Subsequently, antigen retrieval was performed with citrate buffer, (pH 6.0) followed by two changes with dH$_2$O. The sections were subsequently blocked and incubated with primary antibody (α-E-Cadherin: 1: 200; α-Vimentin: 1:200; α-ILEI: 1:100) for 1.5 h at 25 ^{0}C. The sections were then washed three times with PBS, 5 minutes each, before being incubated with biotinylated secondary antibody for 30 min at 25 ^{0}C. The sections were again washed with PBS and then incubated with Avidin-HRP complex for 30 min at 25 ^{0}C. The stain was developed with diaminobenzidine tetrahydrochloride (DAB) chromogen and observed under Leica DM 2000 microscope with a 10X or 40X objective lens.

Preparation of single cell suspensions from excised tumors: Excised tumors were washed with PBS, and sliced manually with a razor blade. The tissue was then placed in DMEM-F12 media supplemented with 2% calf serum, 10 μg/ml insulin, 100 μg/ml penicillin/streptomycin, and 3 mg/ml collagenase A (Roche) at 37^{0}C for 2 h. The resultant disaggregate was

resuspended in 0.25% trypsin-EDTA for 10 min before being filtered through a 70-μm strainer, and plated on tissue culture dishes.

***In Vivo* luciferase assay:** *In vivo* luciferase assay was performed as described previously (Chaudhury et al., 2010). In brief, cells were stably transfected with a constitutively expressed luciferase construct. Luciferase activity was determined by the Dual Luciferase Reporter assay system (Promega).

Bioluminescent imaging: For the intravenous model, 1 x 10^5 cells in 100μl PBS were injected into the tail vein of 6-week old BalbC athymic nude mice (*nu*/*nu*). Mice were injected with D-luciferin, anesthetized with isoflurane, and imaged with an IVIS Imaging System (Xenogen) 10 min. after luciferin injection. Bioluminescence values at 30 days were compared across the 4 groups.

2.6 Literature Cited

Agafonov, D.E., Kolb, V.A., and Spirin, A.S. (2001). Ribosome-associated protein that inhibits translation at the aminoacyl-tRNA binding stage. EMBO reports. *21*, 399-402.

Anthony, D.D., and Merrick, W.C. (1992). Analysis of 40 S and 80 S complexes with mRNA measured by sucrose density gradients and primer extension inhibition. J. Biol. Chem. *267*, 1554-1562.

Bakin, A.V., Tomlinson, A.K., Bhomick, N.A., Moses, H.L., and Arteaga, C.L. (2000). Phosphatidylinositol 3-kinase is required for transforming growth factor b-mediated epithelial to mesenchymal transition and cell migration. J. Biol. Chem. *275*, 36803-36810.

Berchtold, H., Reshetnikova, L., Reiser, C.O., Schirmer, N.K., Sprinzl, M., and Hilgenfeld, R. (1993). Crystal structure of active elongation factor Tu reveals major domain rearrangements. Nature. *365*, 126–132.

Bierie, B., and Moses, H.L. (2006). TGF-β and cancer. Cytokine Growth Factor Rev. *17*, 29-40.

Chaudhury, A., Hussey, G.S., Ray, P.S., Jin, G., Fox, P.L., and Howe, P.H. (2010). TGFβ-mediated phosphorylation of hnRNP E1 induces EMT via transcript-selective translational induction of Dab2 and ILEI. Nat. Cell Biol. *12*, 286-293.

Clark, I.E., Wyckoff, D., and Gavis, E.R. (2000). Synthesis of the posterior determinant Nanos is spatially restricted by a novel cotranslational regulatory mechanism. Current Biology *10*, 1311-1314.

Collier, B., Goobar-Larsson, L., Sokolowski, M., and Schwartz, S. (1998). Translational inhibition in vitro of human papillomavirus type 16 L2 mRNA mediated through interaction with heterogenous ribonucleoprotein K and poly(rC)-binding proteins 1 and 2. J. Biol. Chem. *263*, 22648-22656.

Dejgaard, K., and Leffers, H. (1996). Characterization of the nucleic-acid-binding activity of KH domains. Different properties of different domains. Eur. J. Biochem. 241, 425-431.

Edmonds BT, Wyckoff J, Yeung YG, Wang Y, Stanley ER, Jones J, Segall J, Condeelis J. (1996). Elongation factor -1 alpha is an overexpressed actin binding protein in metastatic rat mammary adenocarcinoma. J. Cell Sci. 109, 2705-2714.

Evdokimova, V., Tognon, C., Ng, T., Rusanov, P., Melnyk, N., Fink, D., Sorokin, A., Ovchinnikov, L.P., Davicioni, E., Triche, T.J., and Sorensen, P.H.B. (2009). Translational activation of Snail1 and other developmentally regulated transcription factors by YB-1 promotes an epithelial-mesenchymal transition. Cell *15*, 402-415.

Gershtein, E.S., Shatskaya, V.A., Ermilova, V.D., Kushlinksy, N.E., and Krasil'nikov, M.A. (1999). Phosphatidylinositol 3-kinase expression in human breast cancer. Clin. Chem. Acta. *287*, 59-67.

Hampton, M.B., Zhivotovsky, B., Slater, A.F., Burgess, D.H., and Orrenius, S. (1998). Importance of the redox state of cytochrome c during caspase activation in cytosolic extracts. Biochem. J. *329*, 95-99.

Hocevar, B.A., Brown, T.L., and Howe, P.H. (1999). TGF-□ induces fibronectin synthesis through a c-Jun N-terminal kinase-dependent, Smad4-independent pathway. EMBO J. *18*,1345-1356.

Irie, H.Y., Pearline, R.V., Grueneberg, D., Hsia, M., Ravichandran, P., Kothari, N., Natesan, S., and Brugge, J.S. (2005). Distinct roles of Akt1 and Akt2 in regulating cell migration and epithelial mesenchymal transition. J. Cell Biol.*171*, 1023–1034.

Lamouille, S., and Derynck, R. (2007). Cell size and invasion in TGF-β-induced epithelial to mesenchymal transition is regulated by activation of the mTOR pathway. J. Cell Biol. *178*, 437-451.

Ma, L., Young, J., Prabhala, H., Pan, E., Mestdagh, P., Muth, D., Teruya-Feldstein, J., Reinhardt, F., Onder, T.T., Valastyan, S., Westermann, F., Speleman, F., Vandesompele, J., and Weinberg, R. A. (2010). miR-9, a MYC/MYCN-activated microRNA, regulates E-cadherin and cancer metastasis. Nature Cell Biology *12*, 247-256.

Mansilla, F., Dominguez, C.A.G., Yeadon, J.E., Corydon, T.J., Burden, S.J., and Knudsen, C.R. (2008). Translation elongation factor eEF1A binds to a novel myosin binding protein-C-like protein. J. Cell Biochem. *105*, 847-858.

Massague, J. (2008). TGFβ in cancer. Cell *134*, 215-230.

Mazumder, B., and Fox, P.L. (1999). Delayed translational silencing of ceruloplasmin transcript in γ-interferon-activated U937 monocytic cells: role of the 3' untranslated region. Mol. Cell. Biol. *19*, 6898-6905.

Mazumder, B., Seshadri, V., and Fox, P.L. (2003). Translational control by the 3'-UTR: the ends specify the means. TRENDS in Biochemical Sciences. *28*, 91-98.

Meng, Q., Rayala, S.K., Gururaj, A.E., Talukder, A.H., O'Malley, B.W., and Kumar, R. (2007). Signaling-dependent and coordinated regulation of transcription, splicing, and translation resides in a single corregulator, PCBP1. Proc. Natl Acad. Sci. USA *105*, 5866-5871.

Merrick W.C., and Hensold J.O. (2001). Analysis of eukaryotic translation in purified and semipurified systems. Curr. Protoc. Cell Biol. Chapter 11: Unit 11.9.

Micalizzi, D.S., Christensen, K.L., Jedlicka, P., Coletta, R.D., Baron, A.E., Harrell, J.C., Horwitz, K.B., Billheimer, D., Heichman, K.A., Welm, A.L., Scheimann, W.P., and Ford, H.L. (2009). The Six1 homeoprotein induces human mammary carcinoma cells to undergo epithelial-mesenchymal transition and metastasis in mice through increasing TGFβ signaling. J. Clin. Invest. 119: 2678-2690.

Monnier, A., Belle, R., Morales, J., Cormier, P., Boulben, S., and Mulner-Lorillon, O. (2001). Evidence for regulation of protein synthesis at the elongation step by CDK1/cyclin B phosophorylation. Nuc. Acids Res. *29*, 1453-1457.

Mouneimne, G., and Brugge, J.S. (2009). YB-1 Translational Control of Epithelial-Mesenchyme TransitionCancer Cell *15*, 357-359.

Negrutskii, B.S., and El'skaya, A.V. (1998). Eukaryotic translation elongation factor 1a: structure, expression, functions, and possible role in aminoacyl-tRNA channeling. Prog. Nucl. Acid Res. Mol. Biol. *60*, 47-78.

Olsen, P.H., and Ambros, V. (1999). The *lin-4* regulatory RNA controls developmental timing in *Caenorhabditis elegans* by blocking LIN-14 protein synthesis after the initiation of translation. Dev. Biol. *216*, 671-680

Ostareck, D.H., Ostareck-Lederer, A., Wilm, M., Thiele, B.J., and Hentze, M.W. (1997). mRNA silencing in erythroid differentiation: hnRNP K and hnRNP E1 regulate 15-lypoxygenase translation from the 3' end. Cell *89*, 597-606.

Pietenpol, J.A., Howe, P.H., Cunningham, M.R., and Leof, E.B. (1989). Interferon alpha/beta modulation of growth-factor-stimulated mitogenicity in AKR-2B fibroblasts. J. Cell Physiol. *141*, 453-60.

Prunier, C., and Howe, P.H. (2005). Disabled-2 (Dab2) is required for transforming growth factor β-induced epithelial to mesenchymal transition (EMT). J. Biol. Chem. *280*, 17540-17548.

Sampath, P., Mazumder, B., Seshadri, V., Gerber, C.A., Chavatte, L., Kinter, K., Ting, S.M., Dignam, J.D., Kim, S., Driscoll, D.M., and Fox, P.L. (2004). Noncanonical function of glutamyl-prolyl-tRNA synthetase: gene-specific silencing of translation. Cell *119*, 195-208.

Sidiqi, M., Wilce, J.A., Porter, C.J., Barker, A., Leedman, P.J., and Wilce, M.C. (2005). Formation of an alpha CP1-KH3 complex with UC-rich RNA. Eur Biophys J. *34*, 423-429.

Thiery, J.P., and Sleeman, J.P. (2006). Complex networks orchestrate epithelial-mesechymal transitions. Nature Rev. Mol. Cell. Biol. *7*, 131-142.

Waerner, T., Alacakaptan, M., Tamir, I., Oberauer, R., Gal, A., Brabletz, T., Schreiber, M., Jechlinger, M., and Beug H. (2006). ILEI: A cytokine essential for EMT, tumor formation, and late events in metastasis in epithelial cells. Cancer Cell *10*, 227-239.

Wells, S.E., Hillner, P.E,. Vale, R.D., Sachs, A.B. (1998). Circularization of mRNA by eukaryotic translation initiation factors. Mol. Cell. *2*, 135-40.

Wolf, H., Chinali, G., and Parmeggiani, A. (1977). Mechanism of the inhibition of protein synthesis by kirromycin. Eur. J. Biochem. *75*, 67-75.

Yan, G., You, B., Chen, S., Liao, J.K., and Sun, J. (2008). Tumor necrosis factor-a downregulates endothelial nitric oxide mRNA stability via translation elongation factor 1-α1. Circ. Res. *103*, 591-597.

Yang, J., Mani, S.A., Donaher, J.L., Ramaswamy, S., Itzykson, R.A., Come, C., Savagner P., Gitelman, I., Richardson, A., and Weinberg, R.A. (2004). Twist, a master regulator of morphogenesis, plays an essential role in tumor metastasis. Cell *117*, 927–39.

Zavadil, J., and Bottinger, E.P. (2005). TGF-β and epithelial-to-mesenchymal transitions. Oncogene *24*, 5764-5774.

Zuker, M. (2003). Mfold web server for nucleic acid folding and hybridization prediction. Nucleic Acids Res. *31*, 3406–3415.

CHAPTER III

ESTABLISHMENT OF A TGFβ-INDUCED EMT GENE SIGNATURE[2]

3.1 Abstract

A major challenge in the clinical management of human cancers is to accurately stratify patients according to risk and likelihood of a favorable response. Stratification is confounded by significant phenotypic heterogeneity in some tumor types, often without obvious criteria for subdivision. Despite intensive transcriptional array analyses, the identity and validation of cancer specific 'signature genes' remains elusive, partially because the transcriptome does not mirror the proteome. The simplification associated with transcriptomic profiling does not take into consideration changes in the relative expression among transcripts that arise due to post-transcriptional regulatory events. We have previously shown that TGFβ post-transcriptionally regulates epithelial-mesenchymal transition (EMT) by causing increased expression of two

---

transcripts, *Dab2* and *ILEI*, by modulating hnRNP E1 phosphorylation. Using a genome-wide combinatorial approach involving expression profiling and RIP-Chip analysis, we have identified a cohort of translationally regulated mRNAs that are induced during TGFβ-mediated EMT. Coordinated translational regulation by hnRNP E1 constitutes a post-transcriptional regulon inhibiting the expression of related EMT genes, thus enabling the cell to rapidly and coordinately regulate multiple EMT-facilitating genes.

3.2 Introduction

Traditional gain-of-function and loss-of-function approaches have yielded an enormous amount of information in regards to gene function in mammalian development and disease. However, changes in mRNA levels are not always correlative with changes in protein abundance, underlying the importance of post-transcriptional regulation during control of gene expression and activity (Moore, 2005). Indeed, during germ cell development, it has been demonstrated that the 3'-untranslated regions (3'-UTR), when fused to a reporter, are sufficient to confer temporo-spatial specificity for 80% of genes tested (Merrit et al., 2008). Thus, it is clear that the UTRs of mRNA transcripts can significantly impact gene expression. The 'human genome project' reported the mean lengths of 5'-untranslated regions (5'-UTRs) and 3'-UTRs of human mRNAs as 300nt and 770nt, respectively, compared to the mean coding length of 1340nt (Reimann et al., 2002; International Human Genome Sequencing Consortium, 2001), generating renewed interest in the 3'-UTRs of mRNAs to map post-transcriptional regulatory activities.

The epithelial-mesenchymal transition (EMT), in which cells undergo a developmental switch from a polarized, epithelial phenotype to a highly motile fibroblastic or mesenchymal phenotype, has emerged not only as a fundamental process during normal embryonic development and in adult tissue homeostasis, but is also aberrantly activated during metastatic progression (Derynk et al., 2001; Zavadil and Bottinger, 2005; Thiery and Sleeman 2006). EMT is associated with changes in cell-cell adhesion, remodeling of extracellular matrix,

59

and enhanced migratory activity, all properties that enable tumor cells to metastasize (Derynk et al., 2001; Zavadil and Bottinger, 2005; Thiery and Sleeman 2006). Numerous cytokines and autocrine growth factors, including TGFβ, have been implicated in EMT (Bierie and Moses, 2006; Massague, 2008). Our previous studies (Chaudhury et al., 2010; Hussey at el., 2011) and those of others (Waerner et al., 2006; Wang et al., 2010) have shown that regulation of gene expression at the post-transcriptional level plays an indispensable role during TGFβ-induced EMT and metastasis. We identified a transcript-selective translational regulatory pathway in which a ribonucleoprotein (mRNP) complex, consisting of heterogeneous nuclear ribonucleoprotein E1 (hnRNP E1) and eukaryotic elongation factor 1A1 (eEF1A1), binds to a 3'-UTR regulatory BAT (TGFβ activated translation) element and silences translation of *Dab2* and *ILEI* mRNAs, two transcripts which are involved in mediating EMT (Chaudhury et al., 2010; Hussey at el., 2011). TGFβ activates a kinase cascade terminating in the phosphorylation of hnRNP E1, by isoform-specific stimulation of protein kinase Bβ/Akt2, inducing the release of the mRNP complex from the 3'-UTR element, resulting in the reversal of translational silencing and increased expression of *Dab2* and *ILEI* transcripts.

We have previously shown that shRNA-mediated silencing of Dab2 and ILEI in normal murine mammary gland (NMuMG) cells is sufficient to inhibit TGFβ-mediated EMT as analyzed morphologically and by loss of upregulation of N-cadherin and vimentin, mesenchymal cell markers, whereas their overexpression does not induce constitutive EMT, independent of TGFβ

signaling (Chaudhury et al., 2010; Prunier and Howe, 2005). Thus Dab2 and ILEI are required, but not sufficient, for TGFβ-induced EMT. Hence, we, and others based on our studies (Evdokimova, 2012), hypothesized that there are other mRNAs that are being silenced by hnRNP E1 in a similar fashion, and which cumulatively contribute to TGFβ-induced EMT. To address this hypothesis, we adopted a combinatorial approach involving polysome profiling and RIP-Chip analyses using hnRNP E1 and filtered the array data based on the regulatory mechanism of Dab2 and ILEI. This led to the identification and validation of a cohort of target mRNAs that follow the same pattern of regulation as Dab2 and ILEI. Similar to Dab2 and ILEI, the identified target mRNAs harbor a structural BAT element in the 3'-UTR as revealed by *in silico* analysis. This cohort of mRNAs may represent a new TGFβ responsive and hnRNP E1-mediated regulon, operative at a post-transcriptional level in order to mediate TGFβ-induced EMT in a temporal and expedited fashion.

3.3 Results

Experimental design and identification of a TGFβ-induced post-transcriptional EMT gene signature.

To identify potential target mRNA transcripts that are translationally regulated by hnRNP E1 in a TGFβ-dependent manner, we adopted a combinatorial approach involving expression profiling analyses and RNA immunoprecipitation analysis (RIP-Chip). As shown (Figure 3.1 A), we performed a screen using: 1) total mRNA and 2) RNA isolated from monosomal (non-translating) versus polysomal (translating) fractions from TGFβ-treated (24 h) and non-treated NMuMG cells and from the hnRNP E1 knockdown derivative (E1KD), that undergo constitutive EMT even in the absence of TGFβ (Chaudhury et al., 2010; Hussey at el., 2011). In addition, we screened for transcripts that selectively interact with hnRNP E1 in NMuMG cells under unstimulated conditions and subsequently lose their temporal association following TGFβ stimulation (Figure 3.1 A). The samples were individually hybridized to Affymetrix GeneChip® Mouse Genome 430 2.0 arrays.

Following normalization, data was filtered to produce three datasets representing 1) TGFβ translationally regulated genes, 2) genes translationally activated following hnRNP E1 knockdown and 3) hnRNP E1 interacting transcripts (Figure 3.2 B). Genes from the TGFβ translationally regulated dataset were selected as transcripts that displayed an enhanced ratio of association with the actively translating polysomal pool compared to the non-translating

monosomal pool, with no or minor changes in total mRNA expression in NMuMG cells following TGFβ stimulation. mRNA transcripts that displayed enhanced association with polyribosomes irrespective of TGFβ-treatment in E1KD cells were candidates for translationally active genes in an hnRNP E1 knockdown context. Whereas, transcripts which displayed a decreased association with hnRNP E1 in NMuMG cells following TGFβ stimulation, as determined by RIP-Chip analysis, were selected as hnRNP E1 interacting candidates (Figure 3.2 B).

To perform a functional interpretation of our array analysis, all three datasets were queried against GO, Panther and KEGG databases using DAVID and Panther platforms (Table 3.1). Analysis of the TGFβ translationally regulated dataset revealed significant enrichment of categories associated with cell cycle, transcription and ubiquitin-mediated proteolysis. Genes actively translated in E1KD cells are involved in cell cycle, translation and the regulation of the actin cytoskeleton, whereas, transcripts that displayed differential interaction with hnRNP E1 mapped to terms associated with transcription, ubiquitin-mediated proteolysis, in addition to enrichment of several signaling pathways including MAPK, Wnt, integrin and Ras pathway. This analysis is consistent with our findings that TGFβ-mediated translational regulation plays a major role during EMT (Chaudhury et al., 2010; Hussey at el., 2011), as evidenced by enrichment of EMT-associated processes and pathways. In addition, our data indicates that EMT-associated processes are coordinately regulated at both the transcriptional and post-transcriptional level. Enrichment of EMT-associated pathways within the

E1KD and RIP datasets also suggest that hnRNP E1 is a key effector of TGFβ-mediated translational regulation.

Identification of candidate mRNA transcripts translationally regulated by hnRNP E1 in a TGFβ-dependent manner.

In order to identify genes whose expression is translationally regulated by TGFβ through hnRNP E1, the intersection of our three data sets was utilized (Figure 3.1 B) revealing 36 genes, which we have termed BAT genes (Table 3.2). The translational status of the 36 putative BAT genes as determined by isolation of non-translating monosomal (M) fractions (40S, 60S and 80S) and actively translating polysomal (P) fractions from cells treated ± TGFβ for 24 h (Figure 3.2 A) is represented by the signal intensities of monosomal and polysomal association, and is displayed as a heat plot (Figure 3.2 B). The data reveal that the expression of these transcripts (total mRNA) did not vary significantly ± TGFβ in either the parental NMuMG or E1KD cells (Figure 3.2 B). However, in the NMuMG cells, these transcripts preferentially translocated from the M to P fractions following TGFβ stimulation, whereas in the E1KD cells, these transcripts were associated with the P fraction irrespective of TGFβ-treatment (Figure 3.2 B). This methodology accurately identified ILEI as one of the target transcripts, as demonstrated by semi-quantitative RT-PCR analysis of the sample cDNA used for the microarray hybridization (Figure 3.2 C). The ILEI mRNA is polyribosome-associated following TGFβ-treatment in parental NMuMG cells, whereas it is found polyribosome-associated in the E1KD cells in the absence or

64

presence of TGFβ. Total ILEI mRNA levels were not affected by TGFβ stimulation in either cell type (Figure 3.2 C).

Interestingly, several of the identified mRNAs have been previously implicated as targeted transcripts of TGFβ-mediated translational regulation including calpastatin (Barnoy et al., 2000) and epidermal growth factor receptor (Wendt et al., 2010). Additionally, this approach identified several candidates that have been shown to be involved in the EMT process including Eukaryotic initiation factor 5A2 (Zhu et al., 2012), Moesin (Wang et al., 2012), Egfr (Lo et al., 2007) and Inhibin beta-A (Yoshinaga et al., 2004). The data demonstrate, that similar to ILEI, TGFβ induces translocation of these mRNAs from the M to P fractions in the parental NMuMG cells, and that in the E1KD cells these mRNAs are associated with the P fractions irrespective of TGFβ treatment (Figure 3.2 B). These candidates were subsequently used for further validation studies.

Validation of selected genes from the Affymetrix Array.

We next addressed whether the translational regulation of polysome-bound transcripts correlated with respective RNA and protein levels. Initially, we performed a polysome profile expression analysis independent of the pooled microarray samples to further demonstrate the translocation of mRNA from the non-translating M fractions to the actively translating P fractions in non-stimulated and TGFβ-treated cells. In parental NMuMG cells, the target mRNAs are primarily associated with the 80S fraction in non-stimulated cells, and display a complete shift to the actively translating polysomes after 24 h of TGFβ treatment (Figure 3.3 A). These results are in agreement with our previous findings that

hnRNP E1-directed translational regulation targets the 80S stage of translation elongation (Hussey at el., 2011). In contrast, the hnRNP E1 knockdown E1KD cells displayed abundant target mRNA in the actively translating polysomal fractions irrespective of TGFβ treatment (Figure 3.3 B). As a control, semi-quantitative RT-PCR with β-actin specific primers displayed continuous association of the mRNA with the polysomes irrespective of TGFβ-treatment (Figure 3.3 A, B), demonstrating that the translational control is transcript-specific and not due to global regulation of translation.

We next investigated the temporal relationship between total mRNA levels and protein expression levels in TGFβ-treated NMuMG and E1KD cells. With the exception of moesin, total mRNA levels for these target genes, as measured by quantitative real time PCR (qPCR), displayed only minor changes following TGFβ-treatment in both the NMuMG and E1KD cells compared to a ~5 fold increase in Fibronectin (Fn1), a mesenchymal marker and target of TGFβ-mediated transcriptional regulation (Figure 3.3 C, D). These results concur with the microarray data that demonstrate that total mRNA levels for these transcripts were only slightly induced by TGFβ (Figure 3.2). However, it cannot be completely excluded from these results that transcriptional regulation is involved, albeit at a low rate. In contrast, protein expression levels, as analyzed by immunoblot analysis (Figure 3.3 E), revealed that non-stimulated NMuMG cells, despite having abundant message, have low levels of protein for these target genes, and display a rapid, and time-dependent increase in protein expression levels following TGFβ-treatment (Figure 3.3 E). Furthermore, the increased

protein expression levels of these transcripts were shown to correlate with acquisition of a mesenchymal phenotype as demonstrated by increased expression of the mesenchymal marker N-cadherin and decreased expression of Zona occludens 1 (ZO-1). In contrast, in the E1KD cells, although there is not an apparent reduction in the expression of epithelial cell marker ZO-1, the expression of the mesenchymal marker N-cadherin, as well as the protein expression levels of the the BAT genes, were constitutive irrespective of TGFβ-treatment (Fig. 3E).

Target mRNAs are regulated through interaction with hnRNP E1 and a structurally conserved BAT element.

According to the RIP-Chip data, the selected target genes displayed a decrease in association with hnRNP E1 following TGFβ-treatment. The average signal intensity of the association with hnRNP E1 between control and TGFβ-treated samples are represented as a heat plot (Figure 3.4 A). In each case, less of these mRNAs were immunoprecipitated by α-hnRNP E1 in the presence of TGFβ compared to the control, unstimulated NMuMG cells (Figure 3.4 A). To further investigate the temporal association of hnRNP E1 with the selected target genes, we performed a RIP analysis independent of the microarray samples. As shown (Figure 3.4 B), hnRNP E1 interacts with the target transcripts. Immunoprecipitation with α-hnRNP E1 or mouse IgG from cytosolic extracts prepared from NMuMG cells treated with TGFβ for the times indicated, followed by RT-PCR analyses, revealed that while target mRNAs were steadily expressed, hnRNP E1 interaction occurred primarily in non-stimulated cells.

67

These results are in agreement with our previous findings that TGFβ activates a kinase cascade terminating in the phosphorylation of hnRNP E1, by isoform-specific stimulation of protein kinase Bβ/Akt2, inducing the release of the hnRNP E1 from the 3'-UTR *cis* regulatory element, resulting in the reversal of translational silencing and increased expression of EMT-facilitating transcripts (Chaudhury et al., 2010).

We have previously identified the structural BAT element in the 3'-UTRs of Dab2 and ILEI which binds hnRNP E1 and mediates TGFβ-induced translational regulation of these transcripts (Chaudhury et al., 2010). The Dab2 and ILEI BAT elements consist of a proximal stem and an asymmetric bulge followed by a distal stem and terminal loop (Figure 3.4 C). In order to determine whether the selected target genes also contain a respective BAT element, we utilized a consensus BAT element pattern, based on the secondary structure of Dab2 and ILEI BAT elements, to query the non-redundant 3'UTR sequences of the selected target genes using RNAmotif, an RNA secondary structure algorithm (Macke et al., 2001). Putative BAT elements were identified in the target mRNAs with significant folding similarity as identified by the stem-loop and asymmetric bulge (Figure 3.4 D, E).

We next examined the temporal association of hnRNP E1 with the predicted BAT elements using an RNA affinity pull down assay (Figure 3.4 F). The respective BAT element cRNAs were coupled to sepharose beads, and used to precipitate hnRNP E1 from cytosolic S100 extracts isolated from TGFβ-treated and non-treated NMuMG cells. As a negative control, we used the

68

Dab2/U10A element (BAT-M), which contains a U to A substitution at position 10 which unfolds the stem loop structure resulting in diminished binding affinity to hnRNP E1 (Chaudhury et al., 2010; Hussey at el., 2011). Immunoblot analysis confirmed that hnRNP E1 was precipitated by the predicted Egfr and Eif5a2 BAT elements from non-stimulated NMuMG, but TGFβ treatment induced the loss of hnRNP E1 binding in a time-dependent manner. Additionally, pre-treatment of NMuMG cells with the PI3K inhibitor LY294002, blocked the ability of TGFβ to modulate hnRNP E1 interactions (Figure 3.4 F), consistent with our previous observation that inhibition of the PI3K/Akt pathway blocked hnRNP E1 Ser43 phosphorylation (Chaudhury et al., 2010).
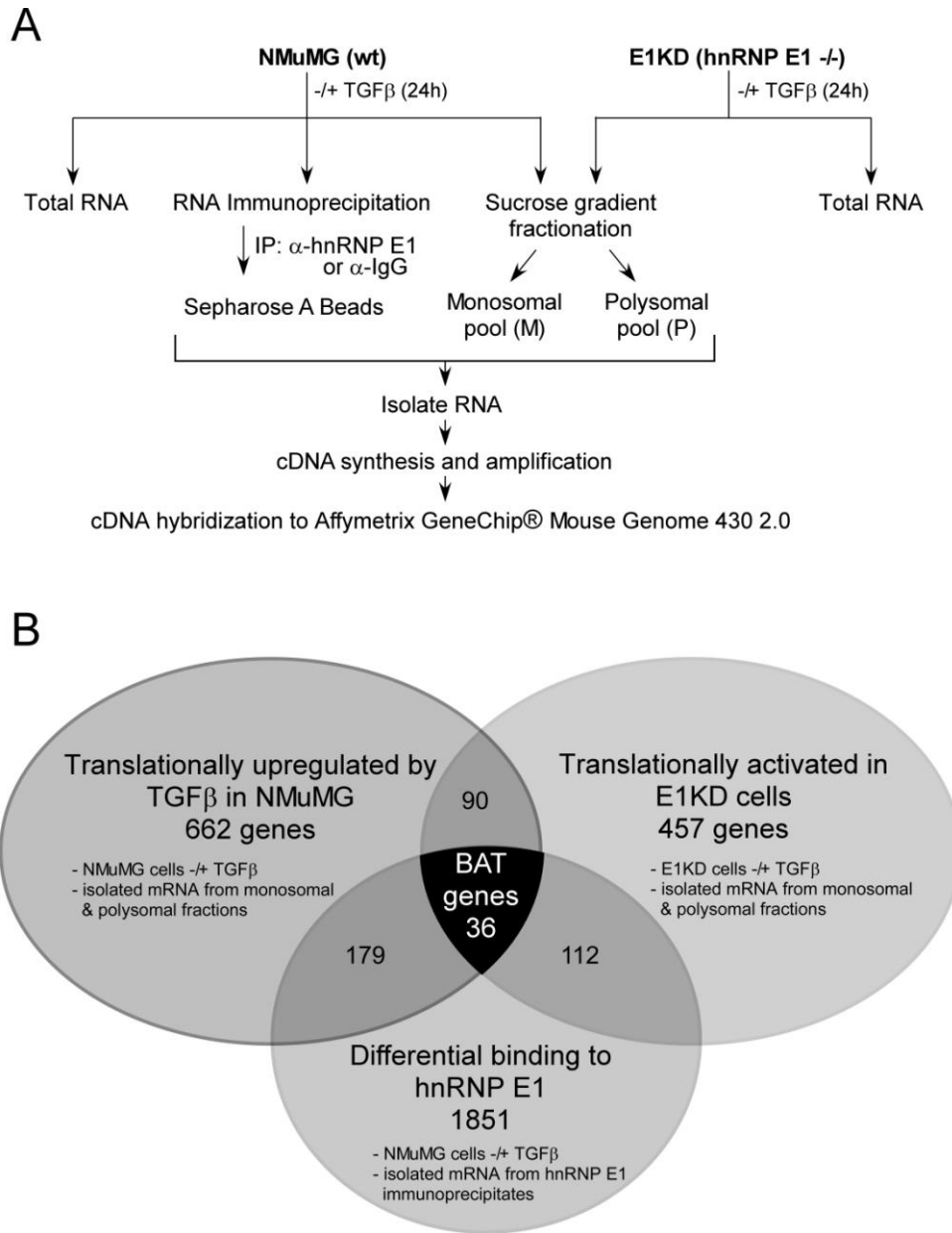
Figure 3.1: Illustration of experimental design. (*A*) Flow chart representing the experimental design. For expression profiling, cytosolic extracts from untreated and TGFβ-treated (24 hr) NMuMG and E1KD cells were fractionated by sucrose gradient centrifugation and RNA was isolated from the non-translating monosomal pool and actively translating polysomal pool, designated as M and P, respectively (n=2). Total unfractionated RNA was isolated from NMuMG and E1KD cells treated ± TGFβ (24 hr) (n=2). For the RIP-Chip analysis, cytosolic extracts from untreated and TGFβ-treated (24 hr) NMuMG cells were immunoprecipitated with α-hnRNP E1 antibody or an isotype control (n=2). (*B*) Venn diagram summarizing the results of the genome wide analysis. Intersection of the three data sets yielded 36 putative BAT genes whose expression is translationally regulated by TGFβ through hnRNP E1.

70
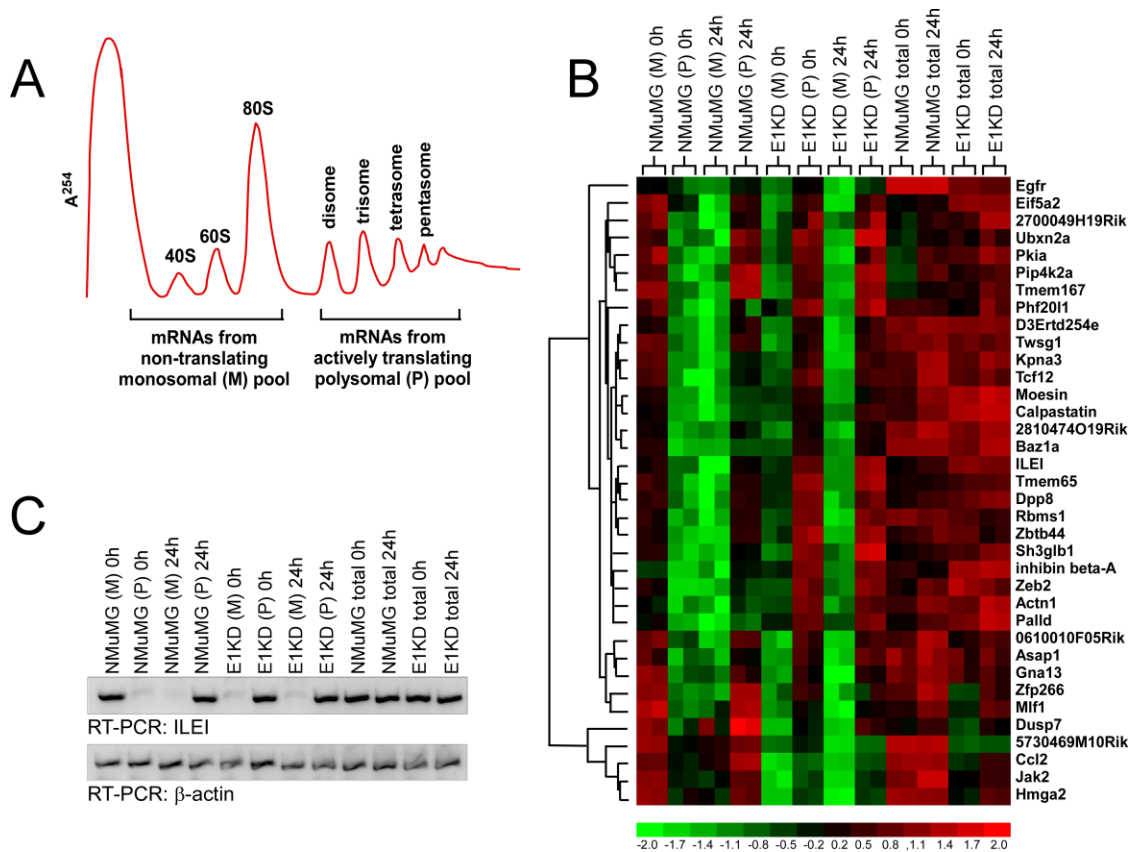
Figure 3.2: Quantitative representation of data. (*A*) Schematic of polysome profile analysis. Monosomal fractions (M; 40S, 60S, and 80S fractions) and polysomal fractions (P) from NMuMG or E1KD cells treated ± TGFβ for 24 hr were isolated by sucrose gradient centrifugation and pooled. (*B*) Heatmap of the raw signal intensity values of the differential gene expression profile for the EMT signature genes compared to total, unfractionated mRNA. Lane 1: NMuMG (M) 0h, 2:NMuMG (P) 24h, 3:(*C*) RT-PCR analysis of microarray RNA samples was used to demonstrate the differential gene expression profile of ILEI.
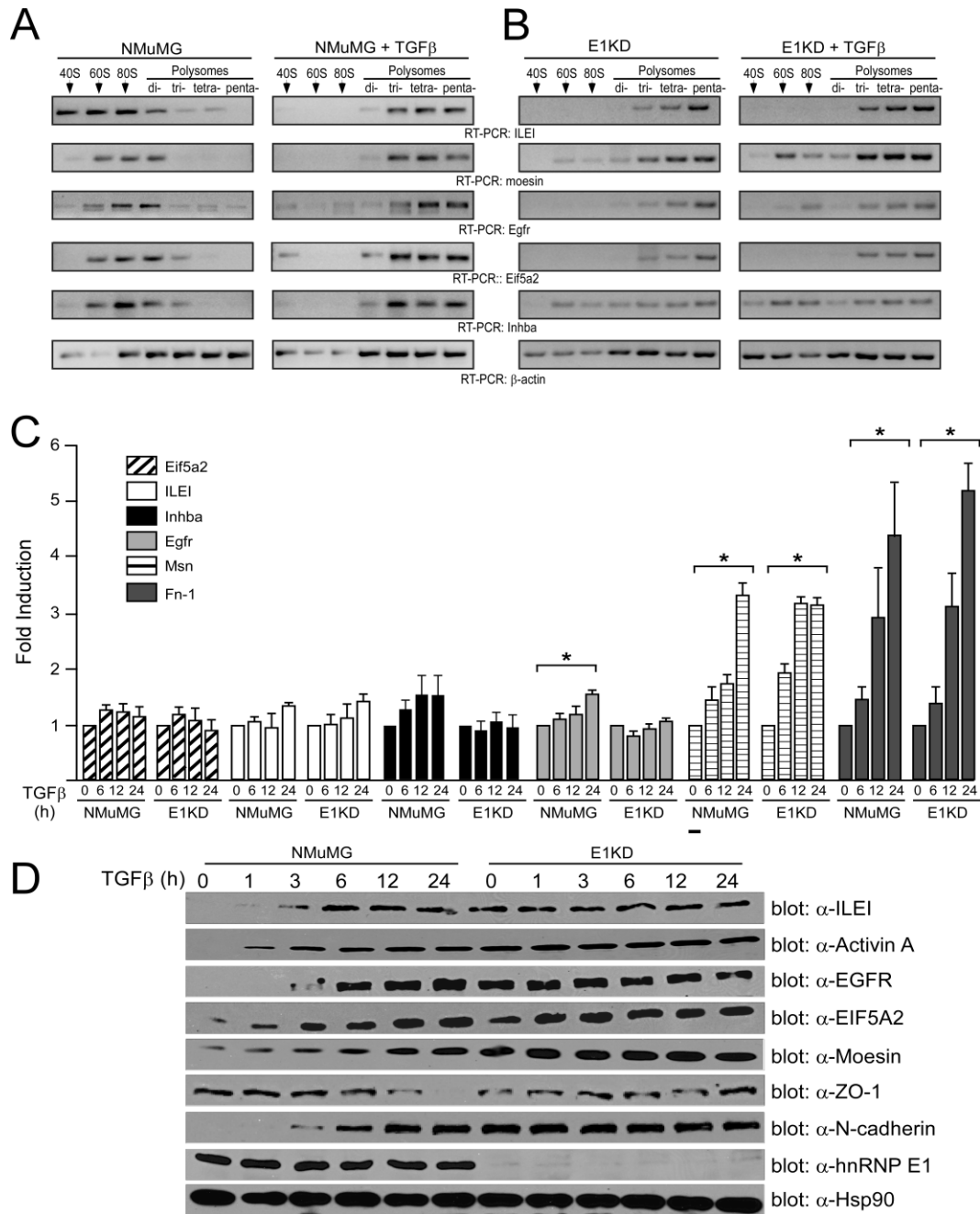
Figure 3.3: Validation of the putative EMT signature gene targets. (*A and B*) RT-PCR analysis using gene specific primers for the potential targets and β-Actin (control) on a polysome profile of NMuMG and E1KD cells ± TGFβ for 24 hr. (*C and D*) Total RNA was isolated from NMuMG and E1KD cells treated with TGFβ for the indicated times and subjected to qPCR analysis to assess steady state mRNA expression levels. Data are presented as means ± s.e., *n*=3 (*P > 0.05) (*E*) Immunoblot analysis examining protein expression levels of the potential targets, α-Hsp90 (control) and α-N-cadherin and α-ZO-1 (EMT markers), in NMuMG and E1KD cells treated with TGFβ for the indicated times.

72
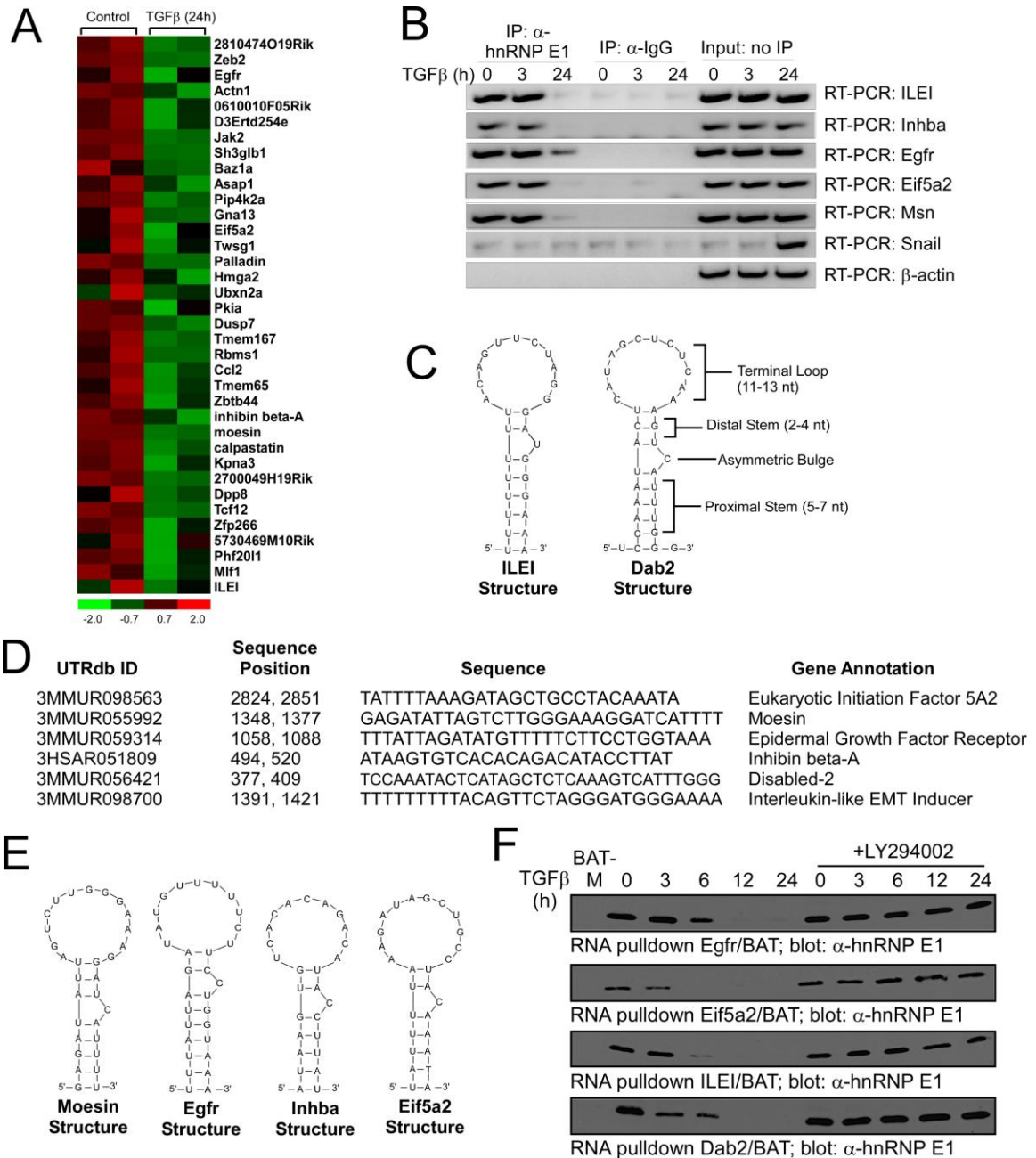
Figure 3.4: Identified mRNAs contain the BAT element and exhibit differential binding to hnRNP E1. (*A*) Heatmap of the RIP-Chip analysis for the putative EMT signature genes. (*B*) NMuMG cells were treated with TGFβ for times indicated, and RT-PCR was performed using gene specific primers for the potential targets, β-Actin (control) and Snail (EMT marker), on a RIP analysis. (*C*) Dab2/BAT and ILEI/BAT structures. Specific regions of the BAT element were selected and used to query the 3'-UTRs of the target mRNAs. (*D and E*) Secondary structures and sequences of target mRNAs with similarities to *Dab2/*BAT. (*F*) RNA affinity pull-down and immunoblot analyses to define the temporal association of hnRNP E1 with the selected BAT elements.

73

Process/Pathway	Database	number of genes mapped to term (expected number)	P-value
TGFβ regulated dataset			
Mitotic cell cycle	GO biological process	34 (8.3)	1.8 E-08
Cell division	GO biological process	36 (9.5)	4.6 E-08
Nucleoside, nucleotide and nucleic acid metabolism	Panther biological process	140 (87.5)	1.6 E-07
Cell cycle	GO biological process	54 (20.8)	5.0 E-07
Mitosis	Panther biological process	27 (9.0)	2.1 E-04
Transcription	GO biological process	101 (59.4)	2.4 E-04
RNA splicing	GO biological process	24 (6.9)	5.8 E-04
RNA processing	GO biological process	37 (14.8)	0.001
Cell cycle	KEGG pathway	16 (4.1)	0.002
mRNA metabolic process	GO biological process	29 (10.4)	0.003
Spliceosome	KEGG pathway	14 (4.0)	0.020
DNA metabolism	Panther biological process	21 (8.1)	0.030
Ubiquitin proteasome pathway	Panther pathway	8 (1.6)	0.043
Pre-mRNA processing	Panther biological process	20 (7.7)	0.046
hnRNP E1 knockdown dataset			
Nucleoside, nucleotide and nucleic acid metabolism	Panther biological process	87 (54.4)	8.4 E-04
Cell cycle	Panther biological process	33 (15.7)	0.014
Translation	GO biological process	20 (6.7)	0.046
Regulation of actin cytoskeleton	KEGG pathway	14 (4.5)	0.055
hnRNP E1 RIP dataset			
Regulation of transcription	GO biological process	268 (187.7)	1.6 E-10
Transcription	GO biological process	220 (137.5)	3.3 E-09
MAPK signaling pathway	KEGG pathway	43 (17.9)	2.6 E-05
Intracellular signaling cascade	Panther biological process	101 (59.4)	3.2 E-05
Regulation of RNA metabolic process	GO biological process	176 (117.3)	4.9 E-05
Intracellular protein traffic	Panther biological process	103 (64.4)	3.5 E-04
Ubiquitin mediated proteolysis	KEGG pathway	26 (9.3)	6.6 E-04
Wnt signaling pathway	Panther pathway	35 (14.6)	6.0 E-04
mRNA transcription	Panther biological process	178 (127.1)	0.001
Pathways in cancer	KEGG pathway	44 (22)	0.002
Colorectal cancer	KEGG pathway	19 (5.9)	0.002
Protein phosphorylation	Panther biological process	77 (48.1)	0.004
Nucleoside, nucleotide and nucleic acid metabolism	Panther biological process	276 (230)	0.004
B cell activation	Panther pathway	13 (3.3)	0.006
Protein catabolic process	GO biological process	76 (44.7)	0.008
EGF receptor signaling pathway	Panther pathway	17 (5.6)	0.013
Angiogenesis	Panther pathway	20 (7.5)	0.018
Ras Pathway	Panther pathway	12 (3.2)	0.022
Protein modification	Panther biological process	115 (82.1)	0.023
Regulation of Rho protein signal transduction	GO biological process	21 (6.8)	0.026
Focal adhesion	KEGG pathway	29 (13.8)	0.026
Endocytosis	Panther biological process	36 (18)	0.029
Integrin signalling pathway	Panther pathway	21 (8.4)	0.029
Natural killer cell mediated cytotoxicity	KEGG pathway	21 (8.4)	0.032
PDGF signaling pathway	Panther pathway	17 (6.3)	0.049

Table 3.1: Number of genes from dataset assigned to a given biological process or pathway is compared to the number of genes expected by chance to map to the term. P-value adjusted for multiple testing using the Bonferroni method.

Accession	Gene Name	Fold Change Total mRNA in NMuMG	Fold Induction Polysomal mRNA in NMuMG	Fold Change Total mRNA in E1KD	Fold Induction Polysomal mRNA in E1KD	Fold Change in hnRNP E1 binding
BM232998	2810474O19Rik	1.6934906	20.82147	1.574616	1.8150383	1.82134
NM_015753	Zeb2	1.8087588	21.33278	0.600818	1.5368752	2.386671
U03425	Egfr	1.0139595	5.856343	0.8066418	1.4240502	1.464086
BC003232	Actn1	1.5691682	6.254957	1.6529006	1.3013419	1.510473
W30094	0610010F05Rik	1.6021398	7.568461	1.2570134	1.0792282	1.389918
AU067741	D3Ertd254e	1.1850928	11.63178	1.0245568	1.6245048	1.552938
NM_008413	Jak2	1.7592982	6.727171	1.4339552	1.2141949	1.918528
BB221842	Sh3glb1	1.1526863	5.540438	1.2834259	1.3995859	1.82134
AV357135	Baz1a	1.0174797	14.02569	1.7411011	1.4948492	1.399586
BE943736	Asap1	1.1289644	5.063026	1.0717735	1.4896775	1.433955
AK012196	Pip4k2a	1.9520635	13.17746	1.201636	1.7171309	2
BI662324	Gna13	1.2184103	7.412704	0.9726549	1.866066	1.574616
AV271901	Eif5a2	1.1289644	6.988583	1	1.4590203	1.337928
BC004850	Twsg1	1.0867349	10.59271	0.9794203	1.4948492	1.274561
BG071905	Palld	1.6132835	9.57983	1.69937	1.5583292	1.735077
X58380	Hmga2	0.9106698	5.676493	1.8986842	1.3613141	1.274561
AV174556	Ubxn2a	1.2397077	7.621104	1.1566882	1.9453099	1.261377
AK010212	Pkia	1.7592982	13.04116	1.3472336	1.771535	1.36604
BC025048	Dusp7	1.270151	7.542276	1.5422108	1.5583292	2.136131
BQ174163	Tmem167	1.2483305	11.27457	1.2789856	1.6021398	1.310393
NM_020296	Rbms1	0.9233823	6.105037	0.8705506	1.7532114	1.30586
AF065933	Ccl2	1.0245568	5.521269	1.9185282	1.0069556	1.607702
BF383782	Tmem65	1.0245568	8.845845	1.082975	1.6934906	1.239708
BC027138	Zbtb44	1.2099941	5.169411	0.8150723	1.5052467	1.29684
NM_008380	Inhba	0.8321987	5.205367	1.1134216	1.5800826	1.274561
NM_010833	Msn	1.9453099	14.22148	1.3058598	1.9930805	1.892115
BB148748	Cast	1.6414832	11.47164	1.1809927	1.8150383	2.034959
BM213828	Kpna3	1.5691682	7.862565	1.3195079	1.8403753	1.494849
AV127581	2700049H19Rik	1.2483305	6.988583	1.5583292	1.1769067	1.618884
BF119821	Dpp8	1.1974787	8.907373	1.201636	1.7290745	1.252664
NM_011544	Tcf12	1.4590203	6.19026	1.082975	1.2397077	1.531558
AW825881	Zfp266	1.4142136	10.37472	1.6643975	1.0606877	1.515717
AK017688	5730469M10Rik	0.9896567	8.310873	1.053361	1.3707828	1.22264
BB268102	Phf20l1	0.952638	5.37029	1.531558	1.9793133	1.324089
AF100171	Mlf1	1.547565	17.44812	1.9318727	1.9656412	1.380317
AK016470	Fam3c	1.226885	7.260153	0.9362722	2.0849315	1.185093

Table 3.2: List of 36 potential BAT genes identified by the combinatorial approach. Despite minor changes in total RNA levels, the target mRNAs display a >5 fold increase in polyribosome association in NMuMG cells post TGFβ treatment compared to E1KD cells where the target mRNAs display constitutive translational activation. Target mRNAs display a decrease in temporal association with hnRNP E1 following TGFβ stimulation for 24 hr.

3.4 Discussion

Despite intensive transcriptional array analysis of human tumors, the identity and validation of 'EMT signature genes' remains elusive (Pradet-Balade et al., 2001; van't Veer et al., 2002; Kang and Massague, 2004), partially because the transcriptome does not mirror the proteome (van der Kelen et al., 2009). To understand how the interplay of RNA-binding proteins affects the regulation of individual transcripts, high-resolution maps of *in vivo* protein-RNA interactions are necessary (Keene and Lager, 2005). An alternative approach is expression profiling on a genome wide scale, whereby non-translating and actively translating pools of mRNAs are isolated by sucrose density gradient fractionation and subsequently subjected to microarray analysis (Zong et al., 1999). RNA-Binding Protein Immunoprecipitation-Microarray (RIP-Chip) profiling is an advanced high-throughput analysis of mRNAs that co-immunoprecipitate with particular mRNA-binding proteins (Penalva et al., 2004). An mRNA-binding protein of interest is immunoprecipitated, and the associated mRNA is isolated and subsequently subjected to microarray analysis. A combinatorial approach involving expression profiling and RIP-chip analysis on a genome-wide basis will yield definitive information on a particular regulatory pathway.

Herein, we have identified a cohort of translationally regulated mRNAs that are upregulated during TGFβ-induced EMT by using a combinatorial approach involving polysome profiling and RIP-Chip analysis. Filtering the Affymetrix array data based on the translational state of transcripts in non-stimulated and TGFβ-treated NMuMG and E1KD cells, and intersecting these

genes sets with the RIP-chip analysis led to the identification of a set of target mRNAs that follow the same pattern of regulation as Dab2 and ILEI, two transcripts necessary for EMT which were previously shown to be translationally regulated by TGFβ through hnRNP E1 (Chaudhury et al., 2010; Hussey et al., 2011). While our confidence in the establishment of this TGFβ-induced post-transcriptional EMT signature was strengthened by the identification of several transcripts which have been previously shown to be translationally regulated by TGFβ, including calpastatin (Barnoy et al., 2000) and epidermal growth factor receptor (Wendt et al., 2010), our approach was not without some limitations. For example, this approach correctly identified ILEI mRNA, a well-characterized target for BAT-mediated translational silencing (Chaudhury et al., 2010; Hussey et al., 2011), however, another previously identified target, Dab2 remained unidentified. This result may be due to a low signal-to-noise ratio of Dab2 expression levels, as the microarray based approach requires that the level of expression of target mRNA exceeds the cutoff limit of detection with a high-signal-to noise ratio (vyas et al., 2009).

Protein expression levels depend on the rate of transcription, as well as other defined control mechanisms, such as mRNA stability (Garcia-Martinez et al., 2004), nuclear export and mRNA localization (Hieronymus and Silver, 2004), translational regulation (Beilharz and Preiss, 2004), and protein degradation (Beyer et al., 2004). Post-transcriptional regulation is mainly controlled by the association of trans-acting RNA binding proteins with cis-regulatory regions in the UTRs of mRNAs. The bioinformatic prediction of putative BAT elements in the

77

identified BAT mRNAs reveals a conserved structure-based homology based upon the functional structural motif previously identified for Dab2 and ILEI. These structures within the 3'-UTRs of the selected target mRNAs all share a stem-loop motif with an asymmetric bulge, albeit with considerable sequence diversity. Although the Egfr and Eif5a2 BAT elements were validated for their ability to bind hnRNP E1, a more comprehensive analysis is still required. This includes, but is not limited to fine mapping and cloning of the 3'-UTR of the candidate genes into reporter vectors to demonstrate functional gain-of-silencing potential.

The BAT element provides further insights into the importance of regulatory elements in the maintenance of homeostasis. Our results are suggestive of a stimulus-dependent upregulation of a post-transcriptional regulon coordinated by the concerted action of a trans-acting mRNP complex and a cis-regulatory element in the 3'-UTR of target genes. Eukaryotic regulons are defined as higher-order genetic units (quasi genome) consisting of monocistronic mRNA subsets under the control of a regulatory RNA binding protein (Keene and Lager, 2005). RNA binding proteins have been shown to specifically bind transcripts encoding functional and colocalized protein classes (Brown et al., 2001; Waggoner and Liebhaber, 2003; Gerber et al., 2004). Post-transcriptional regulons may have evolved as a mechanism to rapidly and coordinately suppress multiple EMT genes.

During the invasive phase of metastasis, a carcinoma cell activates EMT programs by different regulatory pathways. Differentiation to a mesenchymal phenotype enables the cancer cell with the ability to survive through the different

steps of metastatic progression, including localized invasion by primary tumor cells, intravasation, translocation, extravasation and finally micrometastatic colonization at the secondary site (Massague, 2008). Now, we demonstrate a cohort of selective transcripts that are post-transcriptionally upregulated by TGFβ and are correlative with an induction of the EMT phenotype. Akt2-mediated hnRNP E1 phosphorylation post-TGFβ stimulation is the regulatory mechanism mediating the TGFβ-induced translational activation of EMT-facilitating transcripts. We have now shown that hnRNP E1 is a central moiety in this process, and may represent an important molecular target for the development of modulators of this translational regulatory pathway. Furthermore, the continued delineation of the role of the identified target transcripts during EMT will prove to be extremely useful and will allow for their interrogation and manipulation in physiological and pathological situations.

3.5 Materials and Methods

Reagents: Mouse α-hnRNP E1 and α-ZO-1 were obtained from Novus Biologicals. α-ILEI, α-Inhibin beta A and α-EIF5A2 were obtained from Abcam. α-EGFR was obtained from Cell Signaling Technology. α-Moesin was purchased from BD Biosciences. α-Hsp90 and normal mouse IgG were purchased from Santa Cruz Biotechnology. Secondary antibodies, α-mouse and α-rabbit-IgG-HRP were obtained from GE Healthcare Bio-Sciences. Refer to Table 1 for primer sequences.

Cell culture and treatments. NMuMGs were maintained in Dulbecco's modified Eagle's medium supplemented with 10% fetal bovine serum, 10 mg/ml insulin, and antibiotics/antimycotics (100 units/ml penicillin G, 100 mg/ml streptomycin, and 0.25 mg/ml amphotericin B). E1KD (previously termed SH14) were generated in the laboratory and have been described (Chaudhury et al., 2010). TGFβ2 was a generous gift from Genzyme Inc. and was used at a final concentration of 5 ng/ml. Where indicated, cells were treated with 10 μM of LY294002 30 min before TGFβ treatment.

RNA immunoprecipitation: RNA immunoprecipitation was performed as described previously (Penalva et al., 2004). Briefly, the cytosolic extract was incubated with 10 μg of mouse α-hnRNP E1 antibody or mouse α-IgG at 4°C overnight, and precipitated with Protein A-Sepharose (Invitrogen). The beads were washed three times with IP Wash Solution (150 mM NaCl, 50 mM Tris pH 7.5, 0.5% NP40), and immunoprecipitated RNAs isolated by Trizol (Invitrogen) and treated with RNase-free DNase I (Applied Biosystems).

Polysome profiling: Polysome analysis was performed as described previously (Merrick and Hensold, 2001). Briefly, cell lysates were layered onto a 10%-50% sucrose gradient and centrifuged at 100,000 x g at 4^0C for 4 h. Gradient fractions were collected using a fraction collector with continuous monitoring of absorbance at 254 nm. RNA was extracted with Trizol (Invitrogen) and purified with RNeasy minikit (Qiagen).

Microarray data processing: Affymetrix microarray analysis was conducted on two independent samples for each experimental condition. Samples were processed at the MUSC Proteogenomics Facility (http://proteogenomics.musc.edu) using Affymetrix Mouse Genome 430 2.0 GeneChips® in accordance with the manufacturer protocols. The resulting raw data files were deposited in the NCBI Gene Expression Omnibus (Accession #GSE20152). Hybridization data (CEL files) were normalized by RMA algorithm using Affymetrix Expression Console software; detection calls were obtained by Affymetrix MAS5 algorithm. Gene representations not receiving 'present' detection scores in ≥25% of all samples were excluded from further analysis.

Data analysis: The average raw signal intensity values from two independent samples for each experimental condition were determined and used for multiparametric comparisons. Filtering of the genes sets met the following criteria: i) the ratio of the average raw signal intensity of monosomal (M) versus polysomal (P) mRNAs from control NMuMG cells was filtered as ($M_{control}/P_{control} \geq$ 2), whereas in the E1KD cells the parameter was set at ($P_{control}/M_{control} \geq$ 2); ii) the ratio of P vs. M associated mRNAs from TGFβ-treated NMuMG and E1KD cells

was filtered as ($P_{TGF\beta}/M_{TGF\beta} \geq 2$); iii) fold change in total RNA from control vs. TGFβ-treated cells was determined by (Total $RNA_{TGF\square}$/Total $RNA_{control} \leq 2$); and, iv) the ratio of fold induction of polysomal RNA in NMuMG cells post TGF□-stimulation compared to control was filtered at ($[(P_{TGF\beta}/M_{TGF\beta})/(P_{control}/M_{control})] \geq 5$), whereas in the E1KD cells the parameter was set at ($[(P_{TGF\beta}/M_{TGF\beta})/(P_{control}/M_{control}) < 2$). Finally, for the RIP-Chip, the ratio of the average raw signal intensity for mRNAs immunoprecipitated by hnRNP E1 in control NMuMG cells vs. TGFβ-treated was filtered at (IP:E1 Control/TGFβ $\geq$ 1.2), whereas for the IgG immunoprecipitation the parameter was set at (IP:IgG Control/TGFβ $\leq$ 1).

Real-time quantitative PCR (Taqman system): Total RNA was isolated by Trizol extraction. Reverse transcription was performed using the Superscript first strand synthesis system (Invitrogen). Quantitative PCR was performed using an Applied Biosystems 7500 Fast Real-Time PCR System and default cycle conditions. Briefly, reactions were prepared using 50ng cDNA, Taqman® Fast Universal PCR Master Mix and mouse-specific primers for Egfr (cat number Mm00433023_m1), Moesin (Mm00447889_m1), Eif5a2 (Mm00812570_g1), Fam3c (Mm00506842_m1), Inhba (Mm00434339_m1), Fn1 (Mm01256744_m1), and Gapdh (Mm99999915_g1) according to manufacturer's protocol (Life technologies). All samples were run in triplicate and normalized to Gapdh. Data analysis was performed using the relative quantification ($\Delta\Delta C_T$) method (Livak and Schmittgen, 2001).

Preparation of cytosolic extract (S100 Fraction): S100 fractions were prepared from cells as previously described (Mazumder and Fox, 1999) with minor modifications. Briefly, the buffer used for cytosolic extraction contained 20 mM Hepes (pH 7.5), 10 mM KCl, 1.5 mM $MgCl_2$, 1 mM EGTA, 1 mM EDTA, 1 mM DTT and protease inhibitor cocktail (Roche).

RNA pulldown: RiboMax kit (Promega) was used to generate milligram quantity of BAT cRNA. cRNA was bound to CNBr-activated Sepharose beads and incubated for 1 h at 4 ^{0}C with 50 μg of cytosolic extract (S100 Fraction) from NMuMG cells treated ± TGFβ. Following incubation, beads were washed with 0.2 M NaCl and resolved by SDS-PAGE.

Functional pathway search analysis: Functional analysis was performed using the Database for Annotation, Visualization and Integrated Discovery (DAVID), Molecular Signature Database (MSigDB) and Protein Analysis Through Evolutionary Relationships (Panther) platforms. Biological processes and pathway terms from Gene ontology (GO), Kyoto Encyclopedia of Genes and Genomes (KEGG), Panther, Reactome and Biocarta databases were utilized.

Bioinformatic prediction of BAT elements: Analysis of select 3'UTR genes was completed using RNAmotif software (Macke et al., 2001) on a MacBook Pro using an Intel Core-i7, 4gb of RAM, and Mac OS-X 10.6. Software was compiled using GNU's GCC compiler (gcc.gnu.org) in the OS-X terminal utility. Descriptor file was written using Xcode version 3.2 in the C development module. Input file was created in a generic text editor, sequences were obtained

from UTRdb (utrdb.ba.itb.cnr.it). Analysis was run from the OS-X terminal utility,

output was sent to a generic text file to be used for later interpretation.

3.6 Literature Cited

Barnoy S, Supino-Rosin L, Kosower, NS (2000) Regulation of calpain and calpastatin in differentiating myoblasts: mRNA levels, protein synthesis and stability. *Biochem J* 351:413-420.

Beilharz TH, Preiss T (2004) Translational profiling: the genome-wide measure of the nascent proteome. *Brief Funct Genomic Proteomic* 3:103-11.

Beyer A, Hollunder J, Nasheuer HP, Wilhelm T (2004) Post-transcriptional expression regulation in the yeast Saccharomyces cerevisiae on a genomic scale. *Mol Cell Proteomics* 3:1083-92.

Bierie B, Moses HL (2006) TGF-beta and cancer. *Cytokine Growth Factor Rev* 17: 29-40.

Brown V, et al. (2001) Microarray identification of FMRP-associated brain mRNAs and altered mRNA translational profiles in fragile X syndrome. *Cell* 107:477-87.

Chaudhury A, et al. (2010) Transforming growth factor-beta-mediated phosphorylation of hnRNP E1 induces EMT via transcript selective translational induction of Dab2 and ILEI. *Nat Cell Biol* 12:286-93.

Derynck R, Akhurst RJ, Balmain A (2001) TGF-beta signaling in tumor suppression and cancer progression. *Nature Genet* 29:117-29.

Evdokimova V, Tognon CE, Sorensen PHB (2012) On translational regulation and EMT. *Semin Cancer Bio.*
http://dx.doi.org/10.1016/j.semcancer.2012.04.007

Garcia-Martinez J, Aranda A, Perez-Ortin JE (2004) Genomic run-on evaluates transcription rates for all yeast genes and identifies gene regulatory mechanisms. *Mol Cell* 15:303-13.

Gerber AP, Herschlag D, Brown PO (2004) Extensive association of functionally and cytotopically related mRNAs with Puf family RNA-binding proteins in yeast. *PLoS Biol* 2:E79.

Hieronymus H, Silver PA (2004) A systems view of mRNP biology. *Genes Dev* 18:2845-60.

Hussey GS, et al. (2011) Identification of an mRNP complex regulating tumorigenesis at the translational elongation step. *Mol Cell* 41:419-431.

International Human Genome Sequencing Consortium (2001) Initial sequencing and analysis of the human genome. *Nature* 409:860-921.

Kang Y, Massague J (2004) Epithelial-mesenchymal transitions: twist in development and metastasis. *Cell* 118:277-9.

Keene JD, Lager PJ (2005) Post-transcriptional operons and regulons coordinating gene expression. *Chromosome Res* 13:327-37.

Livak KJ, Schmittgen TD (2001) Analysis of relative gene expression data using real-time quantitative PCR and the 2(-Delta Delta C(T)) Method. *Methods* 25:402-408.

Lo HW, et al. (2007) Epidermal growth factor receptor cooperates with signal transducer and activator of transcription 3 to induce epithelial-mesenchymal

transition in cancer cells via up-regulation of TWIST gene expression. *Cancer Res* 67:9066-9076.

Macke TJ, et al. (2001) RNAMotif, an RNA secondary structure definition and search algorithm. Nuc Acids Res 29:4724-35.

Massague J (2008) TGFbeta in Cancer. *Cell* 134:215-30.

Moore MJ (2005) From birth to death: the complex life of eukaryotic mRNAs. *Science* 2:1514-8.

Mazumder B, Fox PL (1999) Delayed translational silencing of ceruloplasmin transcript in gamma interferon-activated U937 monocytic cells: role of the 3' untranslated region. *Mol Cell Biol* 19:6898-905.

Merrick WC, Hensold JO (2001) Analysis of eukaryotic translation in purified and semipurified systems. *Curr. Protoc. Cell Biol.* Chapter 11: Unit 11.9.

Merrit C, Rasaloson D, Ko D, Seydoux G (2008) 3' UTRs are the primary regulators of gene expression in the C. elegans germline. *Curr Biol* 18:1476-82.

Penalva LO, Tenenbaum SA, Keene JD (2004) Gene expression analysis of messenger RNP complexes. *Methods Mol Biol* 257:125-34.

Pradet-Balade B, Boulme F, Beug H, Mullner EW, Garcia-Sanz JA (2001) Translation control: bridging the gap between genomics and proteomics? *Trends Biochem Sci* 26:225-9.

Prunier C, Howe PH (2005) Disabled-2 (Dab2) is required for transforming growth factor beta-induced epithelial to mesenchymal transition (EMT). *J Biol Chem* 280:17540-8.

Reimann I, Huth A, Thiele H, Thiele BJ (2002) Suppression of 15-lipoxygenase synthesis by hnRNP E1 is dependent on repetitive nature of LOX mRNA 3'-UTR control element DICE. *J Mol Biol* 315, 965-74.

Thiery JP, Sleeman JP (2006) Complex networks orchestrate epithelial-mesenchymal transitions. *Nature Rev. Mol Cell Biol* 7:131-42.

van der Kelen K, Beyaert R, Inze D, de Veylder L (2009) Translational control of eukaryotic gene expression. *Crit Rev Biochem Mol Biol* 44:143-68.

van't Veer LJ, et al. (2002) Gene expression profiling predicts clinical outcome of breast cancer. *Nature* 415:530–6.

Vyas K, et al. (2009) Genome-wide polysome profiling reveals an inflammatory posttranscriptional operon in gamma interferon-activated monocytes. *Mol Cell Biol* 29:458-70.

Waerner T, et al. (2006) ILEI: a cytokine essential for EMT, tumor formation, and late events in metastasis in epithelial cells. *Cancer Cell* 10:227-39.

Waggoner SA, Liebhaber SA (2003) Identification of mRNAs associated with alphaCP2-containing RNP complexes. *Mol Cell Biol* 23:7055-67.

Wang H, et al. (2010) PCBP1 suppresses the translation of metastasis-associated PRL-3 phosphatase. *Cancer Cell* 18:52-62.

Wang CC, et al. (2012) Differential expression of moesin in breast cancers and its implication in epithelial-mesenchymal transition*. Histopathology* 61:78-87.

Wendt MK, Smith JA, Schiemann WP (2010) Transforming growth factor-b-induced epithelial-mesenchymal transition facilitates epidermal growth factor-dependent breast cancer progression. *Oncogene* 29:6485-6498.

Yoshinaga K, et al. (2004) N-cadherin is regulated by Activin A and associated with tumor aggressiveness in esophageal carcinoma. *Clin Cancer Res* 10:5702-5707.

Zavadil J, Bottinger EP (2005) TGF-beta and epithelial-to-mesenchymal transitions. *Oncogene* 24:5764-74.

Zhu W, et al. (2012) Ovexpression of EIF5A2 promotes colorectal carcinoma cell aggressiveness by upregulating MTA1 through C-myc to induce epithelial-mesenchymal transition. *Gut* 61:562-575.

Zong Q, Schummer M, Hood L, Morris DR (1999) Messenger RNA translation state: the second dimension of high-throughput expression screening. *Proc Natl Acad Sci U S A* 96:10632-6.

CHAPTER IV

FUTURE PERSPECTIVES:

BAT-MEDIATED EMT AND CANCER STEM CELLS

4.1 Abstract

We have identified a TGFβ-regulated mRNP complex containing the RNA-binding protein hnRNP-E1 which inhibits the translation of genes essential for EMT by blocking eEF1A1 release during translation elongation. Phosphorylation of hnRNP-E1 in response to TGFβ signaling disrupts the hnRNP E1-eEF1A1 interaction, triggering EMT. While many types of cancer cells leaving primary tumors rely on an EMT program to facilitate the initial steps of the invasion-metastasis process, how an EMT program promotes their self-renewal capability is not completed understood. This can in part be addressed by the recent discovery that induction of EMT can stimulate cultured breast cells to adopt characteristics of stem cells including competence of self-renewal and capacity to

differentiate. Herein, we provide evidence that attenuation of the BAT-mRNP complex in normal mammary gland epithelial cells can mediate acquisition of a stem-like phenotype. As an *in vitro* test of mammary gland stem cell function we demonstrate that modulation of hnRNP E1 allowed these cells to effectively grow in mammosphere culture. Furthermore, we demonstrate that this induced EMT in normal mammary gland epithelial cells was able to reconstitute a differentiated mammary gland following implantation into cleared fat pads. These results provide evidence for the requirement of TGFβ-mediated translational activation of EMT-inducer transcripts for facilitating the reprogramming of epithelial cells and to promote their self-renewal capability.

4.2 Introduction

Human carcinomas exhibit a wide range of signaling events to promote migration and invasion. It has become evident that cancer cells can dedifferentiate through activation of specific biological pathways associated with epithelial-mesenchmal transition (EMT), gaining the ability to migrate and invade (Brabletz et al., 2005). Thus, EMT has emerged not only as a fundamental process during normal embryonic development and in adult tissue homeostasis, but has also been demonstrated to be essential for metastatic progression (Derynck et al., 2001; Thiery and Sleeman, 2006; Zavadil and Bottinger, 2005)

Recent reports have suggested that epithelial cells that pass through an EMT acquire a stem cell-like phenotype associated with cancer stem cells (Mani et al., 2008; Morel et al., 2008). It is postulated that many cancers, including breast cancer, are driven by a population of cancer stem cells that display stem cell-like characteristics (Al-Hajj et al., 2003; O'Brien et al., 2007; Ricci-Vitianiet al., 2007; Singh et al., 2004). Cancer stem cells isolated from mammary gland tumors are characterized by their highly tumorigenic potential, their self-renewal capacity, potential for multilineage differentiation, and the ability to generate suspended spherical colonies (mammospheres) when cultured in serum-free medium in non-adherent conditions (Mani et al., 2007). Several cell surface markers have been reported to identify mammary stem cells. For example, a subpopulation of mammary gland stem cells isolated from humor tumors have been shown to express an antigenic phenotype in the $CD44^{hi}/CD24^{low}$ configuration (Al-Hajj et al., 2003; Mani, 2008), whereas enrichment of a

92

population of mammary gland cells from mice exhibit a CD29^{hi}/CD24^{+} pattern (Mani et al., 2007; Visvader and Lindeman, 2006; Wang 2006). Despite recent advances in our understanding of cancer stem cells, the signaling mechanisms that induce and maintain the EMT and stem cell state are not completely understood.

We have described a transcript-selective translational regulatory pathway in which a ribonucleoprotein (mRNP) complex, consisting of heterogeneous nuclear ribonucleoprotein E1 (hnRNP E1) and eukaryotic elogation factor 1-A1, binds to a 3′-UTR regulatory TGF-β-activated translation (BAT) element and silences translation of a cohort of EMT-facilitating transcripts. TGF-β activates a kinase cascade terminating in the phosphorylation of hnRNP E1 by isoform-specific stimulation of protein kinase B/Akt2, which induces the release of the mRNP complex from the 3′-UTR element, resulting in the reversal of translational silencing and increased expression of EMT-facilitating transcripts. In a translational-state microarray analysis, in which differential sedimentation is used to separate the nontranslating, nonpolysomal pool of transcripts from the actively translating, polysome-associated transcripts, *Interleukin-like EMT Inducer* (ILEI) was demonstrated to be translationally upregulated during EMT.

ILEI (previously termed Fam3C) is a member of a recently discovered gene family (Fam3A-D), which was identified using structure-based methods to search for four-helix-bundle cytokines (Zhu et al., 2002). Functionally, ILEI has been demonstrated to be involved in the contribution of EMT. For example, stable overexpression of ILEI in mammary epithelial cells has been reported to

be sufficient to promote EMT and enhance tumor growth and lung metastasis upon teil vein injection (Wearner et al., 2006). Although there has been little progress in the analysis of ILEI-dependent signal transduction or identification of the receptor, a recent report has suggested that overexpression of ILEI in hepatocytes is associated with nuclear accumulation of phosphorylated STAT3 (Lahsnig et al., 2009). As a downstream signaling molecule, STAT3 has been shown to be involved in a variety of tumor related functions including proliferation, embryonic cell-renewal, EMT and migration (Niwa et al, 1998; Yamashita et al., 2002).

We have demonstrated that normal mammary epithelial cells which have undergone an EMT in response to modulation of hnRNP E1 expression levels (E1KD cells), and thus modulation of the BAT mRNP complex, acquire an inherent tumorigenic and metastatic capacity concomitant with increased ILEI expression. Given the highly tumorigenic nature of E1KD cells, we decided to address the association between BAT-mediated EMT and the stem-like phenotype. We show that E1KD cells acquire the ability to form mammospheres *in vitro*, and have the ability to regenerate cleared mammary fat pads in mice. Furthermore, we provide evidence suggesting that acquisition of the stem-like phenotype may be mediated by establishment of ILEI paracrine loops and activation of downstream STAT3 signaling.

4.3 Results

Modulation of hnRNP E1 expression in normal mammary gland epithelial cells mediates stem-like characteristics.

To determine whether modulation of hnRNP E1 expression in normal mammary epithelial cells can mediate stem-cell like traits in addition to the EMT phenotype, we utilized flow cytometry analysis to sort cells based on the expression of CD29 (beta1-integrin) and CD24 (heat-stable antigen), two cell-surface markers whose expression in the CD29^{hi}/CD24^{+} pattern is associated with murine mammary gland stem cells (Wang, 2006). As shown (Figure 4.1 A), the mesenchymal E1KD derivative cells acquired a CD29^{hi}/CD24^{+} antigenic phenotype, whereas this shift was not observed in the parental epithelial cell line. These results suggest that normal mammary epithelial cells which have undergone an EMT in response to knockdown of hnRNP E1 expression develop markers associated with mammary gland stem cells.

We next performed mammosphere assays to further assess the stem-like characteristics of the E1KD cells. The mammosphere assay is a culture system in which cells are grown in serum-free and non-adherent conditions. Under these conditions, differentiated epithelial cells will undergo apoptosis in the absence of anchorage to a substratum, whereas stem cells can survive the anchorage independent conditions (Dontu et al., 2005). As demonstrated (Figure 4.1 B), normal mammary gland epithelial cells are unable to form spheres and cannot survive serial passages in mammosphere assay conditions. In contrast, the

E1KD cells readily formed mammospheres and maintain their self renewal capacity over multiple passages.

While the mammosphere assay offers an *in vitro* analysis of the self-renewal capacity of cells, a more rigorous approach for a qualitative analysis of the self-renewal phenotype, and of the capacity to differentiate involves the *in vivo* regeneration of an entire mammary gland ductal tree (Stingl et al., 2005). As diagramed in Figure 4.1 C, the endogenous epithelium is first surgically removed from a 3-week old mammary gland of a virgin female mouse. Cells are then injected into the cleared mammary fat pad and regeneration of a mammary gland ductal tree is assessed after 6 weeks by whole mount staining of the dissected gland. As shown (Figure 4.1D), transplantation of NMuMG cells into cleared mammary fat pads were unable to regenerate the mammary gland ductal tree (Figure 4.1 D; left panel). In contrast, the E1KD cells, which were stably transfected with a constitutively expressed green fluorescent protein (GFP) construct, were validated for their *in vivo* repopulating activity. As demonstrated by whole mount staining and fluorescence microscopy, transplantation of E1KD cells into cleared fat pads were able to regenerate an entire ductal tree (Figure 4.1 D; right panels). These various observations demonstrate that NMuMG cells which have undergone an EMT in response to modulation of hnRNP E1 expression levels, and thus modulation of the BAT mRNP complex, acquire stem-like characteristics associated with mammary gland stem cells.

E1KD cells increase mammosphere formation in normal mammary epithelial cells.

Recent findings have demonstrated that a combination of both autocrine and paracrine signals are required to promote cells to undergo an epithelial-mesenchymal transition in addition to acquiring self-renewal traits associated with stem cells (Scheel et al., 2011). Furthermore, there is now substantial evidence to suggest that mesenchymal and cancer stem cells are able to promote mammosphere formation in normal epithelial cells by establishment of cytokine networks and microenviromental signals which effect signaling and promote cell survival (Klopp et al., 2010; Liu et al., 2011; Korkaya et al., 2011). Given these finding, we sought to test the hypothesis that secreted factors from E1KD cells in conditioned media can mediate mammosphere formation in normal mammary epithelial cells by establishing paracrine signaling networks. To test this hypothesis, NMuMG cells stably transfected with a constitutively expressed red fluorescent protein (RFP) construct, and E1KD-GFP cells were initially co-cultured in various proportions in a mammosphere assay (Figure 4.2 A, B). NMuMG cells plated with E1KD cells were found to interact as spheres as early as day three after plating and displayed a dose-dependent increase in mammosphere formation (Figure 4.2 A). In addition, fluorescence microscropy validated the proportional presence of NMuMG-RFP and E1KD-GFP cells in the mammospheres (Figure 4.2B).

We next investigated whether direct cell contact between E1KD and NMuMG cells was required by determining the effect of E1KD conditioned media

(E1KD-CM) on mammosphere formation. E1KD-CM was generated by growing E1KD cells in mammosphere culture conditions for 7 days. NMuMG cells were then plated in mammosphere culture with an increasing percentage of volume of E1KD-CM (Figure 4.2 C, D). In comparison to E1KD cells, NMuMG cells alone were not able to form mammospheres (Figure 4.2 C, D). However, a dose-dependent increase in mammosphere formation was detected when NMuMG cells were plated with as little as 10% E1KD-CM. These results suggested that E1KD secreted factors could mediate the acquisition of the self-renewal phenotype required for mammosphere growth.

Evidence for ILEI and Stat3 phosphorylation in mediating hnRNP E1 effects on mammosphere formation.

EMT-associated signaling pathways, including TGFβ and Wnt signaling, have been shown to mediate both the EMT phenotype and the acquisition of self-renewal and stem-like characteristics in normal mammary epithelial cells (Scheel et al., 2011). In addition, it has been demonstrated that mesenchymal stem cells can stimulate a variety of tumor-related functions including proliferation, cell renewal, EMT, and metastasis through the paracrine production of cytokines such as secreted IL6 and activation of STAT3 signaling (Liu et al., 2011). Given the ability of E1KD-CM to support mammosphere growth of normal mammary epithelial cells, we hypothesized that promotion and maintenance of the stem-cell state may depend on activation of similar paracrine loops. Initially, we analyzed activation of STAT3 signaling in NMuMG and E1KD cells by immunoblot analysis (Figure 4.3 A). Treatment of NMuMG cells with TGFβ induced phosphorylation of

STAT3 in a time-dependent manner, whereas STAT3 was constitutively phosphorylated in the E1KD cell line irrespective of TGFβ-treatment. In addition, STAT3 phophorylation was shown to be inhibited in NMuMGs in the presence of LY294002, a PI3K inhibitor (Figure 4.3 A). These results suggested that STAT3 activation may be caused by effectors downstream of the BAT mechanism since phosphorylation of STAT3 was mediated by modulation of hnRNP E1 expression levels, and displayed a TGFβ-dependent and LY2940042-sensitive increase in NMuMG cells.

Our work (Chaudhury et al., 2010), and those of others (Wearner et al., 2006), have shown that ILEI is indispensable during TGFβ-mediated EMT. Although the exact mechanism for how ILEI exerts its biological effects is not completely understood, a recent report has implicated STAT3 as a downstream signaling molecule of ILEI (Lahsnig et al., 2009). To determine whether ILEI may be playing a role in the observed stem-like phenotype, we performed a comparative analysis of ILEI secretion in E1KD and NMuMG conditioned media from cells grown on either adherent plates in normal growth media, or from cells cultured in mammosphere conditions. NMuMG or E1KD cells were seeded on adherent dishes and treated ±TGFβ (24h). After washing with PBS, the cells were incubated an additional 18h in serum-free media. The media was then collected, separated by SDS-PAGE, and subjected to immunoblot analysis. As shown in Figure 4.3B, endogenous and secreted levels of ILEI were induced by TGFβ-stimulation in NMuMG cells, whereas ILEI expression and secretion was constitutive in E1KD derivative cells irrespective of TGFβ-treatment. Next, we

assessed the presence of ILEI by sandwich ELISA from media conditioned by either NMuMG or E1KD cells grown in mammosphere conditions. As shown in Figure 4.3C, ILEI secretion was significantly higher in the E1KD conditioned mammosphere media compared to the NMuMG mammosphere conditioned media. Additionally, ILEI could be successfully immunodepleted from the E1KD conditioned media (Figure 4.3 C).

We next investigated whether E1KD conditioned mammosphere media (E1KD-CM), could induce STAT3 phosphorylation. NMuMG cells treated with E1KD-CM for various times displayed a time-dependent increase in phospo-STAT3 levels as early as 5 minutes, whereas total STAT3 levels remained unaffected. We next assessed whether immunodepletion of ILEI from the E1KD-CM media could prevent STAT3 phosphorylation. NMuMG and E1KD cells treated ±TGFβ (24h), and NMuMG cells treated with either E1KD-CM or ILEI-immunodepleted E1KD-CM were subjected to SDS-PAGE and immunoblot analysis. As shown (Figure 4.3 E) TGFβ-stimulation induced STAT3 phosphorylation in NMuMG cells, whereas phospho-STAT3 levels were constitutively high in the E1KD cells irrespective of TGFβ-treatment. Comparitively, NMuMG cells treated with E1KD-CM were able to induce STAT3 phosphorylation, whereas immunodepletion of ILEI from E1KD-CM prevented STAT3 phosphorylation. Taken together, these results provided evidence suggesting that ILEI may play a role in mediating hnRNP E1 effects on mammosphere formation *via* activation of STAT3 signaling.
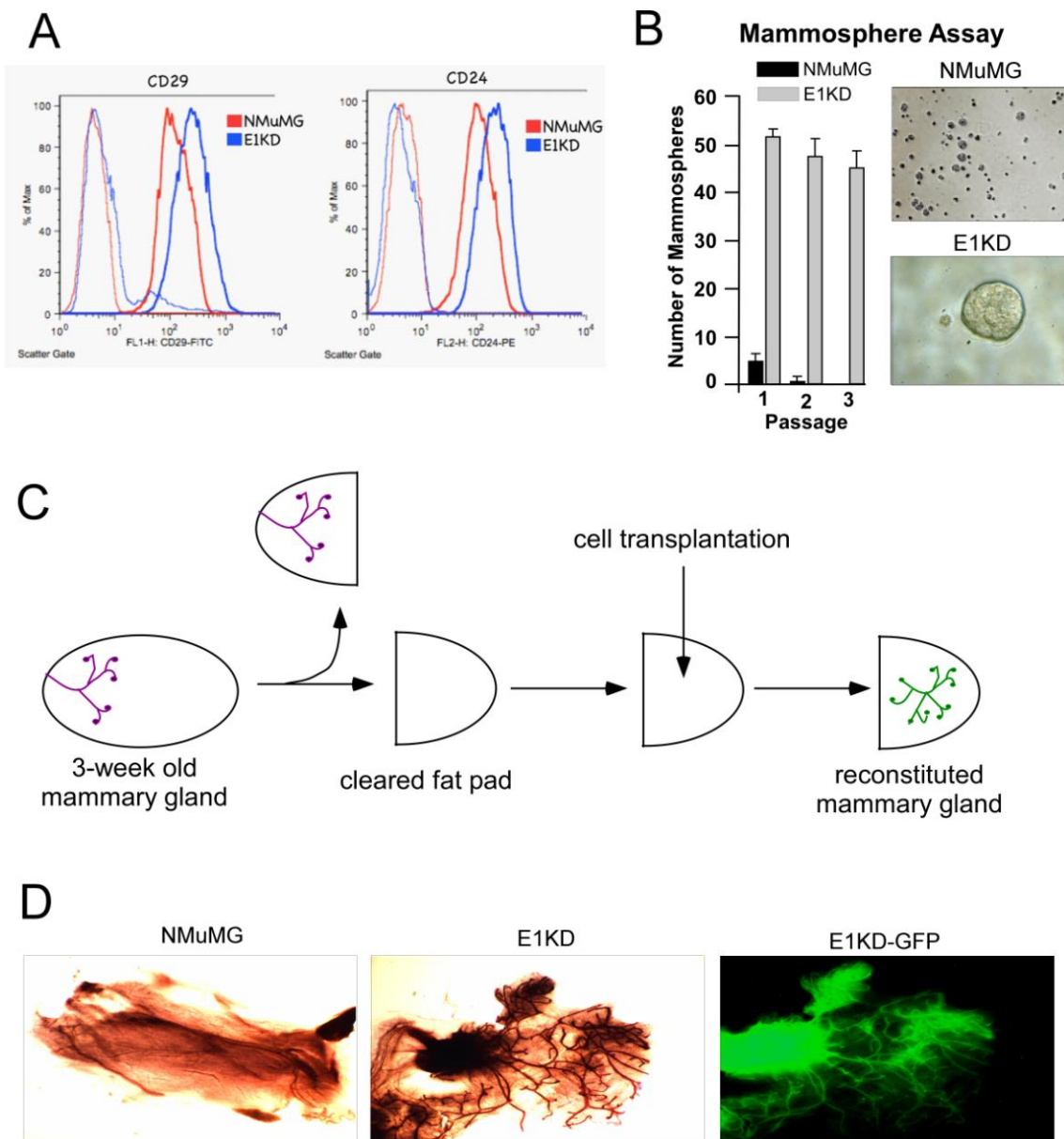
Figure 4.1: Modulation of hnRNP E1 expression in normal mammary gland epithelial cells mediates stem-like characteristics. (A) Single cell suspensions of NMuMG or E1KD cells were stained with cell surface markers CD29-FITC or CD24-PE antibodies and analysed by flow cytometry. (B) Bar graph depicted number of mammospheres formed over multiple passages by NMuMG or E1KD cells (left); Phase-contrast images of mammospheres seeded by NMuMG or E1KD cells (right). (C) Diagram depicting mammary gland repopulation assay. (D) Mammary gland repopulation by 5,000 cells. Results of whole-mount analysis at 6 wks after transplant.
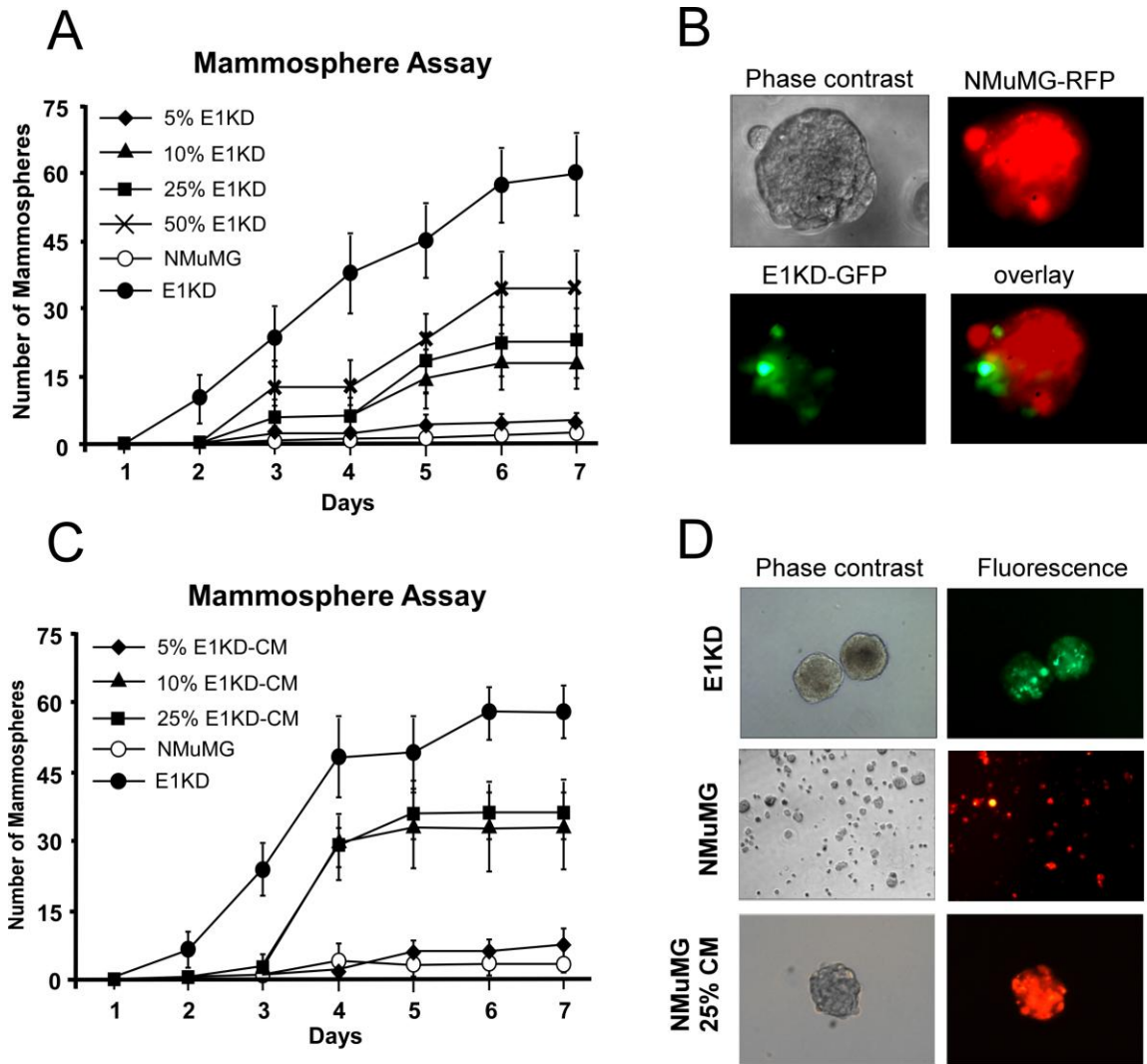
Figure 4.2: E1KD secreted factors mediate the acquisition of the self-renewal phenotype required for mammosphere growth. (A) Number of NMuMG mammospheres formed when plated in mammosphere co-cultures increased with an increasing percentage of E1KD as compared to NMuMG cells alone. (B). Low-magnification image of NMuMG-RFP and E1KD-GFP cells (4:1 co-culture) demonstrating integrated mammosphere formation. (C) Number of NMuMG spheres after plating in the presence of an increasing percentage of volume of E1KD-CM. (D) Images of suspension cultures of E1KD spheres (top panels) or NMuMG suspensions cultures with and without 25% E1KD-CM (bottom panels).
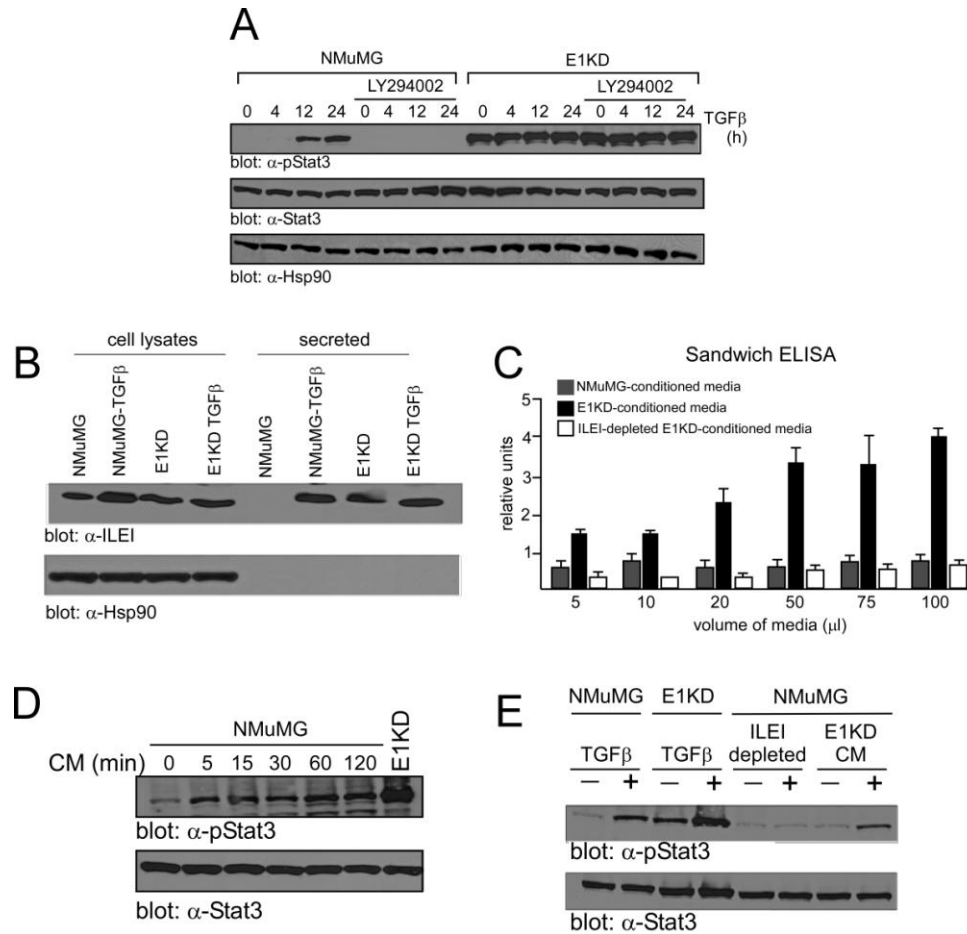
Figure 4.3: Evidence for ILEI and Stat3 phosphorylation in mediating hnRNP E1 effects on mammosphere formation. (A) Immunoblot analysis examining total STAT3 (α-stat3) expression levels, phorphorylation of STAT3 (α-pStat3) and α-Hsp90 (control) in lysates prepared from NMuMG cells treated ± TGFβ for the times indicated in the presence or absence of LY294002. (B) NMuMG or E1KD cells were seeded on adherent dishes and treated ±TGFβ (24h). After washing with PBS, the cells were incubated an additional 18h in serum-free media. The media was then collected, separated by SDS-PAGE, and subjected to immunoblot analysis using α-ILEI, and α-Hsp90 (control) and compared to endogenous levels of ILEI. (C) NMuMG or E1KD conditiond media (CM) was generated by growing cells in mammophere assays for 7 days. Sandwich EISA was used to examine the levels of ILEI in NMuMG-CM, E1KD-CM, or E1KD-CM immunodepleted of ILEI. (D) Immunoblot analysis examining total STAT3 (α-stat3) expression levels, and phorphorylation of STAT3 (α-pStat3) in lysates prepared from NMuMG cells treated with E1KD-CM for the times indicated. E1KD cell lysate was used as a control. (E) Immunoblot analysis examining total STAT3 (α-stat3) expression levels, and phorphorylation of STAT3 (α-pStat3) in lysates prepared from NMuMG and E1KD cells treated ±TGFβ (24h), or NMuMG cells treated with E1KD-CM or ILEI-depleted E1KD-CM.

103

4.4 Discussion

Numerous reports have implicated breast cancer stem cells as a critical target for novel cancer therapeutics given their significant role in the initiation, propagation, recurrence, and therapeutic failures of breast cancer (Morrison et al., 2008; Massard et al., 2006; Ohno et al., 2003; Piccirillo et al., 2006). Thus, an understanding of the molecular mechanisms involved in the regulation of breast cancer stem cells is necessary in order to design effective therapeutic strategies. Recent reports have provided evidence suggesting that the acquisition of the tumorigenic and stem-cell phenotype during the metastatic progression of carcinoma is driven by an epithelial-mesenchymal (EMT) induction (Mani et al., 2008; Morel et al., 2008). EMT, which was initially studied as a feature of embryonic development, is also presumed to be required for tumor invasion and metastasis of carcinoma cells, and is believed to be governed by complex cytokine and growth factor networks influenced by signals from the neoplastic microenvironment (Scheel et al., 2011).

An important finding that is built upon in this study is that a single factor, hnRNP E1, is responsible for silencing a TGFβ-mediated EMT program through the collaborative effort of a regulatory BAT element in select transcripts. We have previously shown that knockdown of hnRNP E1 in mammary epithelial cells mediates not only the acquisition of an EMT phenotype, but also causes these otherwise normal, non-invasive epithelial cells to display an inherent tumorigenic and metastatic capacity. By utilizing a translational-state microarray analysis, we have identified a cohort of translationally regulated mRNAs that are upregulated

during TGFβ-induced EMT including known effectors of EMT such as *Moesin*, *Activin A*, and *Interleukin-like EMT Inducer* (ILEI). Thus the delineation of the role of this EMT gene signature may aid in elucidating the downstream cellular pathways that are affected by activation of silenced EMT-transcripts. In the present study, we provide evidence that normal mammary epithelial cells which have undergone an EMT in response to modulation of hnRNP E1 expression levels (E1KD cells), and thus modulation of the BAT mRNP complex, acquire the ability to form mammospheres *in vitro*, and have the ability to regenerate cleared mammary fat pads in mice, properties which are associated with cancer stem cells. Furthermore, we demonstrate that E1KD cells can effectively enrich and condition their culture medium with secreted factors that mediate increased mamosphere formation in normal mammary epithelial cells. One of the secreted factors identified in the E1KD-conditioned media was the BAT-regulated and EMT-facilitating transcript ILEI.

In terms of its biological function, several reports have demonstrated that stable overexpression of ILEI can mediate an enhanced tumorigenic and invasive phenotype accompanied by nuclear accumulation of phosphorylated STAT3 (Wearner et al., 2006; Lahsnig et al., 2009), however, the molecular mechanism by which ILEI exerts is biological effects is not understood. Progress in the identification of the ILEI receptor has been complicated by our current inability to produce a sufficient biologically active form of ILEI for *in vitro* studies. Despite these limitations, our finding that constitutive ILEI secretion by E1KD cells is sufficient to elicit a biological reponse, as evidenced by induction of STAT3

105

phosphorylation, may allow for a more detailed interrogation and manipulation of the ILEI-dependent signal transduction pathway.

The preliminary results presented in the current study provide evidence for a unique mechanism whereby EMT induction could elicit a stem-like phenotype through the establishment of ILEI-induced STAT3 signaling. Activation of STAT3 as a downstream signaling molecule of ILEI offers an attractive scenario given the role of STAT3 during induction of EMT (Huang et al., 2011) and in self-renewal of pluripotent embryonic stem cells (Niwa et al., 1998). Interestingly, a recent report has demonstrated that in malignant glioma-initiating cells (GIC), TGFβ promotes oncogenesis and increases GIC self-renewal through the Smad-dependent induction of LIF and the JAK-STAT pathway (Penuelas et al., 2009). Comparable to E1KD cells, GICs are characterized by their highly oncogenic potential, self-renewal and multilineage differentiation properties, and their ability to generate neurospheres. Similarly, our findings that shRNA-mediated knockdown of hnRNP E1 results in increased mammosphere formation and the ability to repopulate a mammary ductal tree through multilineage differentation, may be indicative of activated downstream STAT3 transcriptional programs mediating the acquisition of a stem-cell like phenotype. Future studies are needed, however, to determine the exact role that ILEI plays in either the promotion or maintenance of the stem-like phenotype observed in hnRNP E1 knockown cells. One would hypothesize that modulation of ILEI expression in E1KD cells may attenuate not only STAT3 activation but may also modify the self-renewal ability and capacity for multilineage differentiation. Attenuation of the

BAT mRNP complex *via* TGFβ/Akt2-mediated phosphorylation of hnRNP E1, or by modulation of hnRNP E1 expression may therefore represent a critical checkpoint in the downstream activation of cytokine networks governing acquisition of self-renewal properties during tumorigenesis and metastatic progression.

4.5 Materials and Methods

Reagents: Mouse α-ILEI was obtained from Abcam. α-pStat3 and α-Stat3 were obtained from Cell Signaling Technology. α-Hsp90 and normal mouse IgG were purchased from Santa Cruz Biotechnology. Secondary antibodies, α-mouse and α-rabbit-IgG-HRP were obtained from GE Healthcare Bio-Sciences. α-CD29-FITC conjugated and α-CD24-PE conjugated antibodies were obtained from BD Biosciences.

Cell culture and treatments: NMuMGs were maintained in Dulbecco's modified Eagle's medium supplemented with 10% fetal bovine serum, 10 mg/ml insulin, and antibiotics/antimycotics (100 units/ml penicillin G, 100 mg/ml streptomycin, and 0.25 mg/ml amphotericin B). E1KD (previously termed SH14) were generated in the laboratory and have been described (Chaudhury et al., 2010). TGFβ2 was a generous gift from Genzyme Inc. and was used at a final concentration of 5 ng/ml. Where indicated, cells were treated with 10 μM of LY294002 30 min before TGFβ treatment.

Flow cytometry analyses: Single cell suspensions were subjected to flow cytometry analysis on a FACS Aria instrument (BD Biosciences) using standard protocols.

Mammosphere culture: Single-cell suspensions were grown in 100 μl/well of DMEM:F12 medium with 1:50 B27 (Invitrogen), 20 ng/mL EGF, 20 ng/mL basic fibroblast growth factor (bFGF) in Corning Costar 3474 96-well plates at a density of 5,000 cells/mL. Mammospheres were collected by 70-μm

strainer and dissociated with 0.05% trypsin for 15 min to obtain single-cell suspension.

Transplantation and mammary gland whole mounts: Three-week old females of NSG mice were used as recipients. Their inguinal mammary glands were surgically cleared of the endogenous epithelium as described (Brill et al., 2008). 5000 cells were injected into the cleared fat pads using a 50-μL Hamilton syringe. After 6 weeks, the glands were dissected and the whole mounting was done as described (Landua et al., 2009).

Immunodepletion of E1KD conditioned media: E1KD conditioned media (E1KD-CM) was generated by growing E1KD cells in mammosphere media for 7 days. 0.5ml E1KD-CM was incubated with 10μg α-ILEI and 100μl protein A sepharose overnight. Immunodepletion was repeated three times.

Sandwich ELISA: E1KD and NMuMG mammosphere culture media was collected after 7 days, and ILEI levels were determined by sandwich ELISA. The ELISA plates were coated with α-ILEI (Abcam, ab88337) at 10μg/ml in carbonate buffer, pH 9.3. After overnight incubation at 4°C, excess antibody was washed off with PBST (PBS containing 0.05% Tween-20), and the plates were blocked by the addition of 3% BSA in PBS. Samples were added and incubated overnight at 4°C. Plates were washed again with PBST, and α-ILEI antibody (Abcam, ab56065) was added at 10 μg/ml. After incubation at room temperature for 2 h, the plates were washed three times with PBST and incubated IgG-alkaline phosphatase (1:10,000), followed by 1 mg/ml of *p*-nitrophenyl phosphate (Sigma). The absorbance was read after 30 min at 405 nm.

4.6 Literature Cited

Al-Hajj, M., Wicha, M.S., Benito-Hernandez, A., Morrison, S.J., and Clarke, M.F. (2003) Prospective identification of tumorigenic breast cancer cells. Proc. Natl. Acad. Sci. USA 100, 3983–3988

Brabletz T, Jung A, Spaderna S, Hlubek F and Kirchner T (2005) Migrating cancer stem cells – an integrated concept of malignant tumor progression. *Nat Rev* 5:744-749.

Derynck R, Akhurst RJ, Balmain A (2001) TGF-beta signaling in tumor suppression and cancer progression. *Nature Genet* 29:117-29.

Dontu, G., Abdallah, W.M., Foley, J.M., Jackson, K.W., Clarke, M.F., Kawamura, M.J., Wicha, M.S. (2003) In vitro propagation and transcriptional profiling of human mammary stem/progenitor cells. Genes Dev. 17:1253–1270.

Huang C, Yang G, Jiang T, Zhu G, Li H, Qiu Z (2011) The effects and mechanisms of blockage of STAT3 signaling pathway on IL-6 inducing EMT in human pancreatic cancer cells in vitro. Neoplasma 58:396-405.

Korkaya H, Liu S, Wicha MS (2011) Regulation of cancer stem cells by cytokine networks: Attacking cancer inflammatory roots. Clin Cancer Res 17:6125-6129.

Klopp AH, Lacerda L, Gupta A, Debeb BG, Solley T, et al. (2010) Mesenchymal stem cells promote mammosphere formation and decrease E-cadherin in normal malignant breast cells. PLoS One 5(8):e12180.

Lahsnig C, Mikula M, Petz M, Zulehner G, Schneller D, et al. (2008) ILEI requires oncogenic Ras for the epithelial to mesenchymal transition of hepatocytes and liver carcinoma progression. Oncogene 28:638-650.

Liao MJ, Zhang CC, Zhou B, Zimonjic DB, Mani SA, et al. (2007) Enrichment of a population of mammary gland cells that form mammospheres and have in vivo repopulating activity. Cancer Res. 67:8131-8138.

Liu S, Ginestier C, Ou SG, et al (2011) Breast cancer stem cells are regulated by mesenchymal stem cells through cytokine networks. Cancer Res 71:614-624.

Mani, S.A., Guo, W., Liao, M.J., Eaton, E.N., Ayyanan, A., Zhou, A.Y., Brooks, M., Reinhard, F., Zhang, C.C., Shipitsin, M., et al. (2008). The epithelial-mesenchymal transition generates cells with properties of stem cells. Cell 133, 704–715.

Massard C, Deutsch E, Soria JC (2006) Tumour stem cell-targeted treatment: elimination or differentiation. *Ann Oncol* **17:**1620-1624.

Morel, A.P., Lie` vre, M., Thomas, C., Hinkal, G., Ansieau, S., and Puisieux, A. (2008). Generation of breast cancer stem cells through epithelial-mesenchymal transition. PLoS ONE 3, e2888.

Morrison BJ, Schmidt CW, Lakhani SR, Reynolds BA, Lopez JA (2008) Breast cancer stem cells: implications of breast cancer. Breast Cancer Res 2008, **10**:210-15.

Niwa H et al. (1998) Self-renewal of pluripotent embryonic stem cells is mediated via activation of STAT3. Genes Dev, 12:2048-2060.

O'Brien, C.A., Pollett, A., Gallinger, S., and Dick, J.E. (2007) A human colon cancer cell capable of initiating tumour growth in immunodeficient mice. Nature 445, 106–110.

Ohno R, Asou N, Ohnishi K (2003) Treatment of acute promyelocytic leukemia: strategy toward further increase of cure rate. Leukemia 17:1454-1463.

Penuelas S, Anido J, Preito-Sanchez RM, Folch G, Barba I, et al. (2009) TGF-b increases glioma-initiating cell self-renewal through the induction of LIF in human glioblastoma. Cancer Cell 15:315-327.

Piccirillo SG, Reynolds BA, Zanetti N, Lamorte G, Binda E, Broggi G, Brem H, Olivi A, Dimeco F, Vescovi AL (2006) Bone morphogenetic proteins inhibit the tumorigenic potential of human brain tumour-initiating cells. Nature 444:761-765

Ricci-Vitiani, L., Lombardi, D.G., Pilozzi, E., Biffoni, M., Todaro, M., Peschle, C., De Maria, R. (2007) Identification and expansion of human coloncancer-initiating cells. Nature 445, 111–115.

Scheel C, Eaton EN, Li SH, Chaffer CL, Reinhardt F, et al. (2011) Paracrine and autocrine signals induce and maintain mesenchymal and stem cell states in the breast. Cell 145:926-90.

Singh, S.K., Hawkins, C., Clarke, I.D., Squire, J.A., Bayani, J., Hide, T., Henkelman, R.M., Cusimano, M.D., and Dirks, P.B. (2004). Identification of human brain tumour initiating cells. Nature 432, 396–401.

Stingl J, Raouf A, Emerman JT, Eaves CJ (2005) Epithelial progenitors in the normal human mammary gland. J Mammary Gland Biol Neoplasia 10:49–59.

112

Thiery, J.P., and Sleeman, J.P. (2006) Complex networks orchestrate epithelial-mesechymal transitions. *Nature Rev. Mol. Cell. Biol.* 7, 131-142.

Visvader JE and Lindeman GJ (2006) Mammary stem cells and mammopoiesis. Cancer Res. 66:9798-9801.

Waerner, T., Alacakaptan, M., Tamir, I., Oberauer, R., Gal, A., Brabletz, T., Schreiber, M., Jechlinger, M., and Beug H. (2006) ILEI: A cytokine essential for EMT, tumor formation, and late events in metastasis in epithelial cells. *Cancer Cell* 10, 227-239.

Wang, RH (2006) The new portrait of mammary gland stem cells. *Int. J. Biol. Sci.* 2:186-187.

Yamashita S, Miyagi C et al. (2002) STAT3 controls cell movements during Zebrafish Gastrulation. Dev. Cell 2L363-375.

Zhu, Y., Xu, G., Patel, A.,McLaughlin, M.M., Silverman, C., Knecht, K., Sweitzer, S., Li, X., McDonnell, P., Mirabile, R., et al. (2002). Cloning, expression, and initial characterization of a novel cytokine-like gene family. Genomics 80: 144–150.

Zavadil, J., and Bottinger, E.P. (2005) TGF-β and epithelial-to-mesenchymal transitions. *Oncogene* 24, 5764-5774.

CHAPTER V

GENERAL SUMMARY

Tumor metastasis is the most common cause of mortality in cancer patients (Ma et al., 2010). Understanding the molecular mechanisms that cause tumors to metastasize can provide critical knowledge that is necessary for the development of targeted therapies that have a distinct mechanism separate from conventional therapeutics. One approach that has yielded important information in regards to gene function during tumorigenesis and metastatic progression involves strategies that focus on tumor phenotype and transcriptional array analysis aimed at identifying cancer-specific 'signature genes'. However, given the significant phenotypic heterogeneity in some tumor types and the fact that mRNA expression profiling (i.e., the transcriptome) does not accurately mirror the proteome, these approaches often neglect the role of post-transcriptional control in gene expression (Moore 2005). It has become evident that the 5´-and 3´-

untranslated regions (UTRs) of mRNA transcripts can significantly impact gene expression (Merrit et al., 2008).

Gene expression is regulated at multiple synthetic and degradative steps including transcription, splicing, mRNA transport, mRNA stability, translation, protein stability and post-translational modification (Hay and Sonenberg, 2004). Translational control has recently attracted much attention and has been demonstrated to regulate varied physiological processes, such as proliferation, differentiation, cellular stress, inflammation and carcinogenesis, and at a cellular level, it is postulated to be energetically and kinetically more efficient, allowing for more well defined and rigorous regulatory checkpoints (Ruggero et al., 2003; Sampath et al., 2004; Standart and Jackson, 1994). Efficient mRNA translation requires a series of protein–mRNA and protein–protein interactions. Structural elements of the mRNA, including the 5′ cap, 5′-UTR, 3′-UTR and poly(A) tail, are important determinants of these interactions, and have been implicated in translational regulation (Mazumder et al., 2003). In particular, structural elements in 5′-or 3′-UTRs of mRNAs have been shown to be involved in transcript-specific translational control, and there is accumulating evidence for the special role of 3′-UTR cis-regulatory elements during regulation of mRNA localization, stability and translation initiation (Ostareck et al., 1997; Sachs et al., 1997; Zoladek et al., 1995). In addition, post-transcriptional regulation of gene expression requires trans-acting factors consisting of RNA-binding proteins and noncoding RNAs that affect splicing, nuclear export, decay, cellular localization and translation (Varani and Nagai, 1998; Cusack, 1999). Identification of RNAs associated with RNA-

binding proteins in a cellular context is paramount to our understanding of the post-transcriptional control of gene expression, and expression profiling on a genome-wide scale is a commonly employed method aimed at identifying RNAs regulated post-transcriptionally (Keene and Lager, 2005).

Our studies (Chaudhury et al., 2010; Hussey et al., 2011) and those of others (Waerner et al., 2006; Wang et al., 2010) have demonstrated that regulation of gene expression at the post-transcriptional level plays an indispensable role in TGF-β-induced epithelial–mesenchymal transition (EMT) and metastasis. It has become evident that cancer cells can dedifferentiate through activation of specific biological pathways associated with EMT, gaining the ability to migrate and invade. Thus, EMT has emerged not only as a fundamental process during normal embryonic development and in adult tissue homeostasis, but has also been demonstrated to be essential for metastatic progression (Derynck et al., 2001; Thiery and Sleeman, 2006; Zavadil and Bottinger, 2005). EMT is associated with changes in cell–cell adhesion, remodeling of the extracellular matrix and enhanced migratory activity; all properties that enable tumor cells to metastasize. Numerous cytokines and auto-crine growth factors, including TGF-β, have been implicated in EMT (Bierie and Moses, 2006).

We have identified a transcript-selective translational regulatory pathway in which a ribonucleoprotein (mRNP) complex, consisting of heterogeneous nuclear ribonucleoprotein E1 (hnRNP E1) and eukaryotic elogation factor 1-A1 (eEF1A1), binds to a 3′-UTR regulatory TGFβ-activated translation (BAT)

element and silences translation of Disabled-2 (*Dab2*) and Interleukin-like EMT-inducer (*ILEI*), two mRNAs involved in mediating EMT. TGF-β activates a kinase cascade terminating in the phosphorylation of hnRNP E1 by isoform-specific stimulation of protein kinase B/Akt2, which induces the release of the mRNP complex from the 3´-UTR element, resulting in the reversal of translational silencing and increased expression of *Dab2* and *ILEI* transcripts (Chaudhury et al., 2010). We have previously shown that shRNA-mediated silencing of Dab2 and ILEI in normal murine mammary gland (NMuMG) cells is sufficient to inhibit TGFβ-mediated EMT as analyzed morphologically and by loss of upregulation of N-cadherin and vimentin, mesenchymal cell markers, whereas their overexpression does not induce constitutive EMT, independent of TGFβ signaling (Chaudhury et al., 2010; Prunier and Howe, 2005). Thus Dab2 and ILEI are required, but not sufficient, for TGFβ-induced EMT. Hence, we, and others based on our studies (Evdokimova, 2012), hypothesized that there are other mRNAs that are being silenced by hnRNP E1 in a similar fashion, and which cumulatively contribute to TGFβ-induced EMT. By utilizing a translational-state microarray analysis (also known as polysome profiling), in which differential sedimentation is used to separate the nontranslating, nonpolysomal pool of transcripts from the actively translating, polysome-associated transcripts, and intersecting this data with a RIP-Chip analysis, we have identified a cohort of translationally regulated mRNAs that are upregulated during TGFβ-induced EMT and follow the same pattern of regulation as Dab2 and ILEI.

Mechanistically, we have delineated a novel transcript-selective translational pathway and demonstrated that two proteins, hnRNP E1 and eEF1A1, constitute an mRNP complex that binds to the 3′-UTR of these mRNAs and regulates their translation in a TGFβ-dependent manner (Hussey et al., 2011). This represents an unusual case of agonist- or stimulus-dependent upregulation of translation through a 3′-UTR element. Our data also suggest that TGFβ-regulated translation is mediated through eEF1A1 function during the translational elongation step as opposed to numerous other examples where translational control occurs at the initiation step (Curtis et al., 1995; Beckman et al., 2005; van der Kelen et al., 2009). Thus, analysis and elucidation of this post-transcriptional regulatory pathway is of note in that it allowed for the identity of 'EMT signature' genes.

These findings may also have significant implications towards potential prognostic and clinical applications. Our data demonstrate that Akt2-mediated phosphorylation of Ser43 of hnRNP E1 is a trigger for the release of binding and translational silencing mediated by the mRNP complex through the 3′-UTR of 'EMT inducer' mRNAs. Thus, Ser43 represents a key regulatory site; in the dephosphorylated state it mediates translational silencing, whereas its phosphorylation, in response to TGFβ, relieves translational silencing and allows transition to the mesenchymal phenotype. If, in fact, the EMT transition is reflective of the metastatic process, then one might predict that the phosphorylation status of Ser43 may be indicative of metastatic progression and the prognosis of patients.

Investigation and modulation of the EMT process has been the focus of intense investigation, yet few confirmed and *bona fide* EMT mediators have been identified (Kang and Massagu, 2004; Pradet-Balade et al., 2001; Ramswamy et al., 2003). We postulate that the continued delineation of the role of the identified target transcripts during EMT and the development of modulators of the BAT translational regulatory pathway will allow for its interrogation and manipulation during the EMT transition in physiological and pathological situations. However, further studies are needed to understand this transcript-selective translational pathway in human patients, as opposed to cultured cell lines, and for its potential manipulation through targeted therapeutics.

BIBLIOGRAPHY

Afti A, Djelloul S, Chastre E, Davis R, and Gespach C (1997) Evidence for a role of Rho-like GTPases and stress-activated protein kinase/c-Jun N-terminal kinase (SAPK/JNK) in transforming growth factor beta-mediated signaling. *J. Biol. Chem.* 272: 1429-1432.

Beckmann K, Grskovic M, Gebauer F *et al.* (2005) A dual inhibitory mechanism restricts msl-2 mRNA translation for dosage compensation in *Drosophila. Cell* 122, 429–540.

Bierie, B., and Moses, H.L. (2006) TGF-β and cancer. *Cytokine Growth Factor Rev.* 17, 29-40.

Black BL, Lu J, and Olsen EN (1997) The MEF2A 3' untranslated region functions as a cis-acting translational repressor. *Mol. Cell. Biol.* 17: 2756-2763.

Brabletz T, Jung A, Spaderna S, Hlubek F and Kirchner T (2005) Migrating cancer stem cells – an integrated concept of malignant tumor progression. *Nat Rev* 5:744-749.

Brown V, et al. (2001) Microarray identification of FMRP-associated brain mRNAs and altered mRNA translational profiles in fragile X syndrome. *Cell* 107:477-87.

Buck E, Eyzaguirre A, Barr S, Thompson S, Sennello R, Young D, Iwata KK, Gibson NW, Cagnoni P, and Haley JD (2007) Loss of homotypic cell adhesion by epithelial-mesenchymal transition or mutation limits sensitivity to epidermal growth factor receptor inhibition. *Mol. Cancer Ther.* 6:532-541.

Chaudhury, A., Hussey, G.S., Ray, P.S., Jin, G., Fox, P.L., and Howe, P.H. (2010) TGFβ-mediated phosphorylation of hnRNP E1 induces EMT via transcript-selective translational induction of Dab2 and ILEI. *Nat. Cell Biol.* 12, 286-293.

Curtis D, Lehmann R, Zamore PD (1995) Translational regulation in development. *Cell* 81, 171–178.

Cusack S (1999) RNA–protein complexes. *Curr. Opin. Struct. Biol.* 9, 66–73.

De Moor CH and Richter JD (1999) Cytoplasmic polyadenylation elements mediate masking and unmasking of cyclin B1 mRNA. *EMBO J.* 18: 2294-2304.

De Moor CH, Meijer H, and Lissenden S (2005) Mechanisms of translation control by the 3'-UTR in development and differentiation. *Sem. Cell Dev. Biol.* 16: 49-58.

Derynck R, Akhurst RJ, Balmain A (2001) TGF-beta signaling in tumor suppression and cancer progression. *Nature Genet* 29:117-29.

Fu L and Benchimol S (1997) Participation of the human p53 3'UTR in translational repression and activation following γ-irradiation. *EMBO J.* 16: 4117-4125.

Gebauer F and Hentze MW (2004) Molecular mechanisms of translational control. *Nat. Rev. Mol. Cell Biol.* 5: 827-835.

Hanafusa H, Ninomiya-Tsuji J, Masuyama N, Nishita M, Fujisawa J, Shibuya H, Matsumoto K, and Nishida E (1999) Involvement of the p38 mitogen-activated

protein kinase pathway in transforming growth factor-beta-induced gene expression. *J. Biol. Chem.* 274: 27161-27167.

Hartsough MT and Mulder K (1995) Transforming growth factor beta activation of p44mapk in proliferating cultures of epithelial cells. *J. Biol. Chem.* 270: 7117-7124.

Hay N and Sonenberg (2004) Upstream and downstream of mTOR. *Genes Dev* 18:1926-1945.

Hieronymus H, Silver PA (2004) A systems view of mRNP biology. *Genes Dev* 18:2845-60.

Hocevar, B.A., Brown, T.L., and Howe, P.H. (1999) TGF-β induces fibronectin synthesis through a c-Jun N-terminal kinase-dependent, Smad4-independent pathway. *EMBO J.* 18,1345-1356.

Hocevar BA, Smine A, Xu XX, and Howe PH (2001) The adaptor molecule Disabled-2 links the transforming growth factor beta receptors to the Smad pathway. *EMBO J.* 20: 2789-2801.

Hocevar BA, Prunier C, and Howe PH (2005) Disabled-2 (Dab2) mediates transforming growth factor beta (TGFbeta)-stimulated fibronectin synthesis through TGFbeta-activated kinase 1 and activation of the JNK pathway. *J. Biol. Chem.* 280: 25920-25927.

Holcik M and Sonenberg N (2005) Translational control in stress and apoptosis. *Nat. Rev. Mol. Cell Biol.* 6: 318-327.

Howe P (2003) Transforming growth factor beta (Chapter 49). *The cytokine Handbook, 4ᵗʰ Edition. Volume2*; 1119-1152. Edited by Angus W. Thomson & Michael T. Lotze. Academic Press (Elsevier Science), London, UK.

Hussey GS, Chaudhury A, Dawson AE, Lindner DJ, Knudsen CR, Wilce MC, Merrick WC, Howe PH (2011) Identification of an mRNP complex regulating tumorigenesis at the translational elongation step. *Mol Cel.* 41(4):419-431.

Izquierdo JM and Cuezva JM (1997) Control of the translational efficiency of beta-F1-ATPase mRNA depends on the regulation of a protein that binds the 3' untranslated region of the mRNA. *Mol. Cell. Biol.* 17: 5255-5268.

Kang Y, Massague J (2004) Epithelial-mesenchymal transitions: twist in development and metastasis. *Cell* 118:277-9.

Keene JD, Lager PJ (2005) Post-transcriptional operons and regulons coordinating gene expression. *Chromosome Res* 13:327-37.

Ma, L, et al. (2010) miR-9, a MYC/MYCN-activated microRNA, regulates E-cadherin and cancer metastasis. *Nat Cell Biol* 12, 247-256.

Mazumder, B, and Fox, PL (1999) Delayed translational silencing of ceruloplasmin transcript in γ interferon-activated U937 monocytic cells: role of the 3' untranslated region. *Mol. Cell. Biol.* 19, 6898-6905.

Mazumder, B, Seshadri, V, and Fox, PL (2003) Translational control by the 3'-UTR: the ends specify the means. *TRENDS in Biochemical Sciences.* 28, 91-98.

Mbongolo Mbella EG, Bertrand S, Huez G, and Octave JN (2000) A GG nucleotide sequence of the 3' untranslated region of amyloid precursor protein

123

mRNA plays a key role in the regulation of translation and the binding of proteins. *Mol. Cell. Biol.* 20: 4572-4579.

Merrit C, Rasaloson D, Ko D, Seydoux G (2008) 3' UTRs are the primary regulators of gene expression in the C. elegans germline. *Curr Biol* 18:1476-82.

Moore MJ (2005) From birth to death: the complex life of eukaryotic mRNAs. *Science* 2:1514-8.

Musci I, Skorecki KL, ande Goldberg HJ (1996) Extracellular signal-regulated kinase and the small GTP-binding protein, Rac, contribute to the effects of transforming growth factor-beta1 on gene expression. *J. Biol. Chem.* 271: 16567-16572.

Ostareck, DH, Ostareck-Lederer, A, Wilm, M, Thiele, BJ, and Hentze, MW (1997) mRNA silencing in erythroid differentiation: hnRNP K and hnRNP E1 regulate 15-lypoxygenase translation from the 3' end. *Cell* 89, 597-606.

Pradet-Balade B, Boulme F, Beug H, Mullner EW, Garcia-Sanz JA (2001) Translation control: bridging the gap between genomics and proteomics? *Trends Biochem Sci* 26:225-9.

Preiss T and Hentze MW (1999) From factor to mechanism: translation and translational control in eukaryotes. *Curr. Opin. Genet. Dev.* 9: 515-521.

Prunier, C, and Howe, PH (2005) Disabled-2 (Dab2) is required for transforming growth factor β-induced epithelial to mesenchymal transition (EMT). *J. Biol. Chem.* 280, 17540-17548.

Ramswamy S, Ross KN, Lander ES *et al.* (2003) A molecular signature of metastasis in primary solid tumors. *Nature Genet.* 33, 49–54.

Ruggero D, Pandolifi PP (2003) Does the ribosome translate cancer? *Nature Rev. Cancer* 3, 179–192.

Sachs AB, Sarnow P, Hentze MW (1997) Starting at the beginning, middle, and end: translation initiation in eukaryotes. *Cell* 89, 831–838.

Sampath, P, Mazumder, B, Seshadri, V, Gerber, CA, Chavatte, L, Kinter, K, Ting, SM, Dignam, JD, Kim, S, Driscoll, DM, and Fox, PL (2004) Noncanonical function of glutamyl-prolyl-tRNA synthetase: gene-specific silencing of translation. *Cell* 119, 195-208.

Sanford LP, Ormsby I, Gittenberger-de Groot AC, Sariola H, Friedman R, Bolvin GP, Cardell EL, and Doetschman T (1997) TGFbeta2 knockout mice have multiple developmental defects that are non-overlapping with other TGFbeta knockout phenotypes. *Development* 124(13): 2659-2670.

Savagner P (2001) Leaving the neighborhood: molecular mechanisms involved during epithelial-mesenchymal transition. *Bioessays.* 23(10): 921-923.

Shi Y and Massague J (2003) Mechanisms of TGF-beta signaling from cell membrane to the nucleus. *Cell* 113(6): 685-700.

Siegel PM and Massague J (2003) Cytostatic and apoptotic actions of TGF-beta in homeostasis and cancer. *Nat. Rev. Cancer* 3(11): 807-821.

Smith ER, Capochichi CD, He J, Smedberg JL, Yang DH, Prowse AH, Godwin AK, Hamilton TC and Xu XX (2001) Disabled-2 mediates c-Fos suppression and

the cell growth regulatory activity of retinoic acid in embryonic carcinoma cells. J. Biol. Chem. 276: 47303-47310.

Standart N, Jackson RJ (1994) Regulation of translation by specific protein/mRNA interactions. *Biochimie* 76, 867–879.

Thiery, J.P., and Sleeman, J.P. (2006) Complex networks orchestrate epithelial-mesechymal transitions. *Nature Rev. Mol. Cell. Biol.* 7, 131-142.

Tseng CP, Ely BD, Li Y, Pong RC and Hsieh HT (1998) Regulation of rat DOC-2 gene during castration-induced rat ventral prostrate degeneration and its growth inhibitory function in human prostatic carcinoma cells. Endocrinology. 139: 3542-3553.

Wang H, et al. (2010) PCBP1 suppresses the translation of metastasis-associated PRL-3 phosphatase. *Cancer Cell* 18:52-62.

van der Kelen K, Beyaert R, Inze D, de Veylder L (2009) Translational control of eukaryotic gene expression. *Crit Rev Biochem Mol Biol* 44:143-68.

Varani G, Nagai K (1998) RNA recognition by RNP proteins during RNA processing. *Ann. Rev. Biophys. Biomol. Struct.* 27, 407–445.

Waerner, T., Alacakaptan, M., Tamir, I., Oberauer, R., Gal, A., Brabletz, T., Schreiber, M., Jechlinger, M., and Beug H. (2006) ILEI: A cytokine essential for EMT, tumor formation, and late events in metastasis in epithelial cells. *Cancer Cell* 10, 227-239.

Zavadil, J., and Bottinger, E.P. (2005) TGF-β and epithelial-to-mesenchymal transitions. *Oncogene* 24, 5764-5774.

Zoladek T, *et al.* (1995) Mutations altering the mitochondrial-cytoplasmic distribution of Mod5p implicate the actin cytoskeleton and mRNA 3´ ends and/ or protein synthesis in mitochondrial delivery. *Mol. Cell. Biol.* 15, 6884–6894.